Chapter 3

Mass Transfer and Diffusion

M*ass transfer* is the net movement of a component in a mixture from one location to another where the component exists at a different concentration. In many separation operations, the transfer takes place between two phases across an interface. Thus, the absorption by a solvent liquid of a solute from a carrier gas involves mass transfer of the solute through the gas to the gas–liquid interface, across the interface, and into the liquid. Mass-transfer models describe this and other processes such as passage of a species through a gas to the outer surface of a porous, adsorbent particle and into the adsorbent pores, where the species is adsorbed on the porous surface. Mass transfer also governs selective permeation through a nonporous, polymeric material of a component of a gas mixture. Mass transfer, as used here, does not refer to the flow of a fluid through a pipe. However, mass transfer might be superimposed on that flow. Mass transfer is not the flow of solids on a conveyor belt.

Mass transfer occurs by two basic mechanisms: (1) *molecular diffusion* by random and spontaneous microscopic movement of individual molecules in a gas, liquid, or solid as a result of thermal motion; and (2) *eddy* (turbulent) *diffusion* by random, macroscopic fluid motion. Both molecular and/or eddy diffusion frequently involve the movement of different species in opposing directions. When a net flow occurs in one of these directions, the total rate of mass transfer of individual species is increased or decreased by this bulk flow or *convection effect,* which may be considered a third mechanism of mass transfer. Molecular diffusion is extremely slow, whereas eddy diffusion is orders of magnitude more rapid. Therefore, if industrial separation processes are to be conducted in equipment of reasonable size, fluids must be agitated and interfacial areas maximized. If mass transfer in solids is involved, using small particles to decrease the distance in the direction of diffusion will increase the rate.

When separations involve two or more phases, the extent of the separation is limited by phase equilibrium, because, with time, the phases in contact tend to equilibrate by mass transfer between phases. When mass transfer is rapid, equilibration is approached in seconds or minutes, and design of separation equipment may be based on phase equilibrium, not mass transfer. For separations involving barriers, such as membranes, differing species mass-transfer rates through the membrane govern equipment design.

In a binary mixture, molecular diffusion of component A with respect to B occurs because of different potentials or driving forces, which include differences (gradients) of concentration (ordinary diffusion), pressure (pressure diffusion), temperature (thermal diffusion), and external force fields (forced diffusion) that act unequally on the different chemical species present. Pressure diffusion requires a large pressure gradient, which is achieved for gas mixtures with a centrifuge. Thermal diffusion columns or cascades can be employed to separate liquid and gas mixtures by establishing a temperature gradient. More widely applied is forced diffusion in an electrical field, to cause ions of different charges to move in different directions at different speeds.

In this chapter, only molecular diffusion caused by concentration gradients is considered, because this is the most common type of molecular diffusion in separation processes. Furthermore, emphasis is on binary systems, for which molecular-diffusion theory is relatively simple and applications are relatively straightforward. Multicomponent molecular diffusion, which is important in many applications, is considered briefly in Chapter 12. Diffusion in multicomponent systems is much more complex than diffusion in binary systems, and is a more appropriate topic for advanced study using a text such as Taylor and Krishna [1].

Molecular diffusion occurs in solids and in fluids that are stagnant or in laminar or turbulent motion. Eddy diffusion occurs in fluids in turbulent motion. When both molecular diffusion and eddy diffusion occur, they take place in parallel and are additive. Furthermore, they take place because of the same concentration difference (gradient). When mass transfer occurs under turbulent-flow conditions, but across an interface or to a solid surface, conditions may be laminar or nearly stagnant near the interface or solid surface. Thus, even though eddy diffusion may be the dominant mechanism in the bulk of the fluid, the overall rate of mass transfer may be controlled by molecular diffusion because the eddy-diffusion mechanism is damped or even eliminated as the interface or solid surface is approached.

Mass transfer of one or more species results in a total net rate of bulk flow or flux in one direction relative to a fixed

plane or stationary coordinate system. When a net flux occurs, it carries all species present. Thus, the molar flux of an individual species is the sum of all three mechanisms. If N_i is the molar flux of species i with mole fraction x_i, and N is the total molar flux, with both fluxes in moles per unit time per unit area in a direction perpendicular to a stationary plane across which mass transfer occurs, then

$$N_i = x_i N + \text{molecular diffusion flux of } i + \text{eddy diffusion flux of } i \quad (3\text{-}1)$$

where $x_i N$ is the bulk-flow flux. Each term in (3-1) is positive or negative depending on the direction of the flux relative to the direction selected as positive. When the molecular and eddy-diffusion fluxes are in one direction and N is in the opposite direction, even though a concentration difference or gradient of i exists, the net mass-transfer flux, N_i, of i can be zero.

In this chapter, the subject of mass transfer and diffusion is divided into seven areas: (1) steady-state diffusion in stagnant media, (2) estimation of diffusion coefficients, (3) unsteady-state diffusion in stagnant media, (4) mass transfer in laminar flow, (5) mass transfer in turbulent flow, (6) mass transfer at fluid–fluid interfaces, and (7) mass transfer across fluid–fluid interfaces.

3.0 INSTRUCTIONAL OBJECTIVES

After completing this chapter, you should be able to:

- Explain the relationship between mass transfer and phase equilibrium.
- Explain why separation models for mass transfer and phase equilibrium are useful.
- Discuss mechanisms of mass transfer, including the effect of bulk flow.
- State, in detail, Fick's law of diffusion for a binary mixture and discuss its analogy to Fourier's law of heat conduction in one dimension.
- Modify Fick's law of diffusion to include the bulk flow effect.
- Calculate mass-transfer rates and composition gradients under conditions of equimolar, countercurrent diffusion and unimolecular diffusion.
- Estimate, in the absence of data, diffusivities (diffusion coefficients) in gas and liquid mixtures, and know of some sources of data for diffusion in solids.
- Calculate multidimensional, unsteady-state, molecular diffusion by analogy to heat conduction.
- Calculate rates of mass transfer by molecular diffusion in laminar flow for three common cases: (1) falling liquid film, (2) boundary-layer flow past a flat plate, and (3) fully developed flow in a straight, circular tube.
- Define a mass-transfer coefficient and explain its analogy to the heat-transfer coefficient and its usefulness, as an alternative to Fick's law, in solving mass-transfer problems.
- Understand the common dimensionless groups (Reynolds, Sherwood, Schmidt, and Peclet number for mass transfer) used in correlations of mass-transfer coefficients.
- Use analogies, particularly that of Chilton and Colburn, and more theoretically based equations, such as those of Churchill et al., to calculate rates of mass transfer in turbulent flow.
- Calculate rates of mass transfer across fluid–fluid interfaces using the two-film theory and the penetration theory.

3.1 STEADY-STATE, ORDINARY MOLECULAR DIFFUSION

Suppose a cylindrical glass vessel is partly filled with water containing a soluble red dye. Clear water is carefully added on top so that the dyed solution on the bottom is undisturbed. At first, a sharp boundary exists between the two layers, but after a time the upper layer becomes colored, while the layer below becomes less colored. The upper layer is more colored near the original interface between the two layers and less colored in the region near the top of the upper layer. During this color change, the motion of each dye molecule is random, undergoing collisions mainly with water molecules and sometimes with other dye molecules, moving first in one direction and then in another, with no one direction preferred. This type of motion is sometimes referred to as a *random-walk process,* which yields a mean-square distance of travel for a given interval of time, but not a direction of travel. Thus, at a given horizontal plane through the solution in the cylinder, it is not possible to determine whether, in a given time interval, a given molecule will cross the plane or not. However, on the average, a fraction of all molecules in the solution below the plane will cross over into the region above and the same fraction will cross over in the opposite direction. Therefore, if the concentration of dye molecules in the lower region is greater than in the upper region, a net rate of mass transfer of dye molecules will take place from the

lower to the upper region. After a long time, a dynamic equilibrium will be achieved and the concentration of dye will be uniform throughout the solution. Based on these observations, it is clear that:

1. Mass transfer by ordinary molecular diffusion occurs because of a concentration, difference or gradient; that is, a species diffuses in the direction of decreasing concentration.
2. The mass-transfer rate is proportional to the area normal to the direction of mass transfer and not to the volume of the mixture. Thus, the rate can be expressed as a flux.
3. Net mass transfer stops when concentrations are uniform.

Fick's Law of Diffusion

The above observations were quantified by Fick in 1855, who proposed an extension of Fourier's 1822 heat-conduction theory. Fourier's first law of heat conduction is

$$q_z = -k\frac{dT}{dz} \tag{3-2}$$

where q_z is the heat flux by conduction in the positive z-direction, k is the thermal conductivity of the medium, and dT/dz is the temperature gradient, which is negative in the direction of heat conduction. Fick's first law of molecular diffusion also features a proportionality between a flux and a gradient. For a binary mixture of A and B,

$$J_{A_z} = -D_{AB}\frac{dc_A}{dz} \tag{3-3a}$$

and

$$J_{B_z} = -D_{BA}\frac{dc_B}{dz} \tag{3-3b}$$

where, in (3-3a), J_{A_z} is the molar flux of A by ordinary molecular diffusion relative to the molar-average velocity of the mixture in the positive z direction, D_{AB} is the *mutual diffusion coefficient* of A in B, discussed in the next section, c_A is the molar concentration of A, and dc_A/dz is the concentration gradient of A, which is negative in the direction of ordinary molecular diffusion. Similar definitions apply to (3-3b). The molar fluxes of A and B are in opposite directions. If the gas, liquid, or solid mixture through which diffusion occurs is isotropic, then values of k and D_{AB} are independent of direction. Nonisotropic (anisotropic) materials include fibrous and laminated solids as well as single, noncubic crystals. The diffusion coefficient is also referred to as the *diffusivity* and the mass diffusivity (to distinguish it from thermal and momentum diffusivities).

Many alternative forms of (3-3a) and (3-3b) are used, depending on the choice of driving force or potential in the gradient. For example, we can express (3-3a) as

$$J_A = -cD_{AB}\frac{dx_A}{dz} \tag{3-4}$$

where, for convenience, the z subscript on J has been dropped, c = total molar concentration or molar density ($c = 1/v = \rho/M$), and x_A = mole fraction of species A.

Equation (3-4) can also be written in the following equivalent mass form, where j_A is the mass flux of A by ordinary molecular diffusion relative to the mass-average velocity of the mixture in the positive z-direction, ρ is the mass density, and w_A is the mass fraction of A:

$$j_A = -\rho D_{AB}\frac{dw_A}{dz} \tag{3-5}$$

Velocities in Mass Transfer

It is useful to formulate expressions for velocities of chemical species in the mixture. If these velocities are based on the molar flux, N, and the molar diffusion flux, J, the molar average velocity of the mixture, v_M, relative to stationary coordinates is given for a binary mixture as

$$v_M = \frac{N}{c} = \frac{N_A + N_B}{c} \tag{3-6}$$

Similarly, the velocity of species i, defined in terms of N_i, is relative to stationary coordinates:

$$v_i = \frac{N_i}{c_i} \tag{3-7}$$

Combining (3-6) and (3-7) with $x_i = c_i/c$ gives

$$v_M = x_A v_A + x_B v_B \tag{3-8}$$

Alternatively, species diffusion velocities, v_{i_D}, defined in terms of J_i, are relative to the molar-average velocity and are defined as the difference between the species velocity and the molar-average velocity for the mixture:

$$v_{i_D} = \frac{J_i}{c_i} = v_i - v_M \tag{3-9}$$

When solving mass-transfer problems involving net movement of the mixture, it is not convenient to use fluxes and flow rates based on v_M as the frame of reference. Rather, it is preferred to use mass-transfer fluxes referred to stationary coordinates with the observer fixed in space. Thus, from (3-9), the total species velocity is

$$v_i = v_M + v_{i_D} \tag{3-10}$$

Combining (3-7) and (3-10),

$$N_i = c_i v_M + c_i v_{i_D} \tag{3-11}$$

Combining (3-11) with (3-4), (3-6), and (3-7),

$$N_A = \frac{n_A}{A} = x_A N - cD_{AB}\left(\frac{dx_A}{dz}\right) \tag{3-12}$$

and

$$N_B = \frac{n_B}{A} = x_B N - cD_{BA}\left(\frac{dx_B}{dz}\right) \tag{3-13}$$

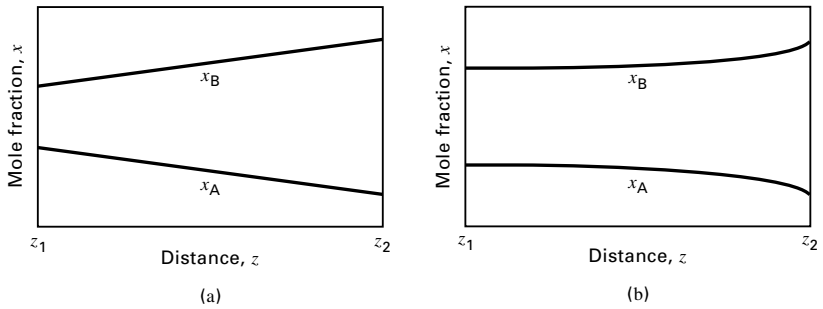

Figure 3.1 Concentration profiles for limiting cases of ordinary molecular diffusion in binary mixtures across a stagnant film: (a) equimolar counterdiffusion (EMD); (b) unimolecular diffusion (UMD).

where in (3-12) and (3-13), n_i is the molar flow rate in moles per unit time, A is the mass-transfer area, the first terms on the right-hand sides are the fluxes resulting from bulk flow, and the second terms on the right-hand sides are the ordinary molecular diffusion fluxes. Two limiting cases are important:

1. Equimolar counterdiffusion (EMD)
2. Unimolecular diffusion (UMD)

Equimolar Counterdiffusion

In equimolar counterdiffusion (EMD), the molar fluxes of A and B in (3-12) and (3-13) are equal but opposite in direction; thus,

$$N = N_A + N_B = 0 \tag{3-14}$$

Thus, from (3-12) and (3-13), the diffusion fluxes are also equal but opposite in direction:

$$J_A = -J_B \tag{3-15}$$

This idealization is closely approached in distillation. From (3-12) and (3-13), we see that in the absence of fluxes other than molecular diffusion,

$$N_A = J_A = -cD_{AB}\left(\frac{dx_A}{dz}\right) \tag{3-16}$$

and

$$N_B = J_B = -cD_{BA}\left(\frac{dx_B}{dz}\right) \tag{3-17}$$

If the total concentration, pressure, and temperature are constant and the mole fractions are maintained constant (but different) at two sides of a stagnant film between z_1 and z_2, then (3-16) and (3-17) can be integrated from z_1 to any z between z_1 and z_2 to give

$$J_A = \frac{cD_{AB}}{z - z_1}(x_{A_1} - x_A) \tag{3-18}$$

and

$$J_B = \frac{cD_{BA}}{z - z_1}(x_{B_1} - x_B) \tag{3-19}$$

Thus, in the steady state, the mole fractions are linear in distance, as shown in Figure 3.1a. Furthermore, because c is constant through the film, where

$$c = c_A + c_B \tag{3-20}$$

by differentiation,

$$dc = 0 = dc_A + dc_B \tag{3-21}$$

Thus,

$$dc_A = -dc_B \tag{3-22}$$

From (3-3a), (3-3b), (3-15), and (3-22),

$$\frac{D_{AB}}{dz} = \frac{D_{BA}}{dz} \tag{3-23}$$

Therefore, $D_{AB} = D_{BA}$.

This equality of diffusion coefficients is always true in a binary system of constant molar density.

EXAMPLE 3.1

Two bulbs are connected by a straight tube, 0.001 m in diameter and 0.15 m in length. Initially the bulb at end 1 contains N_2 and the bulb at end 2 contains H_2. The pressure and temperature are maintained constant at 25°C and 1 atm. At a certain time after allowing diffusion to occur between the two bulbs, the nitrogen content of the gas at end 1 of the tube is 80 mol% and at end 2 is 25 mol%. If the binary diffusion coefficient is 0.784 cm^2/s, determine:

(a) The rates and directions of mass transfer of hydrogen and nitrogen in mol/s

(b) The species velocities relative to stationary coordinates, in cm/s

SOLUTION

(a) Because the gas system is closed and at constant pressure and temperature, mass transfer in the connecting tube is equimolar counterdiffusion by molecular diffusion.

The area for mass transfer through the tube, in cm^2, is $A = 3.14(0.1)^2/4 = 7.85 \times 10^{-3}$ cm^2. The total gas concentration (molar density) is $c = \frac{P}{RT} = \frac{1}{(82.06)(298)} = 4.09 \times 10^{-5}$ mol/cm^3. Take the reference plane at end 1 of the connecting tube. Applying (3-18) to

N_2 over the length of the tube,

$$n_{N_2} = \frac{cD_{N_2,H_2}}{z_2 - z_1}[(x_{N_2})_1 - (x_{N_2})_2]A$$
$$= \frac{(4.09 \times 10^{-5})(0.784)(0.80 - 0.25)}{15}(7.85 \times 10^{-3})$$
$$= 9.23 \times 10^{-9} \text{ mol/s} \qquad \text{in the positive } z\text{-direction}$$
$$n_{H_2} = 9.23 \times 10^{-9} \text{ mol/s} \qquad \text{in the negative } z\text{-direction}$$

(b) For equimolar counterdiffusion, the molar-average velocity of the mixture, v_M, is 0. Therefore, from (3-9), species velocities are equal to species diffusion velocities. Thus,

$$v_{N_2} = (v_{N_2})_D = \frac{J_{N_2}}{c_{N_2}} = \frac{n_{N_2}}{Acx_{N_2}}$$
$$= \frac{9.23 \times 10^{-9}}{[(7.85 \times 10^{-3})(4.09 \times 10^{-5})x_{N_2}]}$$
$$= \frac{0.0287}{x_{N_2}} \qquad \text{in the positive } z\text{-direction}$$

Similarly,

$$v_{H_2} = \frac{0.0287}{x_{H_2}} \qquad \text{in the negative } z\text{-direction}$$

Thus, species velocities depend on species mole fractions, as follows:

z, cm	x_{N_2}	x_{H_2}	v_{N_2}, cm/s	v_{H_2}, cm/s
0 (end 1)	0.800	0.200	0.0351	−0.1435
5	0.617	0.383	0.0465	−0.0749
10	0.433	0.567	0.0663	−0.0506
15 (end 2)	0.250	0.750	0.1148	−0.0383

Note that species velocities vary across the length of the connecting tube, but at any location, z, $v_M = 0$. For example, at $z = 10$ cm, from (3-8),

$$v_M = (0.433)(0.0663) + (0.567)(-0.0506) = 0$$

Unimolecular Diffusion

In unimolecular diffusion (UMD), mass transfer of component A occurs through stagnant (nonmoving) component B. Thus,

$$N_B = 0 \tag{3-24}$$

and

$$N = N_A \tag{3-25}$$

Therefore, from (3-12),

$$N_A = x_A N_A - cD_{AB}\frac{dx_A}{dz} \tag{3-26}$$

which can be rearranged to a Fick's-law form,

$$N_A = -\frac{cD_{AB}}{(1 - x_A)}\frac{dx_A}{dz} = -\frac{cD_{AB}}{x_B}\frac{dx_A}{dz} \tag{3-27}$$

The factor $(1 - x_A)$ accounts for the bulk-flow effect. For a mixture dilute in A, the bulk-flow effect is negligible or small. In mixtures more concentrated in A, the bulk-flow effect can be appreciable. For example, in an equimolar mixture of A and B, $(1 - x_A) = 0.5$ and the molar mass-transfer flux of A is twice the ordinary molecular-diffusion flux.

For the stagnant component, B, (3-13) becomes

$$0 = x_B N_A - cD_{BA}\frac{dx_B}{dz} \tag{3-28}$$

or

$$x_B N_A = cD_{BA}\frac{dx_B}{dz} \tag{3-29}$$

Thus, the bulk-flow flux of B is equal but opposite to its diffusion flux.

At quasi-steady-state conditions, that is, with no accumulation, and with constant molar density, (3-27) becomes in integral form:

$$\int_{z_1}^{z} dz = -\frac{cD_{AB}}{N_A}\int_{x_{A_1}}^{x_A}\frac{dx_A}{1 - x_A} \tag{3-30}$$

which upon integration yields

$$N_A = \frac{cD_{AB}}{z - z_1}\ln\left(\frac{1 - x_A}{1 - x_{A_1}}\right) \tag{3-31}$$

Rearrangement to give the mole-fraction variation as a function of z yields

$$x_A = 1 - (1 - x_{A_1})\exp\left[\frac{N_A(z - z_1)}{cD_{AB}}\right] \tag{3-32}$$

Thus, as shown in Figure 3.1b, the mole fractions are nonlinear in distance.

An alternative and more useful form of (3-31) can be derived from the definition of the log mean. When $z = z_2$, (3-31) becomes

$$N_A = \frac{cD_{AB}}{z_2 - z_1}\ln\left(\frac{1 - x_{A_2}}{1 - x_{A_1}}\right) \tag{3-33}$$

The log mean (LM) of $(1 - x_A)$ at the two ends of the stagnant layer is

$$(1 - x_A)_{LM} = \frac{(1 - x_{A_2}) - (1 - x_{A_1})}{\ln[(1 - x_{A_2})/(1 - x_{A_1})]}$$
$$= \frac{x_{A_1} - x_{A_2}}{\ln[(1 - x_{A_2})/(1 - x_{A_1})]} \tag{3-34}$$

Combining (3-33) with (3-34) gives

$$N_A = \frac{cD_{AB}}{z_2 - z_1}\frac{(x_{A_1} - x_{A_2})}{(1 - x_A)_{LM}} = \frac{cD_{AB}}{(1 - x_A)_{LM}}\frac{(-\Delta x_A)}{\Delta z}$$
$$= \frac{cD_{AB}}{(x_B)_{LM}}\frac{(-\Delta x_A)}{\Delta z} \tag{3-35}$$

EXAMPLE 3.2

As shown in Figure 3.2, an open beaker, 6 cm in height, is filled with liquid benzene at 25°C to within 0.5 cm of the top. A gentle breeze of dry air at 25°C and 1 atm is blown by a fan across the mouth of the beaker so that evaporated benzene is carried away by convection after it transfers through a stagnant air layer in the beaker. The vapor pressure of benzene at 25°C is 0.131 atm. The mutual diffusion coefficient for benzene in air at 25°C and 1 atm is 0.0905 cm^2/s. Compute:

(a) The initial rate of evaporation of benzene as a molar flux in mol/cm^2-s

(b) The initial mole-fraction profiles in the stagnant air layer

(c) The initial fractions of the mass-transfer fluxes due to molecular diffusion

(d) The initial diffusion velocities, and the species velocities (relative to stationary coordinates) in the stagnant layer

(e) The time in hours for the benzene level in the beaker to drop 2 cm from the initial level, if the specific gravity of liquid benzene is 0.874. Neglect the accumulation of benzene and air in the stagnant layer as it increases in height

SOLUTION

Let A = benzene, B = air.

$$c = \frac{P}{RT} = \frac{1}{(82.06)(298)} = 4.09 \times 10^{-5} \text{ mol/cm}^3$$

(a) Take $z_1 = 0$. Then $z_2 - z_1 = \Delta z = 0.5$ cm. From Dalton's law, assuming equilibrium at the liquid benzene–air interface,

$$x_{A_1} = \frac{p_{A_1}}{P} = \frac{0.131}{1} = 0.131 \qquad x_{A_2} = 0$$

$$(1 - x_A)_{LM} = \frac{0.131}{\ln[(1-0)/(1-0.131)]} = 0.933 = (x_B)_{LM}$$

From (3-35),

$$N_A = \frac{(4.09 \times 10^{-5})(0.0905)}{0.5}\left(\frac{0.131}{0.933}\right) = 1.04 \times 10^{-6} \text{ mol/cm}^2\text{-s}$$

(b) $$\frac{N_A(z - z_1)}{cD_{AB}} = \frac{(1.04 \times 10^{-6})(z - 0)}{(4.09 \times 10^{-5})(0.0905)} = 0.281\, z$$

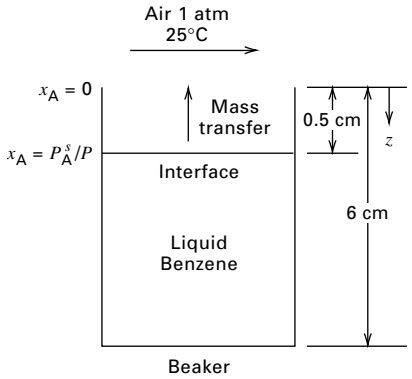

Figure 3.2 Evaporation of benzene from a beaker—Example 3.2.

From (3-32),

$$x_A = 1 - 0.869 \exp(0.281\, z) \tag{1}$$

Using (1), the following results are obtained:

z, cm	x_A	x_B
0.0	0.1310	0.8690
0.1	0.1060	0.8940
0.2	0.0808	0.9192
0.3	0.0546	0.9454
0.4	0.0276	0.9724
0.5	0.0000	1.0000

These profiles are only slightly curved.

(c) From (3-27) and (3-29), we can compute the bulk flow terms, $x_A N_A$ and $x_B N_A$, from which the molecular diffusion terms are obtained.

	$x_i N$ Bulk-Flow Flux, mol/cm^2-s × 10^6		J_i Molecular-Diffusion Flux, mol/cm^2-s × 10^6	
z, cm	A	B	A	B
0.0	0.1360	0.9040	0.9040	−0.9040
0.1	0.1100	0.9300	0.9300	−0.9300
0.2	0.0840	0.9560	0.9560	−0.9560
0.3	0.0568	0.9832	0.9832	−0.9832
0.4	0.0287	1.0113	1.0113	−1.0113
0.5	0.0000	1.0400	1.0400	−1.0400

Note that the molecular-diffusion fluxes are equal but opposite, and the bulk-flow flux of B is equal but opposite to its molecular-diffusion flux, so that its molar flux, N_B, is zero, making B (air) stagnant.

(d) From (3-6),

$$v_M = \frac{N}{c} = \frac{N_A}{c} = \frac{1.04 \times 10^{-6}}{4.09 \times 10^{-5}} = 0.0254 \text{ cm/s} \tag{2}$$

From (3-9), the diffusion velocities are given by

$$v_{i_d} = \frac{J_i}{c_i} = \frac{J_i}{x_i c} \tag{3}$$

From (3-10), the species velocities relative to stationary coordinates are

$$v_i = v_{i_d} + v_M \tag{4}$$

Using (2) to (4), we obtain

	v_{i_d} Molecular-Diffusion Velocity, cm/s		J_i Species Velocity, cm/s	
z, cm	A	B	A	B
0.0	0.1687	−0.0254	0.1941	0
0.1	0.2145	−0.0254	0.2171	0
0.2	0.2893	−0.0254	0.3147	0
0.3	0.4403	−0.0254	0.4657	0
0.4	0.8959	−0.0254	0.9213	0
0.5	∞	−0.0254	∞	0

Note that v_B is zero everywhere, because its molecular-diffusion velocity is negated by the molar-mean velocity.

(e) The mass-transfer flux for benzene evaporation can be equated to the rate of decrease in the moles of liquid benzene per unit cross section of the beaker. Letting z = distance down from the mouth of the beaker and using (3-35) with $\Delta z = z$,

$$N_A = \frac{cD_{AB}}{z}\frac{(-\Delta x_A)}{(1-x_A)_{LM}} = \frac{\rho_L}{M_L}\frac{dz}{dt} \tag{5}$$

Separating variables and integrating,

$$\int_0^t dt = t = \frac{\rho_L(1-x_A)_{LM}}{M_L c D_{AB}(-\Delta x_A)}\int_{z_1}^{z_2} z\,dz \tag{6}$$

The coefficient of the integral on the right-hand side of (6) is constant at

$$\frac{0.874(0.933)}{78.11(4.09\times10^{-5})(0.0905)(0.131)} = 21{,}530 \text{ s/cm}^2$$

$$\int_{z_1}^{z_2} z\,dz = \int_{0.5}^{2.5} z\,dz = 3 \text{ cm}^2$$

From (6), $t = 21{,}530(3) = 64{,}590$ s or 17.94 h, which is a long time because of the absence of turbulence.

Table 3.1 Diffusion Volumes from Fuller, Ensley, and Giddings [*J. Phys. Chem,* **73,** 3679–3685 (1969)] for Estimating Binary Gas Diffusivity by the Method of Fuller et al. [3]

Atomic Diffusion Volumes Atomic and Structural Diffusion-Volume Increments			
C	15.9	F	14.7
H	2.31	Cl	21.0
O	6.11	Br	21.9
N	4.54	I	29.8
Aromatic ring	−18.3	S	22.9
Heterocyclic ring	−18.3		
Diffusion Volumes of Simple Molecules			
He	2.67	CO	18.0
Ne	5.98	CO_2	26.7
Ar	16.2	N_2O	35.9
Kr	24.5	NH_3	20.7
Xe	32.7	H_2O	13.1
H_2	6.12	SF_6	71.3
D_2	6.84	Cl_2	38.4
N_2	18.5	Br_2	69.0
O_2	16.3	SO_2	41.8
Air	19.7		

3.2 DIFFUSION COEFFICIENTS

Diffusivities or diffusion coefficients are defined for a binary mixture by (3-3) to (3-5). Measurement of diffusion coefficients must involve a correction for any bulk flow using (3-12) and (3-13) with the reference plane being such that there is no net molar bulk flow.

The binary diffusivities, D_{AB} and D_{BA}, are mutual or binary diffusion coefficients. Other coefficients include D_{i_M}, the diffusivity of i in a multicomponent mixture; D_{ii}, the self-diffusion coefficient; and the tracer or interdiffusion coefficient. In this chapter, and throughout this book, the focus is on the mutual diffusion coefficient, which will be referred to as the diffusivity or diffusion coefficient.

Diffusivity in Gas Mixtures

As discussed by Poling, Prausnitz, and O'Connell [2], a number of theoretical and empirical equations are available for estimating the value of $D_{AB} = D_{BA}$ in gases at low to moderate pressures. The theoretical equations, based on Boltzmann's kinetic theory of gases, the theorem of corresponding states, and a suitable intermolecular energy-potential function, as developed by Chapman and Enskog, predict D_{AB} to be inversely proportional to pressure and almost independent of composition, with a significant increase for increasing temperature. Of greater accuracy and ease of use is the following empirical equation of Fuller, Schettler, and Giddings [3], which retains the form of the Chapman–Enskog theory but utilizes empirical constants derived from experimental data:

$$D_{AB} = D_{BA} = \frac{0.00143T^{1.75}}{PM_{AB}^{1/2}[(\sum_V)_A^{1/3} + (\sum_V)_B^{1/3}]^2} \tag{3-36}$$

where D_{AB} is in cm^2/s, P is in atm, T is in K,

$$M_{AB} = \frac{2}{(1/M_A) + (1/M_B)} \tag{3-37}$$

and $\sum_V$ = summation of atomic and structural diffusion volumes from Table 3.1, which includes diffusion volumes of some simple molecules.

Experimental values of binary gas diffusivity at 1 atm and near-ambient temperature range from about 0.10 to 10.0 cm^2/s. Poling, et al. [2] compared (3-36) to experimental data for 51 different binary gas mixtures at low pressures over a temperature range of 195–1,068 K. The average deviation was only 5.4%, with a maximum deviation of 25%. Only 9 of 69 estimated values deviated from experimental values by more than 10%. When an experimental diffusivity is available at values of T and P that are different from the desired conditions, (3-36) indicates that D_{AB} is proportional to $T^{1.75}/P$, which can be used to obtain the desired value. Some representative experimental values of binary gas diffusivity are given in Table 3.2.

Table 3.2 Experimental Binary Diffusivities of Some Gas Pairs at 1 atm

Gas pair, A-B	Temperature, K	D_{AB}, cm^2/s
Air—carbon dioxide	317.2	0.177
Air—ethanol	313	0.145
Air—helium	317.2	0.765
Air—*n*-hexane	328	0.093
Air—water	313	0.288
Argon—ammonia	333	0.253
Argon—hydrogen	242.2	0.562
Argon—hydrogen	806	4.86
Argon—methane	298	0.202
Carbon dioxide—nitrogen	298	0.167
Carbon dioxide—oxygen	293.2	0.153
Carbon dioxide—water	307.2	0.198
Carbon monoxide—nitrogen	373	0.318
Helium—benzene	423	0.610
Helium—methane	298	0.675
Helium—methanol	423	1.032
Helium—water	307.1	0.902
Hydrogen—ammonia	298	0.783
Hydrogen—ammonia	533	2.149
Hydrogen—cyclohexane	288.6	0.319
Hydrogen—methane	288	0.694
Hydrogen—nitrogen	298	0.784
Nitrogen—benzene	311.3	0.102
Nitrogen—cyclohexane	288.6	0.0731
Nitrogen—sulfur dioxide	263	0.104
Nitrogen—water	352.1	0.256
Oxygen—benzene	311.3	0.101
Oxygen—carbon tetrachloride	296	0.0749
Oxygen—cyclohexane	288.6	0.0746
Oxygen—water	352.3	0.352

From Marrero, T. R., and E. A. Mason, *J. Phys. Chem. Ref. Data,* **1,** 3–118 (1972).

EXAMPLE 3.3

Estimate the diffusion coefficient for the system oxygen (A)/benzene (B) at 38°C and 2 atm using the method of Fuller et al.

SOLUTION

From (3-37),

$$M_{AB} = \frac{2}{(1/32) + (1/78.11)} = 45.4$$

From Table 3.1, $(\sum_V)_A = 16.3$ and $(\sum_V)_B = 6(15.9) + 6(2.31) - 18.3 = 90.96$

From (3-36), at 2 atm and 311.2 K,

$$D_{AB} = D_{BA} = \frac{0.00143(311.2)^{1.75}}{(2)(45.4)^{1/2}[16.3^{1/3} + 90.96^{1/3}]^2} = 0.0495 \text{ cm}^2/\text{s}$$

At 1 atm, the predicted diffusivity is 0.0990 cm^2/s, which is about 2% below the experimental value of 0.101 cm^2/s in Table 3.2. The experimental value for 38°C can be extrapolated by the temperature dependency of (3-36) to give the following prediction at 200°C:

$$D_{AB} \text{ at } 200^\circ\text{C and 1 atm} = 0.102\left(\frac{200 + 273.2}{38 + 273.2}\right)^{1.75} = 0.212 \text{ cm}^2/\text{s}$$

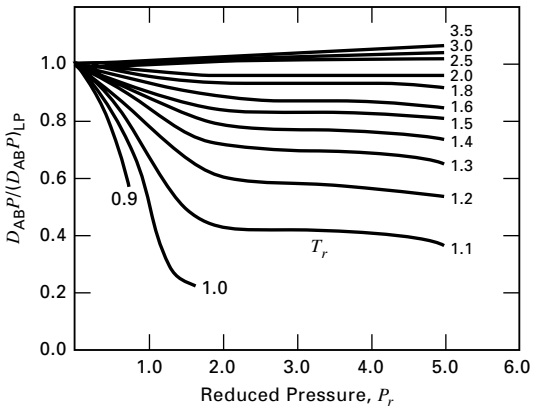

Figure 3.3 Takahashi [4] correlation for effect of high pressure on binary gas diffusivity.

For binary mixtures of light gases, at pressures to about 10 atm, the pressure dependence on diffusivity is adequately predicted by the simple inverse relation (3-36), that is, $PD_{AB} =$ a constant for a given temperature and gas mixture. At higher pressures, deviations from this relation are handled in a manner somewhat similar to the modification of the ideal-gas law by the compressibility factor based on the theorem of corresponding states. Although few reliable experimental data are available at high pressure, Takahasi [4] has published a tentative corresponding-states correlation, shown in Figure 3.3, patterned after an earlier correlation for self-diffusivities by Slattery [5]. In the Takahashi plot, $D_{AB}P/(D_{AB}P)_{LP}$ is given as a function of reduced temperature and pressure, where $(D_{AB}P)_{LP}$ is at low pressure where (3-36) applies. Mixture-critical temperature and pressure are molar-average values. Thus, a finite effect of composition is predicted at high pressure. The effect of high pressure on diffusivity is important in supercritical extraction, discussed in Chapter 11.

EXAMPLE 3.4

Estimate the diffusion coefficient for a 25/75 molar mixture of argon and xenon at 200 atm and 378 K. At this temperature and 1 atm, the diffusion coefficient is 0.180 cm^2/s. Critical constants are

	T_c, K	P_c, atm
Argon	151.0	48.0
Xenon	289.8	58.0

SOLUTION

Calculate reduced conditions:

$T_c = 0.25(151) + 0.75(289.8) = 255.1$ K;
$T_r = T/T_c = 378/255.1 = 1.48$
$P_c = 0.25(48) + 0.75(58) = 55.5$;
$P_r = P/P_c = 200/55.5 = 3.6$

From Figure 3.3, $\dfrac{D_{AB}P}{(D_{AB}P)_{LP}} = 0.82$

$$D_{AB} = \frac{(D_{AB}P)_{LP}}{P}\left[\frac{D_{AB}P}{(D_{AB}P)_{LP}}\right] = \frac{(0.180)(1)}{200}(0.82) = 7.38 \times 10^{-4} \text{ cm/s}$$

Diffusivity in Liquid Mixtures

Diffusion coefficients in binary liquid mixtures are difficult to estimate because of the lack of a rigorous model for the liquid state. An exception is the case of a dilute solute (A) of very large, rigid, spherical molecules diffusing through a stationary solvent (B) of small molecules with no slip of the solvent at the surface of the solute molecules. The resulting relation, based on the hydrodynamics of creeping flow to describe drag, is the Stokes–Einstein equation:

$$(D_{AB})_\infty = \frac{RT}{6\pi\mu_B R_A N_A} \tag{3-38}$$

where R_A is the radius of the solute molecule and N_A is Avagadro's number. Although (3-38) is very limited in its application to liquid mixtures, it has long served as a starting point for more widely applicable empirical correlations for the diffusivity of solute (A) in solvent (B), where both A and B are of the same approximate molecular size. Unfortunately, unlike the situation in binary gas mixtures, $D_{AB} = D_{BA}$ in binary liquid mixtures can vary greatly with composition as shown in Example 3.7. Because the Stokes–Einstein equation does not provide a basis for extending dilute conditions to more concentrated conditions, extensions of (3-38) have been restricted to binary liquid mixtures dilute in A, up to 5 and perhaps 10 mol%.

One such extension, which gives reasonably good predictions for small solute molecules, is the empirical Wilke–Chang [6] equation:

$$(D_{AB})_\infty = \frac{7.4 \times 10^{-8}(\phi_B M_B)^{1/2} T}{\mu_B v_A^{0.6}} \tag{3-39}$$

where the units are cm^2/s for D_{AB}; cP (centipoises) for the solvent viscosity, μ_B; K for T; and cm^3/mol for v_A, the liquid molar volume of the solute at its normal boiling point. The parameter ϕ_B is an association factor for the solvent, which is 2.6 for water, 1.9 for methanol, 1.5 for ethanol, and 1.0 for unassociated solvents such as hydrocarbons. Note that the effects of temperature and viscosity are identical to the prediction of the Stokes–Einstein equation, while the effect of the radius of the solute molecule is replaced by v_A, which can be estimated by summing the atomic contributions in Table 3.3, which also lists values of v_A for dissolved light gases. Some representative experimental values of diffusivity in dilute binary liquid solutions are given in Table 3.4.

Table 3.3 Molecular Volumes of Dissolved Light Gases and Atomic Contributions for Other Molecules at the Normal Boiling Point

	Atomic Volume $(m^3/kmol) \times 10^3$		Atomic Volume $(m^3/kmol) \times 10^3$
C	14.8	Ring	
H	3.7	Three-membered, as in ethylene oxide	−6
O (except as below)	7.4	Four-membered	−8.5
Doubly bonded as carbonyl	7.4	Five-membered	−11.5
Coupled to two other elements:		Six-membered	−15
In aldehydes, ketones	7.4	Naphthalene ring	−30
In methyl esters	9.1	Anthracene ring	−47.5
In methyl ethers	9.9		
In ethyl esters	9.9		Molecular Volume $(m^3/kmol) \times 10^3$
In ethyl ethers	9.9		
In higher esters	11.0		
In higher ethers	11.0	Air	29.9
In acids (—OH)	12.0	O_2	25.6
Joined to S, P, N	8.3	N_2	31.2
N		Br_2	53.2
Doubly bonded	15.6	Cl_2	48.4
In primary amines	10.5	CO	30.7
In secondary amines	12.0	CO_2	34.0
Br	27.0	H_2	14.3
Cl in RCHClR′	24.6	H_2O	18.8
Cl in RCl (terminal)	21.6	H_2S	32.9
F	8.7	NH_3	25.8
I	37.0	NO	23.6
S	25.6	N_2O	36.4
P	27.0	SO_2	44.8

Source: G. Le Bas, *The Molecular Volumes of Liquid Chemical Compounds,* David McKay, New York (1915).

Table 3.4 Experimental Binary Liquid Diffusivities for Solutes, A, at Low Concentrations in Solvents, B

Solvent, B	Solute, A	Temperature, K	Diffusivity, D_{AB}, $cm^2/s \times 10^5$
Water	Acetic acid	293	1.19
	Aniline	293	0.92
	Carbon dioxide	298	2.00
	Ethanol	288	1.00
	Methanol	288	1.26
Ethanol	Allyl alcohol	293	0.98
	Benzene	298	1.81
	Oxygen	303	2.64
	Pyridine	293	1.10
	Water	298	1.24
Benzene	Acetic acid	298	2.09
	Cyclohexane	298	2.09
	Ethanol	288	2.25
	n-Heptane	298	2.10
	Toluene	298	1.85
n-Hexane	Carbon tetrachloride	298	3.70
	Methyl ethyl ketone	303	3.74
	Propane	298	4.87
	Toluene	298	4.21
Acetone	Acetic acid	288	2.92
	Formic acid	298	3.77
	Nitrobenzene	293	2.94
	Water	298	4.56

From Poling et al. [2].

EXAMPLE 3.5

Use the Wilke–Chang equation to estimate the diffusivity of aniline (A) in a 0.5 mol% aqueous solution at 20°C. At this temperature, the solubility of aniline in water is about 4 g/100 g of water or 0.77 mol% aniline. The experimental diffusivity value for an infinitely dilute mixture is 0.92×10^{-5} cm^2/s.

SOLUTION

$\mu_B = \mu_{H_2O} = 1.01$ cP at 20°C

$v_A =$ liquid molar volume of aniline at its normal boiling point of 457.6 K = 107 cm^3/mol

$\phi_B = 2.6$ for water $\quad M_B = 18$ for water $\quad T = 293$ K

From (3-39),

$$D_{AB} = \frac{(7.4 \times 10^{-8})[2.6(18)]^{0.5}(293)}{1.01(107)^{0.6}} = 0.89 \times 10^{-5} \text{ cm}^2/\text{s}$$

This value is about 3% less than the experimental value for an infinitely dilute solution of aniline in water.

More recent liquid diffusivity correlations due to Hayduk and Minhas [7] give better agreement than the Wilke–Chang equation with experimental values for nonaqueous solutions. For a dilute solution of one normal paraffin (C_5 to C_{32}) in another (C_5 to C_{16}),

$$(D_{AB})_\infty = 13.3 \times 10^{-8} \frac{T^{1.47} \mu_B^\epsilon}{v_A^{0.71}} \tag{3-40}$$

where

$$\epsilon = \frac{10.2}{v_A} - 0.791 \tag{3-41}$$

and the other variables have the same units as in (3-39).

For general nonaqueous solutions,

$$(D_{AB})_\infty = 1.55 \times 10^{-8} \frac{T^{1.29} \left(\mathcal{P}_B^{0.5} / \mathcal{P}_A^{0.42} \right)}{\mu_B^{0.92} v_B^{0.23}} \tag{3-42}$$

where $\mathcal{P}$ is the parachor, which is defined as

$$\mathcal{P} = v\sigma^{1/4} \tag{3-43}$$

When the units of the liquid molar volume, v, are cm^3/mol and the surface tension, σ, are g/s^2 (dynes/cm), then the units of the parachor are cm^3-$g^{1/4}/s^{1/2}$-mol. Normally, at near-ambient conditions, $\mathcal{P}$ is treated as a constant, for which an extensive tabulation is available from Quayle [8], who also provides a group-contribution method for estimating parachors for compounds not listed. Table 3.5 gives values of parachors for a number of compounds, while Table 3.6 contains structural contributions for predicting the parachor in the absence of data.

The following restrictions apply to (3-42):

1. Solvent viscosity should not exceed 30 cP.
2. For organic acid solutes and solvents other than water, methanol, and butanols, the acid should be treated as a dimer by doubling the values of $\mathcal{P}_A$ and v_A.
3. For a nonpolar solute in monohydroxy alcohols, values of v_B and $\mathcal{P}_B$ should be multiplied by $8\mu_B$, where the viscosity is in centipoise.

Liquid diffusion coefficients for a solute in a dilute binary system range from about 10^{-6} to 10^{-4} cm^2/s for solutes of molecular weight up to about 200 and solvents with viscosity up to about 10 cP. Thus, liquid diffusivities are five orders of magnitude less than diffusivities for binary gas mixtures at 1 atm. However, diffusion rates in liquids are not necessarily five orders of magnitude lower than in gases because, as seen in (3-5), the product of the concentration (molar density) and the diffusivity determines the rate of diffusion for a given concentration gradient in mole fraction. At 1 atm, the molar density of a liquid is three times that of a gas and, thus, the diffusion rate in liquids is only two orders of magnitude lower than in gases at 1 atm.

Table 3.5 Parachors for Representative Compounds

	Parachor, cm^3-$g^{1/4}/s^{1/2}$-mol		Parachor, cm^3-$g^{1/4}/s^{1/2}$-mol		Parachor, cm^3-$g^{1/4}/s^{1/2}$-mol
Acetic acid	131.2	Chlorobenzene	244.5	Methyl amine	95.9
Acetone	161.5	Diphenyl	380.0	Methyl formate	138.6
Acetonitrile	122	Ethane	110.8	Naphthalene	312.5
Acetylene	88.6	Ethylene	99.5	*n*-Octane	350.3
Aniline	234.4	Ethyl butyrate	295.1	1-Pentene	218.2
Benzene	205.3	Ethyl ether	211.7	1-Pentyne	207.0
Benzonitrile	258	Ethyl mercaptan	162.9	Phenol	221.3
n-Butyric acid	209.1	Formic acid	93.7	*n*-Propanol	165.4
Carbon disulfide	143.6	Isobutyl benzene	365.4	Toluene	245.5
Cyclohexane	239.3	Methanol	88.8	Triethyl amine	297.8

Source: Meissner, *Chem. Eng. Prog.,* **45,** 149–153 (1949).

Table 3.6 Structural Contributions for Estimating the Parachor

Carbon–hydrogen:		R—[—CO—]—R′(ketone)	
C	9.0	$R + R' = 2$	51.3
H	15.5	$R + R' = 3$	49.0
CH_3	55.5	$R + R' = 4$	47.5
CH_2 in —$(CH_2)_n$		$R + R' = 5$	46.3
$n < 12$	40.0	$R + R' = 6$	45.3
$n > 12$	40.3	$R + R' = 7$	44.1
		—CHO	66
Alkyl groups			
1-Methylethyl	133.3	O (not noted above)	20
1-Methylpropyl	171.9	N (not noted above)	17.5
1-Methylbutyl	211.7	S	49.1
2-Methylpropyl	173.3	P	40.5
1-Ethylpropyl	209.5	F	26.1
1,1-Dimethylethyl	170.4	Cl	55.2
1,1-Dimethylpropyl	207.5	Br	68.0
1,2-Dimethylpropyl	207.9	I	90.3
1,1,2-Trimethylpropyl	243.5	Ethylenic bonds:	
C_6H_5	189.6	Terminal	19.1
		2,3-position	17.7
Special groups:		3,4-position	16.3
—COO—	63.8		
—COOH	73.8	Triple bond	40.6
—OH	29.8		
$—NH_2$	42.5	Ring closure:	
—O—	20.0	Three-membered	12
$—NO_2$	74	Four-membered	6.0
$—NO_3$ (nitrate)	93	Five-membered	3.0
$—CO(NH_2)$	91.7	Six-membered	0.8

Source: Quale [8].

EXAMPLE 3.6

Estimate the diffusivity of formic acid (A) in benzene (B) at 25°C and infinite dilution, using the appropriate correlation of Hayduk and Minhas [7]. The experimental value is 2.28×10^{-5} cm^2/s.

SOLUTION

Equation (3-42) applies, with $T = 298$ K

$\mathscr{P}_A = 93.7$ cm^3-$g^{1/4}/s^{1/2}$-mol $\quad \mathscr{P}_B = 205.3$ cm^3-$g^{1/4}/s^{1/2}$-mol

$\mu_B = 0.6$ cP at 25°C $\quad v_B = 96$ cm^3/mol at 80°C

However, because formic acid is an organic acid, $\mathscr{P}_A$ is doubled to 187.4.

From (3-42),

$$(D_{AB})_\infty = 1.55 \times 10^{-8}\left[\frac{298^{1.29}(205.3^{0.5}/187.4^{0.42})}{0.6^{0.92}96^{0.23}}\right]$$

$$= 2.15 \times 10^{-5} \text{ cm}^2/\text{s}$$

which is within 6% of the the experimental value.

The Stokes–Einstein and Wilke–Chang equations predict an inverse dependence of liquid diffusivity with viscosity. The Hayduk–Minhas equations predict a somewhat smaller dependence on viscosity. From data covering several orders of magnitude variation of viscosity, the liquid diffusivity is found to vary inversely with the viscosity raised to an exponent closer to 0.5 than to 1.0. The Stokes–Einstein and Wilke–Chang equations also predict that $D_{AB}\mu_B/T$ is a constant over a narrow temperature range. Because μ_B decreases exponentially with temperature, D_{AB} is predicted to increase exponentially with temperature. For example, for a dilute solution of water in ethanol, the diffusivity of water increases by a factor of almost 20 when the absolute temperature is increased 50%. Over a wide temperature range, it is preferable to express the effect of temperature on D_{AB} by an Arrhenius-type expression,

$$(D_{AB})_\infty = A \exp\left(\frac{-E}{RT}\right) \tag{3-44}$$

where, typically the activation energy for liquid diffusion, E, is no greater than 6,000 cal/mol.

Equations (3-39), (3-40), and (3-42) for estimating diffusivity in binary liquid mixtures only apply to the solute, A, in a dilute solution of the solvent, B. Unlike binary gas mixtures in which the diffusivity is almost independent of composition, the effect of composition on liquid diffusivity is complex, sometimes showing strong positive or negative deviations from linearity with mole fraction.

Based on a nonideal form of Fick's law, Vignes [9] has shown that, except for strongly associated binary mixtures such as chloroform/acetone, which exhibit a rare negative deviation from Raoult's law, infinite-dilution binary diffusivities, $(D)_\infty$, can be combined with mixture activity-coefficient data or correlations thereof to predict liquid binary diffusion coefficients D_{AB} and D_{BA} over the entire composition range. The Vignes equations are:

$$D_{AB} = (D_{AB})_\infty^{x_B}(D_{BA})_\infty^{x_A}\left(1 + \frac{\partial \ln \gamma_A}{\partial \ln x_A}\right)_{T,P} \tag{3-45}$$

$$D_{BA} = (D_{BA})_\infty^{x_A}(D_{AB})_\infty^{x_B}\left(1 + \frac{\partial \ln \gamma_B}{\partial \ln x_B}\right)_{T,P} \tag{3-46}$$

EXAMPLE 3.7

At 298 K and 1 atm, infinite-dilution diffusion coefficients for the methanol (A)/water (B) system are 1.5×10^{-5} cm^2/s and 1.75×10^{-5} cm^2/s for AB and BA, respectively.

Activity-coefficient data for the same conditions as estimated from the UNIFAC method are as follows:

x_A	γ_A	x_B	γ_B
0.0	2.245	1.0	1.000
0.1	1.748	0.9	1.013
0.2	1.470	0.8	1.044
0.3	1.300	0.7	1.087
0.4	1.189	0.6	1.140
0.5	1.116	0.5	1.201
0.6	1.066	0.4	1.269
0.7	1.034	0.3	1.343
0.8	1.014	0.2	1.424
0.9	1.003	0.1	1.511
1.0	1.000	0.0	1.605

Use the Vignes equations to estimate diffusion coefficients over the entire composition range.

SOLUTION

Using a spreadsheet to compute the derivatives in (3-45) and (3-46), which are found to be essentially equal at any composition, and the diffusivities from the same equations, the following results are obtained with $D_{AB} = D_{BA}$ at each composition. The calculations show a minimum diffusivity at a methanol mole fraction of 0.30.

x_A	D_{AB}, cm^2/s	D_{BA}, cm^2/s
0.20	1.10×10^{-5}	1.10×10^{-5}
0.30	1.08×10^{-5}	1.08×10^{-5}
0.40	1.12×10^{-5}	1.12×10^{-5}
0.50	1.18×10^{-5}	1.18×10^{-5}
0.60	1.28×10^{-5}	1.28×10^{-5}
0.70	1.38×10^{-5}	1.38×10^{-5}
0.80	1.50×10^{-5}	1.50×10^{-5}

If the diffusivity is assumed linear with mole fraction, the value at $x_A = 0.50$ is 1.625×10^{-5}, which is almost 40% higher than the predicted value of 1.18×10^{-5}.

Diffusivities of Electrolytes

In an electrolyte solute, the diffusion coefficient of the dissolved salt, acid, or base depends on the ions, since they are the diffusing entities. However, in the absence of an electric potential, only the molecular diffusion of the electrolyte molecule is of interest. The infinite-dilution diffusivity of a single salt in an aqueous solution in cm^2/s can be estimated from the Nernst–Haskell equation:

$$(D_{AB})_\infty = \frac{RT[(1/n_+) + (1/n_-)]}{F^2[(1/\lambda_+) + (1/\lambda_-)]} \tag{3-47}$$

where

n_+ and n_- = valences of the cation and anion, respectively

λ_+ and λ_- = limiting ionic conductances in (A/cm^2)(V/cm)(g-equiv/cm^3), where A = amps and V = volts

F = Faraday's constant = 96,500 coulombs/g-equiv

T = temperature, K

R = gas constant = 8.314 J/mol-K

Values of λ_+ and λ_- at 25°C are listed in Table 3.7. At other temperatures, these values are multiplied by $T/334\mu_B$,

Table 3.7 Limiting Ionic Conductances in Water at 25°C, in $(A/cm^2)(V/cm)(g\text{-}equiv/cm^3)$

Anion	λ_-	Cation	λ_+
OH^-	197.6	H^+	349.8
Cl^-	76.3	Li^+	38.7
Br^-	78.3	Na^+	50.1
I^-	76.8	K^+	73.5
NO_3^-	71.4	NH_4^+	73.4
ClO_4^-	68.0	Ag^+	61.9
HCO_3^-	44.5	Tl^+	74.7
HCO_2^-	54.6	$(\frac{1}{2})Mg^{2+}$	53.1
$CH_3CO_2^-$	40.9	$(\frac{1}{2})Ca^{2+}$	59.5
$ClCH_2CO_2^-$	39.8	$(\frac{1}{2})Sr^{2+}$	50.5
$CNCH_2CO_2^-$	41.8	$(\frac{1}{2})Ba^{2+}$	63.6
$CH_3CH_2CO_2^-$	35.8	$(\frac{1}{2})Cu^{2+}$	54
$CH_3(CH_2)_2CO_2^-$	32.6	$(\frac{1}{2})Zn^{2+}$	53
$C_6H_5CO_2^-$	32.3	$(\frac{1}{3})La^{3+}$	69.5
$HC_2O_4^-$	40.2	$(\frac{1}{3})Co(NH_3)_6^{3+}$	102
$(\frac{1}{2})C_2O_4^{2-}$	74.2		
$(\frac{1}{2})SO_4^{2-}$	80		
$(\frac{1}{3})Fe(CN)_6^{3-}$	101		
$(\frac{1}{4})Fe(CN)_6^{4-}$	111		

Source: Poling, Prausnitz, and O'Connell [2].

where T and μ_B are in kelvins and centipoise, respectively. As the concentration of the electrolyte increases, the diffusivity at first decreases rapidly by about 10% to 20% and then rises to values at a concentration of 2 N (normal) that approximate the infinite-dilution value. Some representative experimental values from Volume V of the International Critical Tables are given in Table 3.8.

Table 3.8 Experimental Diffusivities of Electrolytes in Aqueous Solutions

Solute	Concentration, Mol/L	Temperature, °C	Diffusivity, D_{AB}, $cm^2/s \times 10^5$
HCl	0.1	12	2.29
HNO_3	0.05	20	2.62
	0.25	20	2.59
H_2SO_4	0.25	20	1.63
KOH	0.01	18	2.20
	0.1	18	2.15
	1.8	18	2.19
NaOH	0.05	15	1.49
NaCl	0.4	18	1.17
	0.8	18	1.19
	2.0	18	1.23
KCl	0.4	18	1.46
	0.8	18	1.49
	2.0	18	1.58
$MgSO_4$	0.4	10	0.39
$Ca(NO_3)_2$	0.14	14	0.85

EXAMPLE 3.8

Estimate the diffusivity of KCl in a dilute solution of water at 18.5°C. The experimental value is 1.7×10^{-5} cm^2/s. At concentrations up to 2N, this value varies only from 1.5×10^{-5} to 1.75×10^{-5} cm^2/s.

SOLUTION

At 18.5°C, $T/334\mu = 291.7/[(334)(1.05)] = 0.832$. Using Table 3.7, at 25°C, the corrected limiting ionic conductances are

$$\lambda_+ = 73.5(0.832) = 61.2 \quad \text{and} \quad \lambda_- = 76.3(0.832) = 63.5$$

From (3-47),

$$D_\infty = \frac{(8.314)(291.7)[(1/1)+(1/1)]}{96{,}500^2[(1/61.2)+(1/63.5)]} = 1.62 \times 10^{-5} cm^2/s$$

which is close to the experimental value.

Diffusivity of Biological Solutes in Liquids

For dilute, aqueous, nonelectrolyte solutions, the Wilke–Chang equation (3-39) can be used for small solute molecules of liquid molar volumes up to 500 cm^3/mol, which corresponds to molecular weights to almost 600. In biological applications, diffusivities of water-soluble protein macromolecules having molecular weights greater than 1,000 are of interest. In general, molecules with molecular weights to 500,000 have diffusivities at 25°C that range from 1×10^{-7} to 8×10^{-7} cm^2/s, which is two orders of magnitude smaller than values of diffusivity for molecules with molecular weights less than 1,000. Data for many globular and fibrous protein macromolecules are tabulated by Sorber [10] with a few diffusivities given in Table 3.9. In the absence of data, the following semiempirical equation given by Geankoplis [11] and patterned after the Stokes–Einstein equation can be used:

$$D_{AB} = \frac{9.4 \times 10^{-15} T}{\mu_B (M_A)^{1/3}} \tag{3-48}$$

where the units are those of (3-39).

Also of interest in biological applications are diffusivities of small, nonelectrolyte molecules in aqueous gels containing up to 10 wt% of molecules such as certain polysaccharides (agar), which have a great tendency to swell. Diffusivities are given by Friedman and Kraemer [12]. In general, the diffusivities of small solute molecules in gels are not less than 50% of the values for the diffusivity of the solute in water, with values decreasing with increasing weight percent of gel.

Diffusivity in Solids

Diffusion in solids takes place by different mechanisms depending on the diffusing atom, molecule, or ion; the nature of the solid structure, whether it be porous or nonporous,

Table 3.9 Experimental Diffusivities of Large Biological Proteins in Aqueous Solutions

Protein	MW	Configuration	Temperature, °C	Diffusivity, D_{AB}, $cm^2/s \times 10^5$
Bovine serum albumin	67,500	globular	25	0.0681
γ–Globulin, human	153,100	globular	20	0.0400
Soybean protein	361,800	globular	20	0.0291
Urease	482,700	globular	25	0.0401
Fibrinogen, human	339,700	fibrous	20	0.0198
Lipoxidase	97,440	fibrous	20	0.0559

crystalline, or amorphous; and the type of solid material, whether it be metallic, ceramic, polymeric, biological, or cellular. Crystalline materials may be further classified according to the type of bonding, as molecular, covalent, ionic, or metallic, with most inorganic solids being ionic. However, ceramic materials can be ionic, covalent, or most often a combination of the two. Molecular solids have relatively weak forces of attraction among the atoms or molecules. In covalent solids, such as quartz silica, two atoms share two or more electrons equally. In ionic solids, such as inorganic salts, one atom loses one or more of its electrons by transfer to one or more other atoms, thus forming ions. In metals, positively charged ions are bonded through a field of electrons that are free to move. Unlike diffusion coefficients in gases and low-molecular-weight liquids, which each cover a range of only one or two orders of magnitude, diffusion coefficients in solids cover a range of many orders of magnitude. Despite the great complexity of diffusion in solids, Fick's first law can be used to describe diffusion if a measured diffusivity is available. However, when the diffusing solute is a gas, its solubility in the solid must also be known. If the gas dissociates upon dissolution in the solid, the concentration of the dissociated species must be used in Fick's law. In this section, many of the mechanisms of diffusion in solids are mentioned, but because they are exceedingly complex to quantify, the mechanisms are considered only qualitatively. Examples of diffusion in solids are considered, together with measured diffusion coefficients that can be used with Fick's first law. Emphasis is on diffusion of gas and liquid solutes through or into the solid, but movement of the atoms, molecules, or ions of the solid through itself is also considered.

Porous Solids

When solids are porous, predictions of the diffusivity of gaseous and liquid solute species in the pores can be made. These methods are considered only briefly here, with details deferred to Chapters 14, 15, and 16, where applications are made to membrane separations, adsorption, and leaching. This type of diffusion is also of great importance in the analysis and design of reactors using porous solid catalysts. It is sufficient to mention here that any of the following four mass-transfer mechanisms or combinations thereof may take place:

1. Ordinary molecular diffusion through pores, which present tortuous paths and hinder the movement of large molecules when their diameter is more than 10% of the pore diameter
2. Knudsen diffusion, which involves collisions of diffusing gaseous molecules with the pore walls when the pore diameter and pressure are such that the molecular mean free path is large compared to the pore diameter
3. Surface diffusion involving the jumping of molecules, adsorbed on the pore walls, from one adsorption site to another based on a surface concentration-driving force
4. Bulk flow through or into the pores

When treating diffusion of solutes in porous materials where diffusion is considered to occur only in the fluid in the pores, it is common to refer to an effective diffusivity, D_{eff}, which is based on (1) the total cross-sectional area of the porous solid rather than the cross-sectional area of the pore and (2) on a straight path, rather than the pore path, which may be tortuous. If pore diffusion occurs only by ordinary molecular diffusion, Fick's law (3-3) can be used with an effective diffusivity. The effective diffusivity for a binary mixture can be expressed in terms of the ordinary diffusion coefficient, D_{AB}, by

$$D_{eff} = \frac{D_{AB}\epsilon}{\tau} \tag{3-49}$$

where ϵ is the fractional porosity (typically 0.5) of the solid and τ is the pore-path tortuosity (typically 2 to 3), which is the ratio of the pore length to the length if the pore were straight in the direction of diffusion. The effective diffusivity is either determined experimentally, without knowledge of the porosity or tortuosity, or predicted from (3-49) based on measurement of the porosity and tortuosity and use of the predictive methods for ordinary molecular diffusivity. As an example of the former, Boucher, Brier, and Osburn [13] measured effective diffusivities for the leaching of processed soybean oil (viscosity = 20.1 cP at 120°F) from 1/16-in.-thick porous clay plates with liquid tetrachloroethylene solvent. The rate of extraction was controlled by the rate of diffusion of the soybean oil in the clay plates. The measured value of

D_{eff} was 1.0×10^{-6} cm^2/s. As might be expected from the effects of porosity and tortuosity, the effective value is about one order of magnitude less than the expected ordinary molecular diffusivity, D, of oil in the solvent.

Crystalline Solids

Diffusion through nonporous crystalline solids depends markedly on the crystal lattice structure and the diffusing entity. As discussed in Chapter 17 on crystallization, only seven different lattice structures are possible. For the cubic lattice (simple, body-centered, and face-centered), the diffusivity is the same in all directions (isotropic). In the six other lattice structures (including hexagonal and tetragonal), the diffusivity can be different in different directions (anisotropic). Many metals, including Ag, Al, Au, Cu, Ni, Pb, and Pt, crystallize into the face-centered cubic lattice structure. Others, including Be, Mg, Ti, and Zn, form anisotropic, hexagonal structures. The mechanisms of diffusion in crystalline solids include:

1. Direct exchange of lattice position by two atoms or ions, probably by a ring rotation involving three or more atoms or ions
2. Migration by small solutes through interlattice spaces called interstitial sites
3. Migration to a vacant site in the lattice
4. Migration along lattice imperfections (dislocations), or gain boundaries (crystal interfaces)

Diffusion coefficients associated with the first three mechanisms can vary widely and are almost always at least one order of magnitude smaller than diffusion coefficients in low-viscosity liquids. As might be expected, diffusion by the fourth mechanism can be faster than by the other three mechanisms. Typical experimental diffusivity values, taken mainly from Barrer [14], are given in Table 3.10. The diffusivities cover gaseous, ionic, and metallic solutes. The values cover an enormous 26-fold range. Temperature effects can be extremely large.

Metals

Important practical applications exist for diffusion of light gases through metals. To diffuse through a metal, a gas must first dissolve in the metal. As discussed by Barrer [14], all light gases do not dissolve in all metals. For example, hydrogen dissolves in such metals as Cu, Al, Ti, Ta, Cr, W, Fe, Ni, Pt, and Pd, but not in Au, Zn, Sb, and Rh. Nitrogen dissolves in Zr, but not in Cu, Ag, or Au. The noble gases do not dissolve in any of the common metals. When H_2, N_2, and O_2 dissolve in metals, they dissociate and may react to form hydrides, nitrides, and oxides, respectively. More complex molecules such as ammonia, carbon dioxide, carbon monoxide, and sulfur dioxide also dissociate. The following example illustrates how pressurized hydrogen gas can slowly leak through the wall of a small, thin pressure vessel.

Table 3.10 Diffusivities of Solutes in Crystalline Metals and Salts

Metal/Salt	Solute	T, °C	D, cm^2/s
Ag	Au	760	3.6×10^{-10}
	Sb	20	3.5×10^{-21}
	Sb	760	1.4×10^{-9}
Al	Fe	359	6.2×10^{-14}
	Zn	500	2×10^{-9}
	Ag	50	1.2×10^{-9}
Cu	Al	20	1.3×10^{-30}
	Al	850	2.2×10^{-9}
	Au	750	2.1×10^{-11}
Fe	H_2	10	1.66×10^{-9}
	H_2	100	1.24×10^{-7}
	C	800	1.5×10^{-8}
Ni	H_2	85	1.16×10^{-8}
	H_2	165	1.05×10^{-7}
	CO	950	4×10^{-8}
W	U	1727	1.3×10^{-11}
AgCl	Ag^+	150	2.5×10^{-14}
	Ag^+	350	7.1×10^{-8}
	Cl^-	350	3.2×10^{-16}
KBr	H_2	600	5.5×10^{-4}
	Br_2	600	2.64×10^{-4}

EXAMPLE 3.9

Gaseous hydrogen at 200 psia and 300°C is stored in a small, 10-cm-diameter, steel pressure vessel having a wall thickness of 0.125 in. The solubility of hydrogen in steel, which is proportional to the square root of the hydrogen partial pressure in the gas, is equal to 3.8×10^{-6} mol/cm^3 at 14.7 psia and 300°C. The diffusivity of hydrogen in steel at 300°C is 5×10^{-6} cm^2/s. If the inner surface of the vessel wall remains saturated at the existing hydrogen partial pressure and the hydrogen partial pressure at the outer surface is zero, estimate the time, in hours, for the pressure in the vessel to decrease to 100 psia because of hydrogen loss by dissolving in and diffusing through the metal wall.

SOLUTION

Integrating Fick's first law, (3-3), where A is H_2 and B is the metal, assuming a linear concentration gradient, and equating the flux to the loss of hydrogen in the vessel,

$$-\frac{dn_A}{dt} = \frac{D_{AB} A \Delta c_A}{\Delta z} \tag{1}$$

Because $p_A = 0$ outside the vessel, $\Delta c_A = c_A$ = solubility of A at the inside wall surface in mol/cm^3 and $c_A = 3.8 \times 10^{-6}\left(\frac{p_A}{14.7}\right)^{0.5}$, where p_A is the pressure of A in psia inside the vessel. Let p_{A_o} and n_{A_o} be the initial pressure and moles of A, respectively, in the vessel. Assuming the ideal-gas law and isothermal conditions,

$$n_A = n_{A_o} p_A / p_{A_o} \tag{2}$$

Differentiating (2) with respect to time,

$$\frac{dn_A}{dt} = \frac{n_{A_o}}{p_{A_o}} \frac{dp_A}{dt} \tag{3}$$

Combining (1) and (3),

$$\frac{dp_A}{dt} = -\frac{D_A A(3.8 \times 10^{-6}) p_A^{0.5} p_{A_o}}{n_{A_o} \Delta z (14.7)^{0.5}} \tag{4}$$

Integrating and solving for t,

$$t = \frac{2n_{A_o} \Delta z (14.7)^{0.5}}{3.8 \times 10^{-6} D_A A p_{A_o}} \left(p_{A_o}^{0.5} - p_A^{0.5}\right)$$

Assuming the ideal-gas law,

$$n_{A_o} = \frac{(200/14.7)[(3.14 \times 10^3)/6)]}{82.05(300 + 273)} = 0.1515 \text{ mol}$$

The mean-spherical shell area for mass transfer, A, is

$$A = \frac{3.14}{2}[(10)^2 + (10.635)^2] = 336 \text{ cm}^2$$

The time for the pressure to drop to 100 psia is

$$t = \frac{2(0.1515)(0.125 \times 2.54)(14.7)^{0.5}}{3.8 \times 10^{-6}(5 \times 10^{-6})(336)(200)}(200^{0.5} - 100^{0.5})$$
$$= 1.2 \times 10^6 \text{ s} = 332 \text{ h}$$

Silica and Glass

Another area of great interest is the diffusion of light gases through various forms of silica, whose two elements, Si and O, make up about 60% of the earth's crust. Solid silica can exist in three principal crystalline forms (quartz, tridymite, and cristobalite) and in various stable amorphous forms, including vitreous silica (a noncrystalline silicate glass or fused quartz). Table 3.11 includes diffusivities, D, and solubilities as Henry's law constants, H, at 1 atm for helium and hydrogen in fused quartz as calculated from correlations of experimental data by Swets, Lee, and Frank [15] and Lee [16], respectively. The product of the diffusivity and the solubility is called the permeability, P_M. Thus,

$$P_M = DH \tag{3-50}$$

Unlike metals, where hydrogen usually diffuses as the atom, hydrogen apparently diffuses as a molecule in glass.

Table 3.11 Diffusivities and Solubilities of Gases in Amorphous Silica at 1 atm

Gas	Temp, C	Diffusivity, cm^2/s	Solubility mol/cm^3-atm
He	24	2.39×10^{-8}	1.04×10^{-7}
	300	2.26×10^{-6}	1.82×10^{-7}
	500	9.99×10^{-6}	9.9×10^{-8}
	1,000	5.42×10^{-5}	1.34×10^{-7}
H_2	300	6.11×10^{-8}	3.2×10^{-14}
	500	6.49×10^{-7}	2.48×10^{-13}
	1,000	9.26×10^{-6}	2.49×10^{-12}
O_2	1,000	6.25×10^{-9} (molecular)	
	1,000	9.43×10^{-15} (network)	

For both hydrogen and helium, diffusivities increase rapidly with increasing temperature. At ambient temperature the diffusivities are three orders of magnitude lower than in liquids. At elevated temperatures the diffusivities approach those observed in liquids. Solubilities vary only slowly with temperature. Hydrogen is orders of magnitude less soluble in glass than helium. For hydrogen, the diffusivity is somewhat lower than in metals. Diffusivities for oxygen are also included in Table 3.11 from studies by Williams [17] and Sucov [18]. At 1000°C, the two values differ widely because, as discussed by Kingery, Bowen, and Uhlmann [19], in the former case, transport occurs by molecular diffusion; while in the latter case, transport is by slower network diffusion as oxygen jumps from one position in the silicate network to another. The activation energy for the latter is much larger than for the former (71,000 cal/mol versus 27,000 cal/mol). The choice of glass can be very critical in high-vacuum operations because of the wide range of diffusivity.

Ceramics

Diffusion rates of light gases and elements in crystalline ceramics are very important because diffusion must precede chemical reactions and causes changes in the microstructure. Therefore, diffusion in ceramics has been the subject of numerous studies, many of which are summarized in Figure 3.4, taken from Kingery et al. [19], where diffusivity is plotted as a function of the inverse of temperature in the high-temperature range. In this form, the slopes of the curves are proportional to the activation energy for diffusion, E, where

$$D = D_o \exp\left(-\frac{E}{RT}\right) \tag{3-51}$$

An insert at the middle-right region of Figure 3.4 relates the slopes of the curves to activation energy. The diffusivity curves cover a ninefold range from 10^{-6} to 10^{-15} cm^2/s, with the largest values corresponding to the diffusion of potassium in β-Al_2O_3 and one of the smallest values for carbon in graphite. In general, the lower the diffusivity, the higher is the activation energy. As discussed in detail by Kingery et al. [19], diffusion in crystalline oxides depends not only on temperature but also on whether the oxide is stoichiometric or not (e.g., FeO and $Fe_{0.95}O$) and on impurities. Diffusion through vacant sites of nonstoichiometric oxides is often classified as metal-deficient or oxygen-deficient. Impurities can hinder diffusion by filling vacant lattice or interstitial sites.

Polymers

Thin, dense, nonporous polymer membranes are widely used to separate gas and liquid mixtures. As discussed in detail in Chapter 14, diffusion of gas and liquid species through polymers is highly dependent on the type of polymer, whether it be crystalline or amorphous and, if the latter, glassy or rubbery. Commercial crystalline polymers are

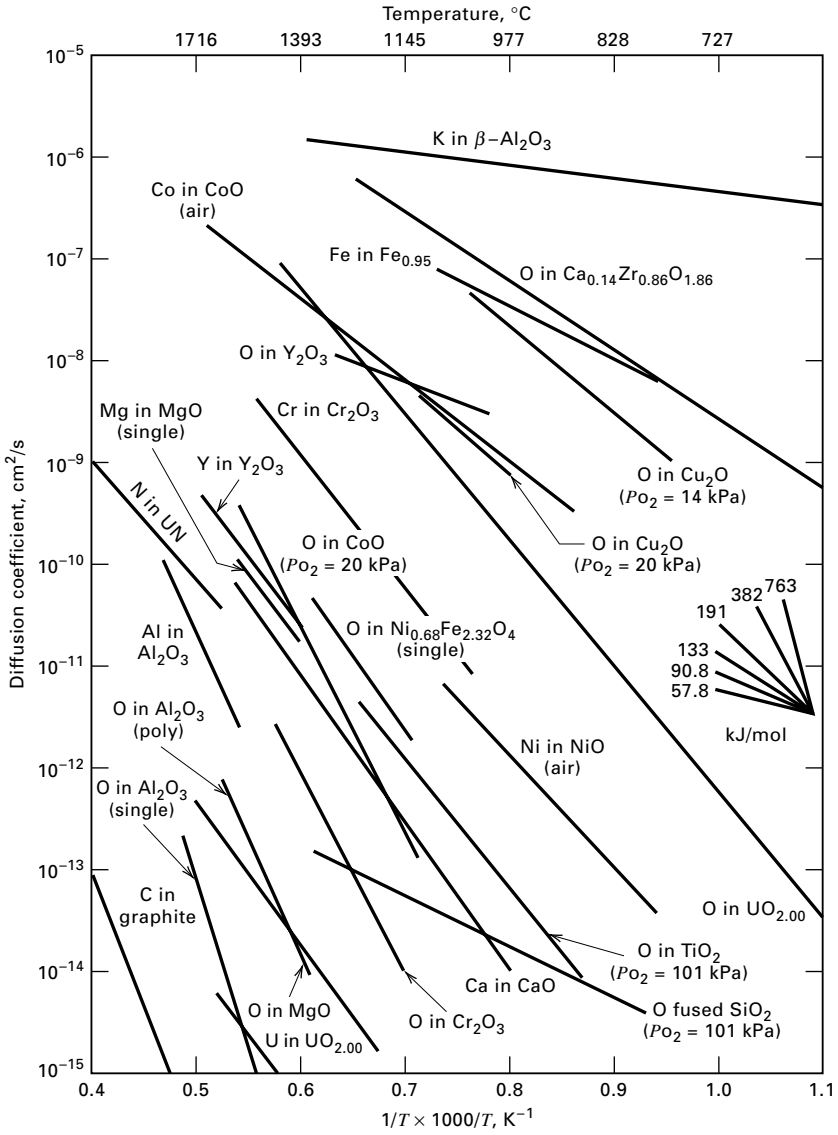

Figure 3.4 Diffusion coefficients for single- and polycrystalline ceramics.
[From W.D. Kingery, H.K. Bowen, and D.R. Uhlmann, *Introduction to Ceramics,* 2nd ed., Wiley Interscience, New York (1976) with permission.]

about 20% amorphous. It is mainly through the amorphous regions that diffusion occurs. As with the transport of gases through metals, transport of gaseous species through polymer membranes is usually characterized by the solution-diffusion mechanism of (3-50). Fick's first law, in the following integrated forms, is then applied to compute the mass transfer flux.

Gas species:

$$N_i = \frac{H_i D_i}{z_2 - z_1}(p_{i_1} - p_{i_2}) = \frac{P_{M_i}}{z_2 - z_1}(p_{i_1} - p_{i_2}) \qquad (3\text{-}52)$$

where p_i is the partial pressure of the gas species at a polymer surface.

Liquid species:

$$N_i = \frac{K_i D_i}{z_2 - z_1}(c_{i_1} - c_{i_2}) \qquad (3\text{-}53)$$

where K_i, the equilibrium partition coefficient, is equal to the ratio of the concentration in the polymer to the concentration, c_i, in the liquid adjacent to the polymer surface. The product $K_i D_i$ is the liquid permeability.

Values of diffusivity for light gases in four polymers, given in Table 14.6, range from 1.3×10^{-9} to 1.6×10^{-6} cm^2/s, which is orders of magnitude less than for diffusion of the same species in a gas.

Diffusivities of liquids in rubbery polymers have been studied extensively as a means of determining viscoelastic parameters. In Table 3.12, taken from Ferry [20], diffusivities are given for different solutes in seven different rubber polymers at near-ambient conditions. The values cover a sixfold range, with the largest diffusivity being that for *n*-hexadecane in polydimethylsiloxane. The smallest diffusivities correspond to the case where the temperature is approaching the glass-transition temperature, where the polymer becomes glassy in structure. This more rigid structure hinders diffusion. In general, as would be expected,

Table 3.12 Diffusivities of Solutes in Rubbery Polymers

Polymer	Solute	Temperature, K	Diffusivity, cm^2/s
Polyisobutylene	*n*-Butane	298	1.19×10^{-9}
	i-Butane	298	5.3×10^{-10}
	n-Pentane	298	1.08×10^{-9}
	n-Hexadecane	298	6.08×10^{-10}
Hevea rubber	*n*-Butane	303	2.3×10^{-7}
	i-Butane	303	1.52×10^{-7}
	n-Pentane	303	2.3×10^{-7}
	n-Hexadecane	298	7.66×10^{-8}
Polymethylacrylate	Ethyl alcohol	323	2.18×10^{-10}
Polyvinylacetate	*n*-Propyl alcohol	313	1.11×10^{-12}
	n-Propyl chloride	313	1.34×10^{-12}
	Ethyl chloride	343	2.01×10^{-9}
	Ethyl bromide	343	1.11×10^{-9}
Polydimethylsiloxane	*n*-Hexadecane	298	1.6×10^{-6}
1,4-Polybutadiene	*n*-Hexadecane	298	2.21×10^{-7}
Styrene-butadiene rubber	*n*-Hexadecane	298	2.66×10^{-8}

smaller molecules have higher diffusivities. A more detailed study of the diffusivity of *n*-hexadecane in random styrene/butadiene copolymers at 25°C by Rhee and Ferry [21] shows a large effect on diffusivity of fractional free volume in the polymer.

Diffusion and permeability in crystalline polymers depend on the degree of crystallinity. Polymers that are 100% crystalline permit little or no diffusion of gases and liquids. For example, the diffusivity of methane at 25°C in polyoxyethylene oxyisophthaloyl decreases from 0.30×10^{-9} to 0.13×10^{-9} cm^2/s when the degree of crystallinity increases from 0 (totally amorphous) to 40% [22]. A measure of crystallinity is the polymer density. The diffusivity of methane at 25°C in polyethylene decreases from 0.193×10^{-6} to 0.057×10^{-6} cm^2/s when the specific gravity increases from 0.914 (low density) to 0.964 (high density) [22]. A plasticizer can cause the diffusivity to increase. For example, when polyvinylchloride is plasticized with 40% tricresyl triphosphate, the diffusivity of CO at 27°C increases from 0.23×10^{-8} to 2.9×10^{-8} cm^2/s [22].

EXAMPLE 3.10

Hydrogen diffuses through a nonporous polyvinyltrimethylsilane membrane at 25°C. The pressures on the sides of the membrane are 3.5 MPa and 200 kPa. Diffusivity and solubility data are given in Table 14.9. If the hydrogen flux is to be 0.64 kmol/m^2-h, how thick in micrometers should the membrane be?

SOLUTION

Equation (3-52) applies. From Table 14.9,

$$D = 160 \times 10^{-11}\ m^2/s \qquad H = S = 0.54 \times 10^{-4}\ mol/m^3\text{-Pa}$$

From (3-50),

$$P_M = DH = (160 \times 10^{-11})(0.54 \times 10^{-4}) = 86.4 \times 10^{-15}\ \text{mol/m-s-Pa}$$

$$p_1 = 3.5 \times 10^6\ \text{Pa} \quad p_2 = 0.2 \times 10^6\ \text{Pa}$$

$$\text{Membrane thickness} = z_2 - z_1 = \Delta z = P_M(p_1 - p_2)/N$$

$$\Delta z = \frac{86.4 \times 10^{-15}(3.5 \times 10^6 - 0.2 \times 10^6)}{[0.64(1000)/3600]} = 1.6 \times 10^{-6}\ \text{m} = 1.6\,\mu\text{m}$$

As discussed in Chapter 14, polymer membranes must be very thin to achieve reasonable gas permeation rates.

Cellular Solids and Wood

As discussed by Gibson and Ashby [23], cellular solids consist of solid struts or plates that form edges and faces of cells, which are compartments or enclosed spaces. Cellular solids such as wood, cork, sponge, and coral exist in nature. Synthetic cellular structures include honeycombs, and foams (some with open cells) made from polymers, metals, ceramics, and glass. The word *cellulose* means "full of little cells."

A widely used cellular solid is wood, whose annual world production of the order of 10^{12} kg is comparable to the production of iron and steel. Chemically, wood consists of lignin, cellulose, hemicellulose, and minor amounts of organic chemicals and elements. The latter are extractable, and the former three, which are all polymers, give wood its structure. Green wood also contains up to 25 wt% moisture in the cell walls and cell cavities. Adsorption or desorption of moisture in wood causes anisotropic swelling and shrinkage.

The structure of wood, which often consists of (1) highly elongated hexagonal or rectangular cells, called tracheids in softwood (coniferous species, e.g., spruce, pine, and fir) and fibers in hardwood (deciduous or broad-leaf species, e.g., oak, birch, and walnut); (2) radial arrays of rectangular-like cells, called rays, which are narrow and short in softwoods but wide and long in hardwoods; and (3) enlarged cells with large pore spaces and thin walls, called sap channels because they conduct fluids up the tree. The sap channels are less than 3 vol% of softwood, but as much as 55 vol% of hardwood.

Because the structure of wood is directional, many of its properties are anisotropic. For example, stiffness and strength are 2 to 20 times greater in the axial direction of the tracheids or fibers than in the radial and tangential directions of the trunk from which the wood is cut. This anisotropy extends to permeability and diffusivity of wood penetrants, such as moisture and preservatives. According to Stamm [24], the permeability of wood to liquids in the axial direction can be up to 10 times greater than in the transverse direction.

Movement of liquids and gases through wood and wood products takes time during drying and treatment with preservatives, fire retardants, and other chemicals. This movement takes place by capillarity, pressure permeability, and diffusion. Nevertheless, wood is not highly permeable because the cell voids are largely discrete and lack direct interconnections. Instead, communication among cells is through circular openings spanned by thin membranes with submicrometer-sized pores, called pits, and to a smaller extent, across the cell walls. Rays give wood some permeability in the radial direction. Sap channels do not contribute to permeability. All three mechanisms of movement of gases and liquids in wood are considered by Stamm [24]. Only diffusion is discussed here.

The simplest form of diffusion is that of a water-soluble solute through wood saturated with water, such that no dimensional changes occur. For the diffusion of urea, glycerine, and lactic acid into hardwood, Stamm [24] lists diffusivities in the axial direction that are about 50% of ordinary liquid diffusivities. In the radial direction, diffusivities are about 10% of the values in the axial direction. For example, at 26.7°C the diffusivity of zinc sulfate in water is 5×10^{-6} cm^2/s. If loblolly pine sapwood is impregnated with zinc sulfate in the radial direction, the diffusivity is found to be 0.18×10^{-6} cm^2/s [24].

The diffusion of water in wood is more complex. Moisture content determines the degree of swelling or shrinkage. Water is held in the wood in different ways: It may be physically adsorbed on cell walls in monomolecular layers, condensed in preexisting or transient cell capillaries, or absorbed in cell walls to form a solid solution.

Because of the practical importance of lumber drying rates, most diffusion coefficients are measured under drying conditions in the radial direction across the fibers. Results depend on temperature and swollen-volume specific gravity. Typical results are given by Sherwood [25] and Stamm [24]. For example, for beech with a swollen specific gravity of 0.4, the diffusivity increases from a value of about 1×10^{-6} cm^2/s at 10°C to 10×10^{-6} cm^2/s at 60°C.

3.3 ONE-DIMENSIONAL, STEADY-STATE AND UNSTEADY-STATE, MOLECULAR DIFFUSION THROUGH STATIONARY MEDIA

For conductive heat transfer in stationary media, Fourier's law is applied to derive equations for the rate of heat transfer for steady-state and unsteady-state conditions in shapes such as slabs, cylinders, and spheres. Many of the results are plotted in generalized charts. Analogous equations can be derived for mass transfer, using simplifying assumptions.

In one dimension, the molar rate of mass transfer of A in a binary mixture with B is given by a modification of (3-12), which includes bulk flow and diffusion:

$$n_A = x_A(n_A + n_B) - cD_{AB}A\left(\frac{dx_A}{dz}\right) \tag{3-54}$$

If A is a dissolved solute undergoing mass transfer, but B is stationary, $n_B = 0$. It is common to assume that c is a constant and x_A is small. The bulk-flow term is then eliminated and (3-54) accounts for diffusion only, becoming Fick's first law:

$$n_A = -cD_{AB}A\left(\frac{dx_A}{dz}\right) \tag{3-55}$$

Alternatively, (3-55) can be written in terms of concentration gradient:

$$n_A = -D_{AB}A\left(\frac{dc_A}{dz}\right) \tag{3-56}$$

This equation is analogous to Fourier's law for the rate of heat conduction, Q:

$$Q = -kA\left(\frac{dT}{dz}\right) \tag{3-57}$$

Steady State

For steady-state, one-dimensional diffusion, with constant D_{AB}, (3-56) can be integrated for various geometries, the most common results being analogous to heat conduction.

1. Plane wall with a thickness, $z_2 - z_1$:

$$n_A = D_{AB}A\left(\frac{c_{A_1} - c_{A_2}}{z_2 - z_1}\right) \tag{3-58}$$

2. Hollow cylinder of inner radius r_1 and outer radius r_2, with diffusion in the radial direction outward:

$$n_A = 2\pi L\frac{D_{AB}(c_{A_1} - c_{A_2})}{\ln(r_2/r_1)} \tag{3-59}$$

or

$$n_A = D_{AB}A_{LM}\left(\frac{c_{A_1} - c_{A_2}}{r_2 - r_1}\right) \tag{3-60}$$

where

A_{LM} = log mean of the areas $2\pi rL$ at r_1 and r_2

L = length of the hollow cylinder

3. Spherical shell of inner radius r_1 and outer radius r_2, with diffusion in the radial direction outward:

$$n_A = \frac{4\pi r_1 r_2 D_{AB}(c_{A_1} - c_{A_2})}{r_2 - r_1} \tag{3-61}$$

or

$$n_A = D_{AB} A_{GM} \left(\frac{c_{A_1} - c_{A_2}}{r_2 - r_1} \right) \tag{3-62}$$

where A_{GM} = geometric mean of the areas $4\pi r^2$ at r_1 and r_2.

When $r_1/r_2 < 2$, the arithmetic mean area is no more than 4% greater than the log mean area. When $r_1/r_2 < 1.33$, the arithmetic mean area is no more than 4% greater than the geometric mean area.

Unsteady State

Equation (3-56) is applied to unsteady-state molecular diffusion by considering the accumulation or depletion of a species with time in a unit volume through which the species is diffusing. Consider the one-dimensional diffusion of species A in B through a differential control volume with diffusion in the z-direction only, as shown in Figure 3.5. Assume constant total concentration, $c = c_A + c_B$, constant diffusivity, and negligible bulk flow. The molar flow rate of species A by diffusion at the plane $z = z$ is given by (3-56):

$$n_{A_z} = -D_{AB} A \left(\frac{\partial c_A}{\partial z} \right)_z \tag{3-63}$$

At the plane, $z = z + \Delta z$, the diffusion rate is

$$n_{A_{z+\Delta z}} = -D_{AB} A \left(\frac{\partial c_A}{\partial z} \right)_{z+\Delta z} \tag{3-64}$$

The accumulation of species A in the control volume is

$$A \frac{\partial c_A}{\partial t} \Delta z \tag{3-65}$$

Since rate in − rate out = accumulation,

$$-D_{AB} A \left(\frac{\partial c_A}{\partial z} \right)_z + D_{AB} A \left(\frac{\partial c_A}{\partial z} \right)_{z+\Delta z} = A \left(\frac{\partial c_A}{\partial t} \right) \Delta z \tag{3-66}$$

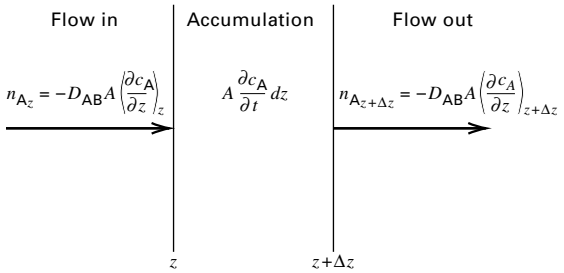

Figure 3.5 Unsteady-state diffusion through a differential volume $A\,dz$.

Rearranging and simplifying,

$$D_{AB} \left[\frac{(\partial c_A/\partial z)_{z+\Delta z} - (\partial c_A/\partial z)_z}{\Delta z} \right] = \frac{\partial c_A}{\partial t} \tag{3-67}$$

In the limit, as $\Delta z \to 0$,

$$\frac{\partial c_A}{\partial t} = D_{AB} \frac{\partial^2 c_A}{\partial z^2} \tag{3-68}$$

Equation (3-68) is Fick's second law for one-dimensional diffusion. The more general form, for three-dimensional rectangular coordinates, is

$$\frac{\partial c_A}{\partial t} = D_{AB} \left(\frac{\partial^2 c_A}{\partial x^2} + \frac{\partial^2 c_A}{\partial y^2} + \frac{\partial^2 c_A}{\partial z^2} \right) \tag{3-69}$$

For one-dimensional diffusion in the radial direction only, for cylindrical and spherical coordinates, Fick's second law becomes, respectively,

$$\frac{\partial c_A}{\partial t} = \frac{D_{AB}}{r} \frac{\partial}{\partial r} \left(r \frac{\partial c_A}{\partial r} \right) \tag{3-70}$$

and

$$\frac{\partial c_A}{\partial t} = \frac{D_{AB}}{r^2} \frac{\partial}{\partial r} \left(r^2 \frac{\partial c_A}{\partial r} \right) \tag{3-71}$$

Equations (3-68) to (3-71) are analogous to Fourier's second law of heat conduction where c_A is replaced by temperature, T, and diffusivity, D_{AB}, is replaced by thermal diffusivity, $\alpha = k/\rho C_P$. The analogous three equations for heat conduction for constant, isotropic properties are, respectively:

$$\frac{\partial T}{\partial t} = \alpha \left(\frac{\partial^2 T}{\partial x^2} + \frac{\partial^2 T}{\partial y^2} + \frac{\partial^2 T}{\partial z^2} \right) \tag{3-72}$$

$$\frac{\partial T}{\partial t} = \frac{\alpha}{r} \frac{\partial}{\partial r} \left(r \frac{\partial T}{\partial r} \right) \tag{3-73}$$

$$\frac{\partial T}{\partial t} = \frac{\alpha}{r^2} \frac{\partial}{\partial r} \left(r^2 \frac{\partial T}{\partial r} \right) \tag{3-74}$$

Analytical solutions to these partial differential equations in either Fick's law or Fourier's law form are available for a variety of boundary conditions. Many of these solutions are derived and discussed by Carslaw and Jaeger [26] and Crank [27]. Only a few of the more useful solutions are presented here.

Semi-infinite Medium

Consider the semi-infinite medium shown in Figure 3.6, which extends in the z-direction from $z = 0$ to $z = \infty$. The x and y coordinates extend from $-\infty$ to $+\infty$, but are not of interest because diffusion takes place only in the z-direction. Thus, (3-68) applies to the region $z \geq 0$. At time $t \leq 0$, the concentration is c_{A_o} for $z \geq 0$. At $t = 0$, the surface of the semi-infinite medium at $z = 0$ is instantaneously brought to the concentration $c_{A_s} > c_{A_o}$ and held there for $t > 0$. Therefore, diffusion into the medium occurs. However, because

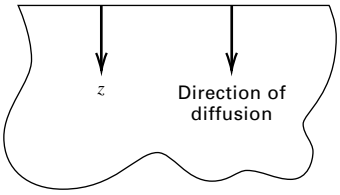

Figure 3.6 One-dimensional diffusion into a semi-infinite medium.

the medium is infinite in the z-direction, diffusion cannot extend to $z = \infty$ and, therefore, as $z \to \infty$, $c_A = c_{A_o}$ for all $t \geq 0$. Because the partial differential equation (3-68) and its one boundary (initial) condition in time and two boundary conditions in distance are linear in the dependent variable, c_A, an exact solution can be obtained. Either the method of combination of variables [28] or the Laplace transform method [29] is applicable. The result, in terms of the fractional accomplished concentration change, is

$$\theta = \frac{c_A - c_{A_o}}{c_{A_s} - c_{A_o}} = \text{erfc}\left(\frac{z}{2\sqrt{D_{AB}t}}\right) \tag{3-75}$$

where the complementary error function, erfc, is related to the error function, erf, by

$$\text{erfc}(x) = 1 - \text{erf}(x) = 1 - \frac{2}{\sqrt{\pi}}\int_0^x e^{-\eta^2} d\eta \tag{3-76}$$

The error function is included in most spreadsheet programs and handbooks, such as *Handbook of Mathematical Functions* [30]. The variation of erf(x) and erfc(x) is as follows:

x	erf(x)	erfc(x)
0	0.0000	1.0000
0.5	0.5205	0.4795
1.0	0.8427	0.1573
1.5	0.9661	0.0339
2.0	0.9953	0.0047
∞	1.0000	0.0000

Equation (3-75) is used to compute the concentration in the semi-infinite medium, as a function of time and distance from the surface, assuming no bulk flow. Thus, it applies most rigorously to diffusion in solids, and also to stagnant liquids and gases when the medium is dilute in the diffusing solute.

In (3-75), when $(z/2\sqrt{D_{AB}t}) = 2$, the complementary error function is only 0.0047, which represents less than a 1% change in the ratio of the concentration change at $z = z$ to the change at $z = 0$. Thus, it is common to refer to $z = 4\sqrt{D_{AB}t}$ as the penetration depth and to apply (3-75) to media of finite thickness as long as the thickness is greater than the penetration depth.

The instantaneous rate of mass transfer across the surface of the medium at $z = 0$ can be obtained by taking the derivative of (3-75) with respect to distance and substituting it into Fick's first law applied at the surface of the medium. Thus, using the Leibnitz rule for differentiating the integral of (3-76), with $x = z/2\sqrt{D_{AB}t}$,

$$\begin{aligned} n_A &= -D_{AB}A\left(\frac{\partial c_A}{\partial z}\right)_{z=0} \\ &= D_{AB}A\left(\frac{c_{A_s} - c_{A_o}}{\sqrt{\pi D_{AB}t}}\right)\exp\left(-\frac{z^2}{4D_{AB}t}\right)\Big|_{z=0} \end{aligned} \tag{3-77}$$

Thus,

$$n_A|_{z=0} = \sqrt{\frac{D_{AB}}{\pi t}}A(c_{A_s} - c_{A_o}) \tag{3-78}$$

We can also determine the total number of moles of solute, $\mathcal{N}_A$, transferred into the semi-infinite medium by integrating (3-78) with respect to time:

$$\begin{aligned} \mathcal{N}_A &= \int_o^t n_A|_{z=0}\, dt = \sqrt{\frac{D_{AB}}{\pi}}A(c_{A_s} - c_{A_o})\int_o^t \frac{dt}{\sqrt{t}} \\ &= 2A(c_{A_s} - c_{A_o})\sqrt{\frac{D_{AB}t}{\pi}} \end{aligned} \tag{3-79}$$

EXAMPLE 3.11

Determine how long it will take for the dimensionless concentration change, $\theta = (c_A - c_{A_o})/(c_{A_s} - c_{A_o})$, to reach 0.01 at a depth $z = 1$ m in a semi-infinite medium, which is initially at a solute concentration c_{A_o}, after the surface concentration at $z = 0$ increases to c_{A_s}, for diffusivities representative of a solute diffusing through a stagnant gas, a stagnant liquid, and a solid.

SOLUTION

For a gas, assume $D_{AB} = 0.1$ cm^2/s. We know that $z = 1$ m $= 100$ cm. From (3-75) and (3-76),

$$\theta = 0.01 = 1 - \text{erf}\left(\frac{z}{2\sqrt{D_{AB}t}}\right)$$

Therefore,

$$\text{erf}\left(\frac{z}{2\sqrt{D_{AB}t}}\right) = 0.99$$

From tables of the error function,

$$\left(\frac{z}{2\sqrt{D_{AB}t}}\right) = 1.8214$$

Solving,

$$t = \left[\frac{100}{1.8214(2)}\right]^2 \frac{1}{0.10} = 7{,}540 \text{ s} = 2.09 \text{ h}$$

In a similar manner, the times for typical gas, liquid, and solid media are:

Semi-infinite Medium	D_{AB}, cm^2/s	Time for $\theta = 0.01$ at 1 m
Gas	0.10	2.09 h
Liquid	1×10^{-5}	2.39 year
Solid	1×10^{-9}	239 centuries

These results show that molecular diffusion is very slow, especially in liquids and solids. In liquids and gases, the rate of mass

transfer can be greatly increased by agitation to induce turbulent motion. For solids, it is best to reduce the diffusion path to as small a dimension as possible by reducing the size of the solid.

Medium of Finite Thickness with Sealed Edges

Consider a rectangular, parallelepiped medium of finite thickness $2a$ in the z-direction, and either infinitely long dimensions in the y- and x-directions or finite lengths of $2b$ and $2c$, respectively, in those directions. Assume that in Figure 3.7a the edges parallel to the z-direction are sealed, so diffusion occurs only in the z-direction and initially the concentration of the solute in the medium is uniform at c_{A_o}. At time $t = 0$, the two unsealed surfaces of the medium at $z = \pm a$ are brought to and held at concentration $c_{A_s} > c_{A_o}$. Because of symmetry, $\partial c_A/\partial z = 0$ at $z = 0$. Assume constant D_{AB}. Again (3-68) applies, and an exact solution can be obtained because both (3-68) and the boundary conditions are linear in c_A. By the method of separation of variables [28] or the Laplace transform method [29], the result from Carslaw and Jaeger [26], in terms of the fractional, unaccomplished concentration change, E, is

$$E = 1 - \theta = \frac{c_{A_s} - c_A}{c_{A_s} - c_{A_o}} = \frac{4}{\pi}\sum_{n=0}^{\infty}\frac{(-1)^n}{(2n+1)} \times \exp[-D_{AB}(2n+1)^2\pi^2 t/4a^2]\cos\frac{(2n+1)\pi z}{2a} \tag{3-80}$$

or, in terms of the complementary error function,

$$E = 1 - \theta = \frac{c_{A_s} - c_A}{c_{A_s} - c_{A_o}} = \sum_{n=0}^{\infty}(-1)^n \times \left[\operatorname{erfc}\frac{(2n+1)a - z}{2\sqrt{D_{AB}t}} + \operatorname{erfc}\frac{(2n+1)a + z}{2\sqrt{D_{AB}t}}\right] \tag{3-81}$$

For large values of $D_{AB}t/a^2$, which is referred to as the Fourier number for mass transfer, the infinite series solutions of (3-80) and (3-81) converge rapidly, but for small values (e.g., short times), they do not. However, in the latter case, the solution for the semi-infinite medium applies for $D_{AB}t/a^2 < \frac{1}{16}$. A convenient plot of the exact solution is given in Figure 3.8.

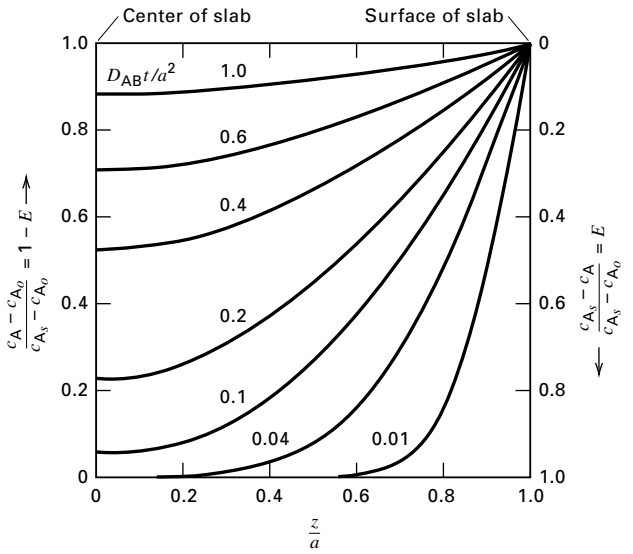

Figure 3.8 Concentration profiles for unsteady-state diffusion in a slab.

[Adapted from H.S. Carslaw and J.C. Jaeger, *Conduction of Heat in Solids,* 2nd ed., Oxford University Press, London (1959).]

The instantaneous rate of mass transfer across the surface of either unsealed face of the medium (i.e., at $z = \pm a$) is obtained by differentiating (3-80) with respect to z, evaluating the result at $z = a$, followed by substitution into Fick's first law to give

$$n_A|_{z=a} = \frac{2D_{AB}(c_{A_s} - c_{A_o})A}{a} \times \sum_{n=0}^{\infty}\exp\left[-\frac{D_{AB}(2n+1)^2\pi^2 t}{4a^2}\right] \tag{3-82}$$

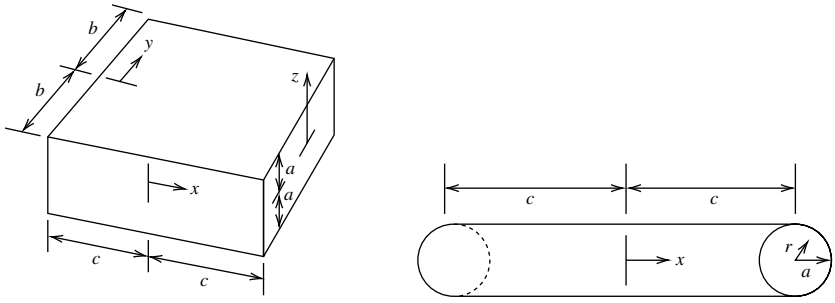

(a) Slab. Edges at $x = +c$ and $-c$ and at $y = +b$ and $-b$ are sealed.

(b) Cylinder. Two circular ends at $x = +c$ and $-c$ are sealed.

(c) Sphere

Figure 3.7 Unsteady-state diffusion in media of finite dimensions.

We can also determine the total number of moles transferred across either unsealed face by integrating (3-82) with respect to time. Thus,

$$\mathcal{N}_A = \int_o^t n_A|_{z=a}\, dt = \frac{8(c_{A_s} - c_{A_o})Aa}{\pi^2} \times \sum_{n=0}^{\infty} \frac{1}{(2n+1)^2} \left\{1 - \exp\left[-\frac{D_{AB}(2n+1)^2\pi^2 t}{4a^2}\right]\right\} \tag{3-83}$$

In addition, the average concentration of the solute in the medium, $c_{A_{avg}}$, as a function of time, can be obtained in the case of a slab from:

$$\frac{c_{A_s} - c_{A_{avg}}}{c_{A_s} - c_{A_o}} = \frac{\int_o^a (1-\theta)\, dz}{a} \tag{3-84}$$

Substitution of (3-80) into (3-84) followed by integration gives

$$E_{avg_{slab}} = (1-\theta_{ave})_{slab} = \frac{c_{A_s} - c_{A_{avg}}}{c_{A_s} - c_{A_o}} = \frac{8}{\pi^2} \sum_{n=0}^{\infty} \frac{1}{(2n+1)^2} \exp\left[-\frac{D_{AB}(2n+1)^2\pi^2 t}{4a^2}\right] \tag{3-85}$$

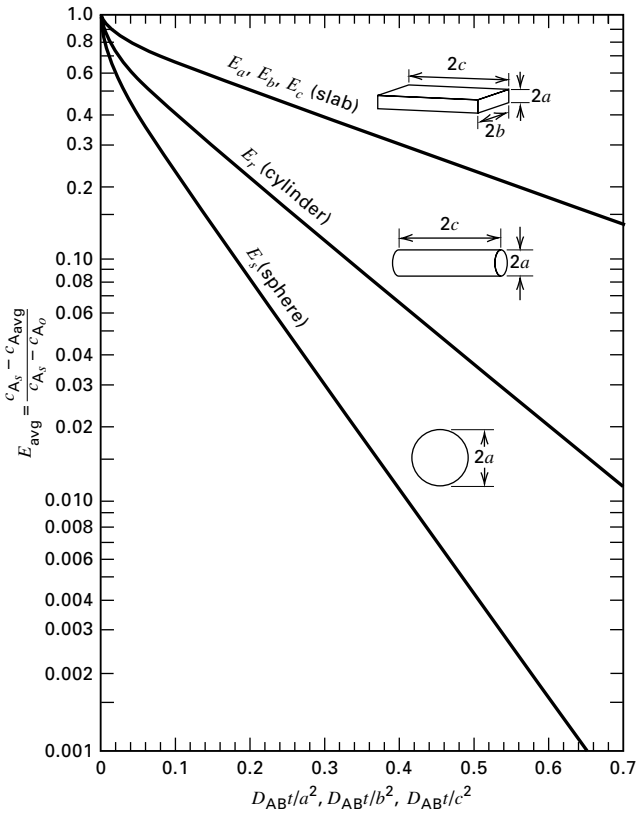

Figure 3.9 Average concentrations for unsteady-state diffusion.

[Adapted from R.E. Treybal, *Mass-Transfer Operations,* 3rd ed., McGraw-Hill, New York (1980).]

This equation is plotted in Figure 3.9. It is important to note that concentrations are in mass of solute per mass of dry solid or mass of solute/volume. This assumes that during diffusion the solid does not shrink or expand so that the mass of dry solid per unit volume of wet solid will remain constant. Then, we can substitute a concentration in terms of mass or moles of solute per mass of dry solid, i.e., the moisture content on the dry basis.

When the edges of the slab in Figure 3.7a are not sealed, the method of Newman [31] can be used with (3-69) to determine concentration changes within the slab. In this method, E or E_{avg} is given in terms of the E values from the solution of (3-68) for each of the coordinate directions by

$$E = E_x E_y E_z \tag{3-86}$$

Corresponding solutions for infinitely long, circular cylinders and spheres are available in Carslaw and Jaeger [26] and are plotted in Figures 3.9, 3.10, and 3.11, respectively. For a short cylinder, where the ends are not sealed, E or E_{ave} is given by the method of Newman as

$$E = E_r E_x \tag{3-87}$$

Some materials such as crystals and wood, have thermal conductivities and diffusivities that vary markedly with direction. For these anisotropic materials, Fick's second law in the form of (3-69) does not hold. Although the general anisotropic case is exceedingly complex, as shown in the following example, the mathematical treatment is relatively simple when the principal axes of diffusivity coincide with the coordinate system.

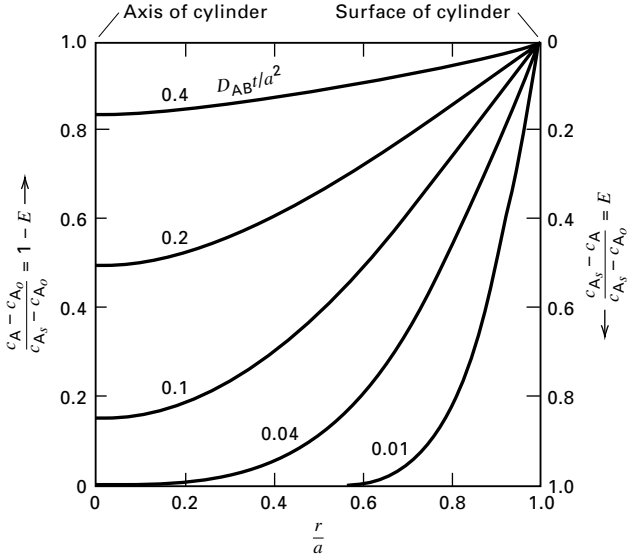

Figure 3.10 Concentration profiles for unsteady-state diffusion in a cylinder.

[Adapted from H.S. Carslaw and J.C. Jaeger, *Conduction of Heat in Solids,* 2nd ed., Oxford University Press, London (1959).]

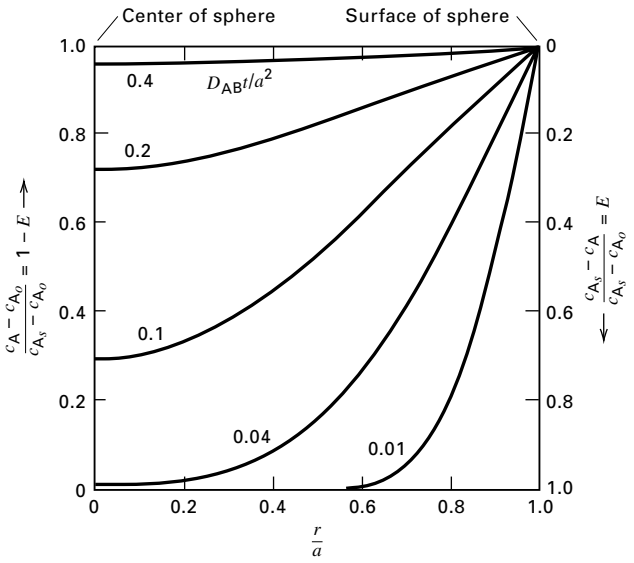

Figure 3.11 Concentration profiles for unsteady-state diffusion in a sphere.

[Adapted from H.S. Carslaw and J.C. Jaeger, *Conduction of Heat in Solids,* 2nd ed., Oxford University Press, London (1959).]

EXAMPLE 3.12

A piece of lumber, measuring $5 \times 10 \times 20$ cm, initially contains 20 wt% moisture. At time 0, all six faces are brought to an equilibrium moisture content of 2 wt%. Diffusivities for moisture at 25°C are 2×10^{-5} cm^2/s in the axial (z) direction along the fibers and 4×10^{-6} cm^2/s in the two directions perpendicular to the fibers. Calculate the time in hours for the average moisture content to drop to 5 wt% at 25°C. At that time, determine the moisture content at the center of the piece of lumber. All moisture contents are on a dry basis.

SOLUTION

In this case, the solid is anisotropic, with $D_x = D_y = 4 \times 10^{-6}$ cm^2/s and $D_z = 2 \times 10^{-5}$ cm^2/s, where dimensions $2c$, $2b$, and $2a$ in the x, y, and z directions are 5, 10, and 20 cm, respectively. Fick's second law for an isotropic medium, (3-69), must be rewritten for this anisotropic material as

$$\frac{\partial c_A}{\partial t} = D_x \left[\frac{\partial^2 c_A}{\partial x^2} + \frac{\partial^2 c_A}{\partial y^2} \right] + D_z \frac{\partial^2 c_A}{\partial z^2} \tag{1}$$

as discussed by Carslaw and Jaeger [26].

To transform (1) into the form of (3-69), let

$$x_1 = x\sqrt{\frac{D}{D_x}} \qquad y_1 = y\sqrt{\frac{D}{D_x}} \qquad z_1 = z\sqrt{\frac{D}{D_z}} \tag{2}$$

where D is chosen arbitrarily. With these changes in variables, (1) becomes

$$\frac{\partial c_A}{\partial t} = D\left(\frac{\partial^2 c_A}{\partial x_1^2} + \frac{\partial^2 c_A}{\partial y_1^2} + \frac{\partial^2 c_A}{\partial z_1^2} \right) \tag{3}$$

Since this is the same form as (3-69) and since the boundary conditions do not involve diffusivities, we can apply Newman's method, using Figure 3.9, where concentration, c_A, is replaced by weight-percent moisture on a dry basis.

From (3-86) and (3-85),

$$E_{\text{ave}_{\text{slab}}} = E_{\text{avg}_x} E_{\text{avg}_y} E_{\text{avg}_z} = \frac{c_{A_{\text{ave}}} - c_{A_s}}{c_{A_o} - c_{A_s}} = \frac{5-2}{20-2} = 0.167$$

Let $D = 1 \times 10^{-5}$ cm^2/s.

z_1 Direction (axial):

$$a_1 = a\left(\frac{D}{D_z}\right)^{1/2} = \frac{20}{2}\left(\frac{1\times10^{-5}}{2\times10^{-5}}\right)^{1/2} = 7.07 \text{ cm}$$

$$\frac{Dt}{a_1^2} = \frac{1\times10^{-5}t}{7.07^2} = 2.0\times10^{-7}t, \text{ s}$$

y_1 Direction:

$$b_1 = b\left(\frac{D}{D_y}\right)^{1/2} = \frac{10}{2}\left(\frac{1\times10^{-5}}{4\times10^{-6}}\right)^{1/2} = 7.906 \text{ cm}$$

$$\frac{Dt}{b_1^2} = \frac{1\times10^{-5}t}{7.906^2} = 1.6\times10^{-7}t, \text{ s}$$

x_1-Direction:

$$c_1 = c\left(\frac{D}{D_x}\right)^{1/2} = \frac{5}{2}\left(\frac{1\times10^{-5}}{4\times10^{-6}}\right)^{1/2} = 3.953 \text{ cm}$$

$$\frac{Dt}{c_1^2} = \frac{1\times10^{-5}t}{3.953^2} = 6.4\times10^{-7}t, \text{ s}$$

Use Figure 3.9 iteratively with assumed values of time in seconds to obtain values of E_{avg} for each of the three coordinates until (3-86) equals 0.167.

t, h	t, s	$E_{\text{avg}_{z_1}}$	$E_{\text{avg}_{y_1}}$	$E_{\text{avg}_{x_1}}$	E_{avg}
100	360,000	0.70	0.73	0.46	0.235
120	432,000	0.67	0.70	0.41	0.193
135	486,000	0.65	0.68	0.37	0.164

Therefore, it takes approximately 136 h.

For 136 h = 490,000 s, the Fourier numbers for mass transfer are

$$\frac{Dt}{a_1^2} = \frac{(1\times10^{-5})(490{,}000)}{7.07^2} = 0.0980$$

$$\frac{Dt}{b_1^2} = \frac{(1\times10^{-5})(490{,}000)}{7.906^2} = 0.0784$$

$$\frac{Dt}{c_1^2} = \frac{(1\times10^{-5})(490{,}000)}{3.953^2} = 0.3136$$

From Figure 3.8, at the center of the slab,

$$E_{\text{center}} = E_{z_1} E_{y_1} E_{x_1} = (0.945)(0.956)(0.605) = 0.547$$

$$= \frac{c_{A_s} - c_{A_{\text{center}}}}{c_{A_s} - c_{A_o}} = \frac{2 - c_{A_{\text{center}}}}{2 - 20} = 0.547$$

Solving,

$$c_A \text{ at the center} = 11.8 \text{ wt\% moisture}$$

3.4 MOLECULAR DIFFUSION IN LAMINAR FLOW

Many mass-transfer operations involve diffusion in fluids in laminar flow. The fluid may be a film flowing slowly down a vertical or inclined surface, a laminar boundary layer that forms as the fluid flows slowly past a thin plate, or the fluid may flow through a small tube or slowly through a large pipe or duct. Mass transfer may occur between a gas and a liquid film, between a solid surface and a fluid, or between a fluid and a membrane surface.

Falling Liquid Film

Consider a thin liquid film, of a mixture of volatile A and nonvolatile B, falling in laminar flow at steady state down one side of a vertical surface and exposed to pure gas, A, on the other side of the film, as shown in Figure 3.12. The surface is infinitely wide in the x-direction (normal to the page). In the absence of mass transfer of A into the liquid film, the liquid velocity in the z-direction, u_z, is zero. In the absence of end effects, the equation of motion for the liquid film in fully developed laminar flow in the downward y-direction is

$$\mu \frac{d^2 u_y}{dz^2} + \rho g = 0 \tag{3-88}$$

Usually, fully developed flow, where u_y is independent of the distance y, is established quickly. If δ is the thickness of the film and the boundary conditions are $u_y = 0$ at $z = \delta$ (no-slip condition at the solid surface) and $du_y/dz = 0$ at $z = 0$ (no drag at the liquid–gas interface), (3-88) is readily integrated to give a parabolic velocity profile:

$$u_y = \frac{\rho g \delta^2}{2\mu}\left[1 - \left(\frac{z}{\delta}\right)^2\right] \tag{3-89}$$

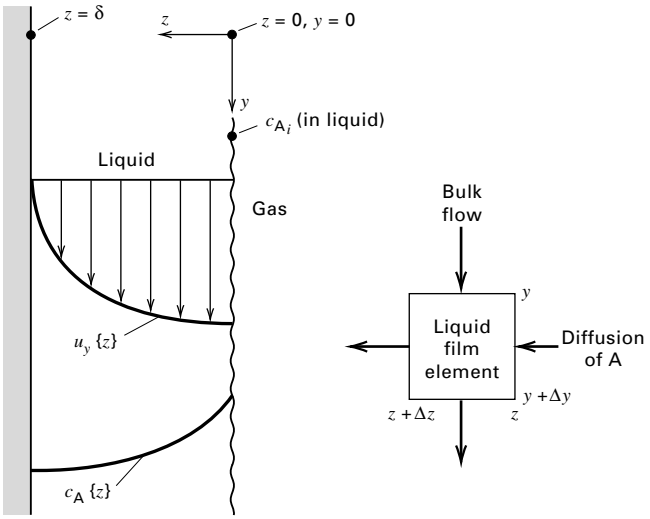

Figure 3.12 Mass transfer from a gas into a falling, laminar liquid film.

Thus, the maximum liquid velocity, which occurs at $z = 0$, is

$$(u_y)_{\max} = \frac{\rho g \delta^2}{2\mu} \tag{3-90}$$

The bulk-average velocity in the liquid film is

$$\bar{u}_y = \frac{\int_0^\delta u_y \, dz}{\delta} = \frac{\rho g \delta^2}{3\mu} \tag{3-91}$$

Thus, the film thickness for fully developed flow is independent of location y and is

$$\delta = \left(\frac{3\bar{u}_y \mu}{\rho g}\right)^{1/2} = \left(\frac{3\mu\Gamma}{\rho^2 g}\right)^{1/3} \tag{3-92}$$

where Γ = liquid film flow rate per unit width of film, W.

For film flow, the Reynolds number, which is the ratio of the inertial force to the viscous force, is

$$N_{\mathrm{Re}} = \frac{4 r_H \bar{u}_y \rho}{\mu} = \frac{4\delta \bar{u}_y \rho}{\mu} = \frac{4\Gamma}{\mu} \tag{3-93}$$

where r_H = hydraulic radius = (flow cross section)/(wetted perimeter) $= (W\delta)/W = \delta$ and, by the equation of continuity, $\Gamma = \bar{u}_y \rho \delta$.

As reported by Grimley [32], for $N_{\mathrm{Re}} < 8$ to 25, depending on the surface tension and viscosity, the flow in the film is laminar and the interface between the liquid film and the gas is flat. The value of 25 is obtained with water. For 8 to $25 < N_{\mathrm{Re}} < 1{,}200$, the flow is still laminar, but ripples and waves may appear at the interface unless suppressed by the addition of wetting agents to the liquid.

For a flat liquid–gas interface and a small rate of mass transfer of A into the liquid film, (3-88) to (3-93) hold and the film velocity profile is given by (3-89). Now consider a mole balance on A for an incremental volume of liquid film of constant density, as shown in Figure 3.12. Neglect bulk flow in the z-direction and axial diffusion in the y-direction. Then, at steady state, neglecting accumulation or depletion of A in the incremental volume,

$$-D_{\mathrm{AB}}(\Delta y)(\Delta x)\left(\frac{\partial c_{\mathrm{A}}}{\partial z}\right)_z + u_y c_{\mathrm{A}}|_y (\Delta z)(\Delta x)$$
$$= -D_{\mathrm{AB}}(\Delta y)(\Delta x)\left(\frac{\partial c_{\mathrm{A}}}{\partial z}\right)_{z+\Delta z} + u_y c_{\mathrm{A}}|_{y+\Delta y}(\Delta z)(\Delta x) \tag{3-94}$$

Rearranging and simplifying (3-94),

$$\left[\frac{u_y c_{\mathrm{A}}|_{y+\Delta y} - u_y c_{\mathrm{A}}|_y}{\Delta y}\right] = D_{\mathrm{AB}}\left[\frac{(\partial c_{\mathrm{A}}/\partial z)_{z+\Delta z} - (\partial c_{\mathrm{A}}/\partial z)_z}{\Delta z}\right] \tag{3-95}$$

In the limit, as $\Delta z \to 0$ and $\Delta y \to 0$,

$$u_y \frac{\partial c_{\mathrm{A}}}{\partial y} = D_{\mathrm{AB}} \frac{\partial^2 c_{\mathrm{A}}}{\partial z^2} \tag{3-96}$$

Substituting (3-89) into (3-96),

$$\frac{\rho g \delta^2}{2\mu}\left[1 - \left(\frac{z}{\delta}\right)^2\right] \frac{\partial c_{\mathrm{A}}}{\partial y} = D_{\mathrm{AB}} \frac{\partial^2 c_{\mathrm{A}}}{\partial z^2} \tag{3-97}$$

This equation was solved by Johnstone and Pigford [33] and later by Olbrich and Wild [34], for the following boundary conditions:

$$\begin{aligned} c_A &= c_{A_i} \quad \text{at } z = 0 \quad \text{for } y > 0 \\ c_A &= c_{A_0} \quad \text{at } y = 0 \quad \text{for } 0 < z < \delta \\ \partial c_A/\partial z &= 0 \quad \text{at } z = \delta \quad \text{for } 0 < y < L \end{aligned}$$

where L = height of the vertical surface. The solution of Olbrich and Wild is in the form of an infinite series, giving c_A as a function of z and y. However, of more interest is the average concentration at $y = L$, which, by integration, is

$$\bar{c}_{A_y} = \frac{1}{\bar{u}_y \delta} \int_0^\delta u_y c_{A_y}\, dz \tag{3-98}$$

For the condition $y = L$, the result is

$$\begin{aligned} \frac{c_{A_i} - \bar{c}_{A_L}}{c_{A_i} - c_{A_0}} &= 0.7857 e^{-5.1213\eta} + 0.09726 e^{-39.661\eta} \\ &\quad + 0.036093^{-106.25\eta} + \cdots \end{aligned} \tag{3-99}$$

where

$$\eta = \frac{2 D_{AB} L}{3\delta^2 \bar{u}_y} = \frac{8/3}{N_{Re} N_{Sc} (\delta/L)} = \frac{8/3}{(\delta/L) N_{Pe_M}} \tag{3-100}$$

$$\begin{aligned} N_{Sc} &= \text{Schmidt number} = \frac{\mu}{\rho D_{AB}} \\ &= \frac{\text{momentum diffusivity}, \mu/\rho}{\text{mass diffusivity}, D_{AB}} \end{aligned} \tag{3-101}$$

$$\begin{aligned} N_{Pe_M} &= N_{Re} N_{Sc} = \text{Peclet number for mass transfer} \\ &= \frac{4\delta \bar{u}_y}{D_{AB}} \end{aligned} \tag{3-102}$$

The Schmidt number is analogous to the Prandtl number, used in heat transfer:

$$N_{Pr} = \frac{C_P \mu}{k} = \frac{(\mu/\rho)}{(k/\rho C_P)} = \frac{\text{momentum diffusivity}}{\text{thermal diffusivity}}$$

The Peclet number for mass transfer is analogous to the Peclet number for heat transfer:

$$N_{Pe_H} = N_{Re} N_{Pr} = \frac{4\delta \bar{u}_y C_P \rho}{k}$$

Both Peclet numbers are ratios of convective transport to molecular transport.

The total rate of absorption of A from the gas into the liquid film for height L and width W is

$$n_A = \bar{u}_y \delta W (\bar{c}_{A_L} - c_{A_0}) \tag{3-103}$$

Mass-Transfer Coefficients

Mass-transfer problems involving fluids are most often solved using mass-transfer coefficients, analogous to heat-transfer coefficients. For the latter, *Newton's law of cooling* defines a heat-transfer coefficient, h:

$$Q = hA\, \Delta T \tag{3-104}$$

where

Q = rate of heat transfer
A = area for heat transfer (normal to the direction of heat transfer)
ΔT = temperature-driving force for heat transfer

For mass transfer, a composition driving force replaces ΔT. As discussed later in this chapter, because composition can be expressed in a number of ways, different mass-transfer coefficients are defined. If we select Δc_A as the driving force for mass transfer, we can write

$$n_A = k_c A\, \Delta c_A \tag{3-105}$$

which defines a mass-transfer coefficient, k_c, in mol/time-area-driving force, for a concentration driving force. Unfortunately, no name is in general use for (3-105).

For the falling laminar film, we take $\Delta c_A = c_{A_i} - \bar{c}_A$, which varies with vertical location, y, because even though c_{A_i} is independent of y, the average film concentration, $\bar{c}_A$, increases with y. To derive an expression for k_c, we equate (3-105) to Fick's first law at the gas–liquid interface:

$$k_c A (c_{A_i} - \bar{c}_A) = -D_{AB} A \left(\frac{\partial c_A}{\partial z} \right)_{z=0} \tag{3-106}$$

Although this is the most widely used approach for defining a mass-transfer coefficient, in this case of a falling film it fails because $(\partial c_A/\partial z)$ at $z = 0$ is not defined. Therefore, for this case we use another approach as follows. For an incremental height, we can write for film width W,

$$n_A = \bar{u}_y \delta W\, d\bar{c}_A = k_c (c_{A_i} - \bar{c}_A) W\, dy \tag{3-107}$$

This defines a local value of k_c, which varies with distance y because $\bar{c}_A$ varies with y. An average value of k_c, over a height L, can be defined by separating variables and integrating (3-107):

$$\begin{aligned} k_{c_{avg}} &= \frac{\int_0^L k_c\, dy}{L} = \frac{\bar{u}_y \delta \int_{c_{A_0}}^{c_{A_L}} [d\bar{c}_A/(c_{A_i} - \bar{c}_A)]}{L} \\ &= \frac{\bar{u}_y \delta}{L} \ln \frac{c_{A_i} - c_{A_0}}{c_{A_i} - \bar{c}_{A_L}} \end{aligned} \tag{3-108}$$

In general, the argument of the natural logarithm in (3-108) is obtained from the reciprocal of (3-99). For values of η in (3-100) greater than 0.1, only the first term in (3-99) is significant (error is less than 0.5%). In that case,

$$k_{c_{avg}} = \frac{\bar{u}_y \delta}{L} \ln \frac{e^{5.1213\eta}}{0.7857} \tag{3-109}$$

Since $\ln e^x = x$,

$$k_{c_{avg}} = \frac{\bar{u}_y \delta}{L} (0.241 + 5.1213\eta) \tag{3-110}$$

In the limit, for large η, using (3-100) and (3-102), (3-110) becomes

$$k_{c_{avg}} = 3.414 \frac{D_{AB}}{\delta} \tag{3-111}$$

In a manner suggested by the Nusselt number, $N_{Nu} = h\delta/k$ for heat transfer, where δ = a characteristic length, we define a Sherwood number for mass transfer, which for a falling film of characteristic length δ is

$$N_{Sh_{avg}} = \frac{k_{c_{avg}} \delta}{D_{AB}} \tag{3-112}$$

From (3-111), $N_{\mathrm{Sh}_{\mathrm{avg}}} = 3.414$, which is the smallest value that the Sherwood number can have for a falling liquid film.

The average mass-transfer flux of A is given by

$$N_{\mathrm{A}_{\mathrm{avg}}} = \frac{n_{\mathrm{A}_{\mathrm{avg}}}}{A} = k_{c_{\mathrm{avg}}}(c_{\mathrm{A}_i} - \bar{c}_{\mathrm{A}})_{\mathrm{mean}} \qquad (3\text{-}113)$$

For values $\eta < 0.001$ in (3-100), when the liquid-film flow regime is still laminar without ripples, the time of contact of the gas with the liquid is short and mass transfer is confined to the vicinity of the gas–liquid interface. Thus, the film acts as if it were infinite in thickness. In this limiting case, the downward velocity of the liquid film in the region of mass transfer is just $u_{y_{\max}}$, and (3-96) becomes

$$u_{y_{\max}} \frac{\partial c_{\mathrm{A}}}{\partial y} = D_{\mathrm{AB}} \frac{\partial^2 c_{\mathrm{A}}}{\partial z^2} \qquad (3\text{-}114)$$

Since from (3-90) and (3-91), $u_{y_{\max}} = 3\bar{u}_y/2$, (3-114) can be rewritten as

$$\frac{\partial c_{\mathrm{A}}}{\partial y} = \left(\frac{2D_{\mathrm{AB}}}{3\bar{u}_y}\right) \frac{\partial^2 c_{\mathrm{A}}}{\partial z^2} \qquad (3\text{-}115)$$

where the boundary conditions are

$$\begin{aligned} c_{\mathrm{A}} &= c_{\mathrm{A}_0} \quad \text{for } z > 0 \quad \text{and } y > 0 \\ c_{\mathrm{A}} &= c_{\mathrm{A}_i} \quad \text{for } z = 0 \quad \text{and } y > 0 \\ c_{\mathrm{A}} &= c_{\mathrm{A}_0} \quad \text{for large } z \quad \text{and } y > 0 \end{aligned}$$

Equation (3-115) and the boundary conditions are equivalent to the case of the semi-infinite medium, as developed above. Thus, by analogy to (3-68), (3-75), and (3-76) the solution is

$$E = 1 - \theta = \frac{c_{\mathrm{A}_i} - c_{\mathrm{A}}}{c_{\mathrm{A}_i} - c_{\mathrm{A}_0}} = \mathrm{erf}\left(\frac{z}{2\sqrt{2D_{\mathrm{AB}}y/3\bar{u}_y}}\right) \qquad (3\text{-}116)$$

Assuming that the driving force for mass transfer in the film is $c_{\mathrm{A}_i} - c_{\mathrm{A}_0}$, we can use Fick's first law at the gas–liquid interface to define a mass-transfer coefficient:

$$N_{\mathrm{A}} = -D_{\mathrm{AB}} \left.\frac{\partial c_{\mathrm{A}}}{\partial z}\right|_{z=0} = k_c(c_{\mathrm{A}_i} - c_{\mathrm{A}_0}) \qquad (3\text{-}117)$$

The error function is defined as

$$\mathrm{erf}\, z = \frac{2}{\sqrt{\pi}} \int_0^z e^{-t^2} dt \qquad (3\text{-}118)$$

Using the Leibnitz rule with (3-116) to differentiate this integral function,

$$\left.\frac{\partial c_{\mathrm{A}}}{\partial z}\right|_{z=0} = -(c_{\mathrm{A}_i} - c_{\mathrm{A}_0})\sqrt{\frac{3\bar{u}_y}{2\pi D_{\mathrm{AB}} y}} \qquad (3\text{-}119)$$

Substituting (3-119) into (3-117) and introducing the Peclet number for mass transfer from (3-102), we obtain an expression for the local mass-transfer coefficient as a function of distance down from the top of the wall:

$$k_c = \sqrt{\frac{3D_{\mathrm{AB}}^2 N_{\mathrm{Pe_M}}}{8\pi y\delta}} = \sqrt{\frac{3D_{\mathrm{AB}}\Gamma}{2\pi y\delta\rho}} \qquad (3\text{-}120)$$

The average value of k_c over the height of the film, L, is obtained by integrating (3-120) with respect to y, giving

$$k_{c_{\mathrm{avg}}} = \sqrt{\frac{6D_{\mathrm{AB}}\Gamma}{\pi\delta\rho L}} = \sqrt{\frac{3D_{\mathrm{AB}}^2}{2\pi\delta L} N_{\mathrm{Pe_M}}} \qquad (3\text{-}121)$$

Combining (3-121) with (3-112) and (3-102),

$$N_{\mathrm{Sh}_{\mathrm{avg}}} = \sqrt{\frac{3\delta}{2\pi L} N_{\mathrm{Pe}_M}} = \sqrt{\frac{4}{\pi\eta}} \qquad (3\text{-}122)$$

where, by (3-108), the proper mean to use with $k_{c_{\mathrm{avg}}}$ is the log mean. Thus,

$$\begin{aligned} (c_{\mathrm{A}_i} - \bar{c}_{\mathrm{A}})_{\mathrm{mean}} &= (c_{\mathrm{A}_i} - \bar{c}_{\mathrm{A}})_{\mathrm{LM}} \\ &= \frac{(c_{\mathrm{A}_i} - c_{\mathrm{A}_0}) - (c_{\mathrm{A}_i} - c_{\mathrm{A}_L})}{\ln[(c_{\mathrm{A}_i} - c_{\mathrm{A}_0})/(c_{\mathrm{A}_i} - \bar{c}_{\mathrm{A}_L})]} \end{aligned} \qquad (3\text{-}123)$$

When ripples are present, values of $k_{c_{\mathrm{avg}}}$ and $N_{\mathrm{Sh}_{\mathrm{avg}}}$ can be considerably larger than predicted by these equations.

In the above development, asymptotic, closed-form solutions are obtained with relative ease for large and small values of η, defined by (3-100). These limits, in terms of the average Sherwood number, are shown in Figure 3.13. The

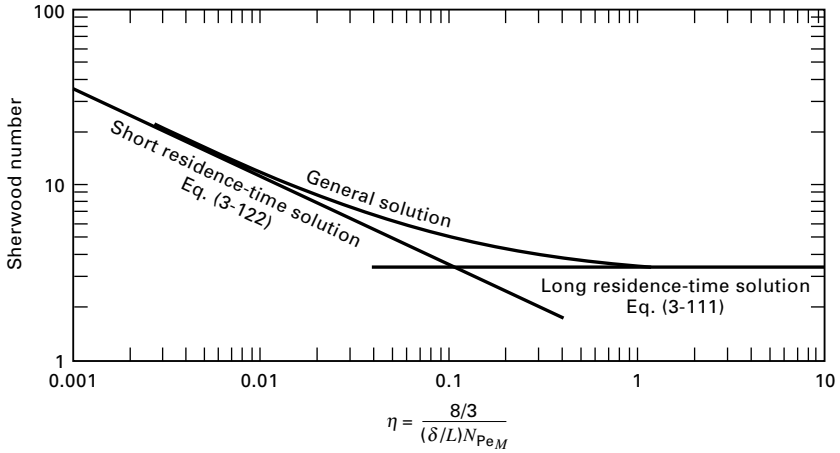

Figure 3.13 Limiting and general solutions for mass transfer to a falling, laminar liquid film.

general solution for intermediate values of η is not available in closed form. Similar limiting solutions for large and small values of appropriate parameters, usually dimensionless groups, have been obtained for a large variety of transport and kinetic phenomena, as discussed by Churchill [35]. Often the two limiting cases can be patched together to provide a reasonable estimate of the intermediate solution, if a single intermediate value is available from experiment or the general numerical solution. The procedure is discussed by Churchill and Usagi [36]. The general solution of Emmert and Pigford [37] to the falling, laminar liquid film problem is included in Figure 3.13.

EXAMPLE 3.13

Water (B) at 25°C, in contact with pure CO_2 (A) at 1 atm, flows as a film down a vertical wall 1 m wide and 3 m high at a Reynolds number of 25. Using the following properties, estimate the rate of adsorption of CO_2 into water in kmol/s:

$$D_{AB} = 1.96 \times 10^{-5} \text{ cm}^2/\text{s}; \qquad \rho = 1.0 \text{ g/cm}^3;$$
$$\mu_L = 0.89 \text{ cP} = 0.00089 \text{ kg/m-s}$$

Solubility of CO_2 in water at 1 atm and 25°C $= 3.4 \times 10^{-5}$ mol/cm^3.

SOLUTION

From (3-93),

$$\Gamma = \frac{N_{Re}\mu}{4} = \frac{25(0.89)(0.001)}{4} = 0.00556 \frac{\text{kg}}{\text{m} - \text{s}}$$

From (3-101),

$$N_{Sc} = \frac{\mu}{\rho D_{AB}} = \frac{(0.89)(0.001)}{(1.0)(1{,}000)(1.96 \times 10^{-5})(10^{-4})} = 454$$

From (3-92),

$$\delta = \left[\frac{3(0.89)(0.001)(0.00556)}{1.0^2(1{,}000)^2(9.807)}\right]^{1/3} = 1.15 \times 10^{-4} \text{ m}$$

From (3-90) and (3-91), $\bar{u}_y = (2/3)u_{y_{max}}$. Therefore,

$$\bar{u}_y = \frac{2}{3}\left[\frac{(1.0)(1{,}000)(9.807)(1.15 \times 10^{-4})^2}{2(0.89)(0.001)}\right] = 0.0486 \text{ m/s}$$

From (3-100),

$$\eta = \frac{8/3}{(25)(454)[(1.15 \times 10^{-4})/3]} = 6.13$$

Therefore, (3-111) applies, giving

$$k_{c_{avg}} = \frac{3.41(1.96 \times 10^{-5})(10^{-4})}{1.15 \times 10^{-4}} = 5.81 \times 10^{-5} \text{ m/s}$$

To determine the rate of absorption, $\bar{c}_{A_L}$ must be determined. From (3-103) and (3-113),

$$n_A = \bar{u}_y \delta W(\bar{c}_{A_L} - c_{A_0}) = k_{c_{avg}} A \frac{(\bar{c}_{A_L} - c_{A_0})}{\ln[(c_{A_i} - c_{A_0})/(c_{A_i} - c_{A_L})]}$$

Thus,

$$\ln\left(\frac{c_{A_i} - c_{A_0}}{c_{A_i} - \bar{c}_{A_L}}\right) = \frac{k_{c_{avg}} A}{\bar{u}_y \delta W}$$

Solving for $\bar{c}_{A_L}$,

$$\bar{c}_{A_L} = c_{A_i} - (c_{A_i} - c_{A_0}) \exp\left(-\frac{k_{c_{avg}} A}{\bar{u}_y \delta W}\right)$$

$$L = 3 \text{ m}, \quad W = 1 \text{ m}, \quad A = WL = (1)(3) = 3 \text{ m}^2$$

$$c_{A_0} = 0, \quad c_{A_i} = 3.4 \times 10^{-5} \text{ mol/cm}^3 = 3.4 \times 10^{-2} \text{ kmol/m}^3$$

$$\bar{c}_{A_L} = 3.4 \times 10^{-2}\left\{1 - \exp\left[-\frac{(5.81 \times 10^{-5})(3)}{(0.0486)(1.15 \times 10^{-4})(1)}\right]\right\}$$
$$= 3.4 \times 10^{-2} \text{ kmol/m}^3$$

Thus, the exiting liquid film is saturated with CO_2, which implies equilibrium at the gas–liquid interface. From (3-103),

$$n_A = 0.0486(1.15 \times 10^{-4})(3.4 \times 10^{-2}) = 1.9 \times 10^{-7} \text{ kmol/s}$$

Boundary-Layer Flow on a Flat Plate

Consider the flow of a fluid (B) over a thin, flat plate parallel with the direction of flow of the fluid upstream of the plate, as shown in Figure 3.14. A number of possibilities for mass transfer of another species, A, into B exist: (1) The plate might consist of material A, which is slightly soluble in B. (2) Component A might be held in the pores of an inert solid plate, from which it evaporates or dissolves into B. (3) The plate might be an inert, dense polymeric membrane, through which species A can pass into fluid B. Let the fluid velocity profile upstream of the plate be uniform at a free-system velocity of u_o. As the fluid passes over the plate, the velocity u_x in the direction of flow is reduced to zero at the wall, which establishes a velocity profile due to drag. At a certain distance z, normal to and out from the solid surface, the fluid velocity is 99% of u_o. This distance, which increases with increasing distance x from the leading edge of the plate, is arbitrarily defined as the velocity boundary-layer thickness, δ. Essentially all flow retardation occurs in the boundary layer, as first suggested by Prandtl [38]. The buildup of this layer, the velocity profile in the layer, and the drag force can be determined for laminar flow by solving the equations of continuity and motion (Navier–Stokes equations) for the x-direction. For a Newtonian fluid of constant density and viscosity, in the absence of pressure gradients in the x- and

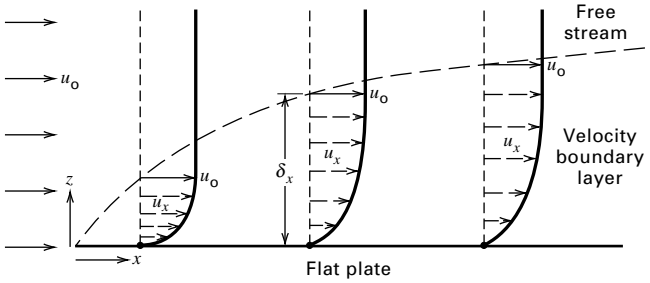

Figure 3.14 Laminar boundary-layer development for flow across a flat plate.

y- (normal to the x–z plane) directions, these equations for the region of the boundary layer are

$$\frac{\partial u_x}{\partial x} + \frac{\partial u_z}{\partial z} = 0 \tag{3-124}$$

$$u_x \frac{\partial u_x}{\partial x} + u_z \frac{\partial u_x}{\partial z} = \frac{\mu}{\rho}\left(\frac{\partial^2 u_x}{\partial z^2}\right) \tag{3-125}$$

The boundary conditions are

$u_x = u_o$ at $x = 0$ for $z > 0$ $\quad u_x = 0$ at $z = 0$ for $x > 0$
$u_x = u_o$ at $z = \infty$ for $x > 0$ $\quad u_z = 0$ at $z = 0$ for $x > 0$

The solution of (3-124) and (3-125) in the absence of heat and mass transfer, subject to these boundary conditions, was first obtained by Blasius [39] and is described in detail by Schlichting [40]. The result in terms of a local friction factor, f_x, a local shear stress at the wall, τ_{w_x}, and a local drag coefficient at the wall, C_{D_x}, is

$$\frac{C_{D_x}}{2} = \frac{f_x}{2} = \frac{\tau_{w_x}}{\rho u_o^2} = \frac{0.322}{N_{\mathrm{Re}_x}^{0.5}} \tag{3-126}$$

where

$$N_{\mathrm{Re}_x} = \frac{x u_o \rho}{\mu} \tag{3-127}$$

Thus, the drag is greatest at the leading edge of the plate, where the Reynolds number is smallest. Average values of the drag coefficient are obtained by integrating (3-126) from $x = 0$ to L, giving

$$\frac{C_{D_{\mathrm{avg}}}}{2} = \frac{f_{\mathrm{avg}}}{2} = \frac{0.664}{(N_{\mathrm{Re}_L})^{0.5}} \tag{3-128}$$

The thickness of the velocity boundary layer increases with distance along the plate:

$$\frac{\delta}{x} = \frac{4.96}{N_{\mathrm{Re}_x}^{0.5}} \tag{3-129}$$

A reasonably accurate expression for the velocity profile was obtained by Pohlhausen [41], who assumed the empirical form $u_x = C_1 z + C_2 z^3$.

If the boundary conditions,

$$u_x = 0 \text{ at } z = 0 \quad u_x = u_o \text{ at } z = \delta \quad \partial u_x/\partial z = 0 \text{ at } z = \delta$$

are applied to evaluate C_1 and C_2, the result is

$$\frac{u_x}{u_o} = 1.5\left(\frac{z}{\delta}\right) - 0.5\left(\frac{z}{\delta}\right)^3 \tag{3-130}$$

This solution is valid only for a laminar boundary layer, which by experiment persists to $N_{\mathrm{Re}_x} = 5 \times 10^5$.

When mass transfer of A into the boundary layer occurs, the following species continuity equation applies at constant diffusivity:

$$u_x \frac{\partial c_A}{\partial x} + u_z \frac{\partial c_A}{\partial z} = D_{AB}\left(\frac{\partial^2 c_A}{\partial x^2}\right) \tag{3-131}$$

If mass transfer begins at the leading edge of the plate and if the concentration in the fluid at the solid–fluid interface is constant, the additional boundary conditions are

$$\begin{aligned} c_A &= c_{A_o} \quad \text{at } x = 0 \quad \text{for } z > 0, \\ c_A &= c_{A_i} \quad \text{at } z = 0 \quad \text{for } x > 0, \\ \text{and} \quad c_A &= c_{A_o} \quad \text{at } z = \infty \quad \text{for } x > 0 \end{aligned}$$

If the rate of mass transfer is low, the velocity profiles are undisturbed. The solution to the analogous problem in heat transfer was first obtained by Pohlhausen [42] for $N_{\mathrm{Pr}} > 0.5$, as described in detail by Schlichting [40]. The results for mass transfer are

$$\frac{N_{\mathrm{Sh}_x}}{N_{\mathrm{Re}_x} N_{\mathrm{Sc}}^{1/3}} = \frac{0.332}{N_{\mathrm{Re}_x}^{0.5}} \tag{3-132}$$

where

$$N_{\mathrm{Sh}_x} = \frac{x k_{c_x}}{D_{AB}} \tag{3-133}$$

and the driving force for mass transfer is $c_{A_i} - c_{A_o}$.

The concentration boundary layer, where essentially all of the resistance to mass transfer resides, is defined by

$$\frac{c_{A_i} - c_A}{c_{A_i} - c_{A_o}} = 0.99 \tag{3-134}$$

and the ratio of the concentration boundary-layer thickness, δ_c, to the velocity boundary thickness, δ, is

$$\delta_c/\delta = 1/N_{\mathrm{Sc}}^{1/3} \tag{3-135}$$

Thus, for a liquid boundary layer, where $N_{\mathrm{Sc}} > 1$, the concentration boundary layer builds up more slowly than the velocity boundary layer. For a gas boundary layer, where $N_{SC} \approx 1$, the two boundary layers build up at about the same rate. By analogy to (3-130), the concentration profile is given by

$$\frac{c_{A_i} - c_A}{c_{A_i} - c_{A_o}} = 1.5\left(\frac{z}{\delta_c}\right) - 0.5\left(\frac{z}{\delta_c}\right)^3 \tag{3-136}$$

Equation (3-132) gives the local Sherwood number. If this expression is integrated over the length of the plate, L, the average Sherwood number is found to be

$$N_{\mathrm{Sh}_{\mathrm{avg}}} = 0.664\, N_{\mathrm{Re}_L}^{1/2} N_{\mathrm{Sc}}^{1/3} \tag{3-137}$$

where

$$N_{\mathrm{Sh}_{\mathrm{avg}}} = \frac{L k_{c_{\mathrm{avg}}}}{D_{AB}} \tag{3-138}$$

EXAMPLE 3.14

Air at 100°C, 1 atm, and a free-stream velocity of 5 m/s flows over a 3-m-long, thin, flat plate of naphthalene, causing it to sublime.

(a) Determine the length over which a laminar boundary layer persists.

(b) For that length, determine the rate of mass transfer of naphthalene into air.

(c) At the point of transition of the boundary layer to turbulent flow, determine the thicknesses of the velocity and concentration boundary layers.

Assume the following values for physical properties:

Vapor pressure of napthalene = 10 torr
Viscosity of air = 0.0215 cP
Molar density of air = 0.0327 kmol/m^3
Diffusivity of napthalene in air = 0.94×10^{-5} m^2/s

SOLUTION

(a) $N_{\mathrm{Re}_x} = 5 \times 10^5$ for transition. From (3-127),

$$x = L = \frac{\mu N_{\mathrm{Re}_x}}{u_o \rho} = \frac{[(0.0215)(0.001)](5 \times 10^5)}{(5)[(0.0327)(29)]} = 2.27 \text{ m}$$

at which transition to turbulent flow begins.

(b) $c_{A_o} = 0 \quad c_{A_i} = \dfrac{10(0.0327)}{760} = 4.3 \times 10^{-4}$ kmol/m^3

From (3-101),

$$N_{\mathrm{Sc}} = \frac{\mu}{\rho D_{AB}} = \frac{[(0.0215)(0.001)]}{[(0.0327)(29)](0.94 \times 10^{-5})} = 2.41$$

From (3-137),

$$N_{\mathrm{Sh}_{\mathrm{avg}}} = 0.664(5 \times 10^5)^{1/2}(2.41)^{1/3} = 630$$

From (3-138),

$$k_{c_{\mathrm{avg}}} = \frac{630(0.94 \times 10^{-5})}{2.27} = 2.61 \times 10^{-3} \text{m/s}$$

For a width of 1 m,

$$A = 2.27 \text{ m}^2$$
$$n_A = k_{c_{\mathrm{avg}}} A(c_{A_i} - c_{A_o}) = 2.61 \times 10^{-3}(2.27)(4.3 \times 10^{-4})$$
$$= 2.55 \times 10^{-6} \text{ kmol/s}$$

(c) From (3-129), at $x = L = 2.27$ m,

$$\delta = \frac{3.46(2.27)}{(5 \times 10^5)^{0.5}} = 0.0111 \text{ m}$$

From (3-135),

$$\delta_c = \frac{0.0111}{(2.41)^{1/3}} = 0.0083 \text{ m}$$

Fully Developed Flow in a Straight, Circular Tube

Figure 3.15 shows the formation and buildup of a laminar velocity boundary layer when a fluid flows from a vessel into a straight, circular tube. At the entrance, plane *a*, the velocity profile is flat. A velocity boundary layer then begins to build up as shown at planes *b*, *c*, and *d*. In this region, the central core outside the boundary layer has a flat velocity profile where the flow is accelerated over the entrance velocity. Finally, at plane *e*, the boundary layer fills the tube. From here the velocity profile is fixed and the flow is said to be fully developed. The distance from the plane *a* to plane *e* is the entry region.

For fully developed laminar flow in a straight, circular tube, by experiment, the Reynolds number, $N_{\mathrm{Re}} = D\bar{u}_x\rho/\mu$, where $\bar{u}_x$ is the flow-average velocity in the axial direction, x, and D is the inside diameter of the tube, must be less than 2,100. For this condition, the equation of motion in the axial direction for horizontal flow and constant properties is

$$\frac{\mu}{r}\frac{\partial}{\partial r}\left(r\frac{\partial u_x}{\partial r}\right) - \frac{dP}{dx} = 0 \tag{3-139}$$

where the boundary conditions are

$$r = 0 \text{ (axis of the tube)}, \quad \partial u_x/\partial r = 0$$
and $$r = r_w \text{(tube wall)}, \quad u_x = 0$$

Equation (3-139) was integrated by Hagen in 1839 and Poiseuille in 1841. The resulting equation for the velocity profile, expressed in terms of the flow-average velocity, is

$$u_x = 2\bar{u}_x\left[1 - \left(\frac{r}{r_w}\right)^2\right] \tag{3-140}$$

or, in terms of the maximum velocity at the tube axis,

$$u_x = u_{x_{\max}}\left[1 - \left(\frac{r}{r_w}\right)^2\right] \tag{3-141}$$

From the form of (3-141), the velocity profile is parabolic in nature.

The shear stress, pressure drop, and Fanning friction factor are obtained from solutions to (3-139):

$$\tau_w = -\mu\left(\frac{\partial u_x}{\partial r}\right)\bigg|_{r=r_w} = \frac{4\mu\bar{u}_x}{r_w} \tag{3-142}$$

$$-\frac{dP}{dx} = \frac{32\mu\bar{u}_x}{D^2} = \frac{2f\rho\bar{u}_x^2}{D} \tag{3-143}$$

with

$$f = \frac{16}{N_{\mathrm{Re}}} \tag{3-144}$$

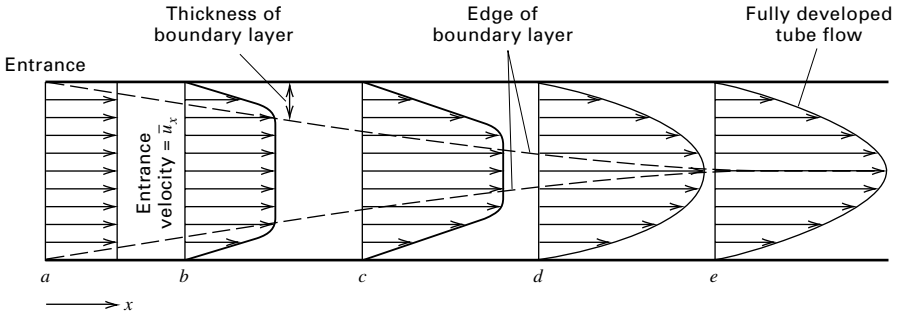

Figure 3.15 Buildup of a laminar velocity boundary layer for flow in a straight, circular tube.

The entry length to achieve fully developed flow is defined as the axial distance, L_e, from the entrance to the point at which the centerline velocity is 99% of the fully developed flow value. From the analysis of Langhaar [43] for the entry region,

$$\frac{L_e}{D} = 0.0575 N_{\text{Re}} \tag{3-145}$$

Thus, at the upper limit of laminar flow, $N_{\text{Re}} = 2{,}100$, $L_e/D = 121$, a rather large ratio. For $N_{\text{Re}} = 100$, the ratio is only 5.75. In the entry region, Langhaar's analysis shows the friction factor is considerably higher than the fully developed flow value given by (3-144). At $x = 0$, f is infinity, but then decreases exponentially with x, approaching the fully developed flow value at L_e. For example, for $N_{\text{Re}} = 1{,}000$, (3-144) gives $f = 0.016$, with $L_e/D = 57.5$. In the region from $x = 0$ to $x/D = 5.35$, the average friction factor from Langhaar is 0.0487, which is about three times higher than the fully developed value.

In 1885, Graetz [44] obtained a theoretical solution to the problem of convective heat transfer between the wall of a circular tube, held at a constant temperature, and a fluid flowing through the tube in fully developed laminar flow. Assuming constant properties and negligible conduction in the axial direction, the energy equation, after substituting (3-140) for u_x, is

$$2\bar{u}_x \left[1 - \left(\frac{r}{r_w}\right)^2\right] \frac{\partial T}{\partial x} = \frac{k}{\rho C_P} \left[\frac{1}{r}\frac{\partial}{\partial r}\left(r\frac{\partial T}{\partial r}\right)\right] \tag{3-146}$$

The boundary conditions are

$$x = 0 \text{ (where heat transfer begins)}, \quad T = T_0, \text{ for all } r$$

$$x > 0, \quad r = r_w, \quad T = T_i \qquad x > 0, \quad r = 0, \quad \partial T/\partial r = 0$$

The analogous species continuity equation for mass transfer, neglecting bulk flow in the radial direction and diffusion in the axial direction, is

$$2\bar{u}_x \left[1 - \left(\frac{r}{r_w}\right)^2\right] \frac{\partial c_{\text{A}}}{\partial x} = D_{\text{AB}} \left[\frac{1}{r}\frac{\partial}{\partial r}\left(r\frac{\partial c_{\text{A}}}{\partial r}\right)\right] \tag{3-147}$$

with analogous boundary conditions.

The Graetz solution of (3-147) for the temperature profile or the concentration profile is in the form of an infinite series, and can be obtained from (3-146) by the method of separation of variables using the method of Frobenius. A detailed solution is given by Sellars, Tribus, and Klein [45]. From the concentration profile, expressions for the mass-transfer coefficient and the Sherwood number are obtained. When x is large, the concentration profile is fully developed and the local Sherwood number, N_{Sh_x}, approaches a limiting value of 3.656. At the other extreme, when x is small such that the concentration boundary layer is very thin and confined to a region where the fully developed velocity profile is linear, the local Sherwood number is obtained from the classic Leveque [46] solution, presented by Knudsen and Katz [47]:

$$N_{\text{Sh}_x} = \frac{k_{c_x} D}{D_{\text{AB}}} = 1.077 \left[\frac{N_{\text{Pe}_{\text{M}}}}{(x/D)}\right]^{1/3} \tag{3-148}$$

where

$$N_{\text{Pe}_{\text{M}}} = \frac{D\bar{u}_x}{D_{\text{AB}}} \tag{3-149}$$

The limiting solutions, together with the general Graetz solution, are shown in Figure 3.16, where it is seen that $N_{\text{Sh}_x} = 3.656$ is valid for $N_{\text{Pe}_{\text{M}}}/(x/D) < 4$ and (3-148) is valid for $N_{\text{Pe}_{\text{M}}}/(x/D) > 100$. The two limiting solutions can be patched together if one point of the general solution is available where the two solutions intersect.

Over a length of tube where mass transfer occurs, an average Sherwood number can be derived by integrating the general expression for the local Sherwood number. An empirical representation for that average, proposed by Hausen [48], is

$$N_{\text{Sh}_{\text{avg}}} = 3.66 + \frac{0.0668[N_{\text{Pe}_{\text{M}}}/(x/D)]}{1 + 0.04[N_{\text{Pe}_{\text{M}}}/(x/D)]^{2/3}} \tag{3-150}$$

which is based on a log-mean concentration driving force.

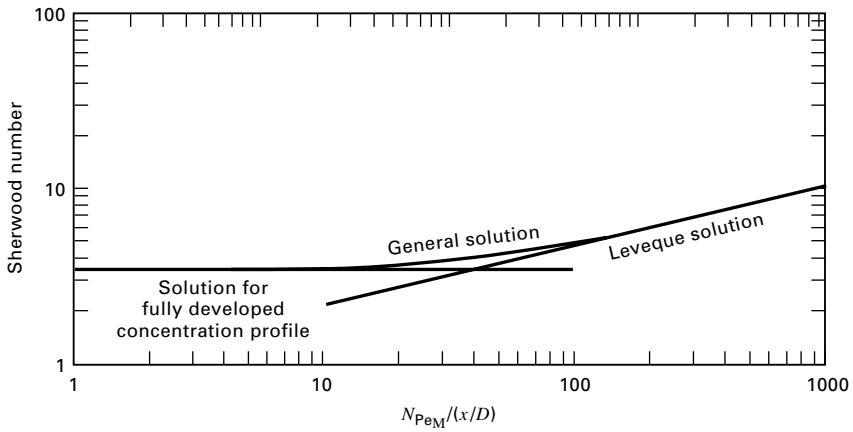

Figure 3.16 Limiting and general solutions for mass transfer to a fluid in laminar flow in a straight, circular tube.

EXAMPLE 3.15

Linton and Sherwood [49] conducted experiments on the dissolution of cast tubes of benzoic acid (A) into water (B) flowing through the tubes in laminar flow. They obtained good agreement with predictions based on the Graetz and Leveque equations. Consider a 5.23-cm-inside-diameter by 32-cm-long tube of benzoic acid, preceded by 400 cm of straight metal pipe of the same inside diameter where a fully developed velocity profile is established. Pure water enters the system at 25°C at a velocity corresponding to a Reynolds number of 100. Based on the following property data at 25°C, estimate the average concentration of benzoic acid in the water leaving the cast tube before a significant increase in the inside diameter of the benzoic acid tube occurs because of dissolution.

Solubility of benzoic acid in water = 0.0034 g/cm^3

Viscosity of water = 0.89 cP = 0.0089 g/cm-s

Diffusivity of benzoic acid in water at infinite dilution = 9.18×10^{-6} cm^2/s

SOLUTION

$$N_{Sc} = \frac{0.0089}{(1.0)(9.18 \times 10^{-6})} = 970$$

$$N_{Re} = \frac{D\bar{u}_x \rho}{\mu} = 100$$

from which

$$\bar{u}_x = \frac{(100)(0.0089)}{(5.23)(1.0)} = 0.170 \text{ cm/s}$$

From (3-149),

$$N_{Pe_M} = \frac{(5.23)(0.170)}{9.18 \times 10^{-6}} = 9.69 \times 10^4$$

$$\frac{x}{D} = \frac{32}{5.23} = 6.12$$

$$\frac{N_{Pe_M}}{(x/D)} = \frac{9.69 \times 10^4}{6.12} = 1.58 \times 10^4$$

From (3-150),

$$N_{Sh_{avg}} = 3.66 + \frac{0.0668(1.58 \times 10^4)}{1 + 0.04(1.58 \times 10^4)^{2/3}} = 44$$

$$k_{c_{avg}} = N_{Sh_{avg}} \left(\frac{D_{AB}}{D}\right) = 44 \frac{(9.18 \times 10^{-6})}{5.23} = 7.7 \times 10^{-5} \text{ cm/s}$$

Using a log-mean driving force,

$$n_A = \bar{u}_x S(\bar{c}_{A_x} - c_{A_0}) = k_{c_{avg}} A \frac{[(c_{A_i} - c_{A_0}) - (c_{A_i} - \bar{c}_{A_x})]}{\ln[(c_{A_i} - c_{A_0})/(c_{A_i} - \bar{c}_{A_x})]}$$

where S is the cross-sectional area for flow. Simplifying,

$$\ln\left(\frac{c_{A_i} - c_{A_0}}{c_{A_i} - \bar{c}_{A_x}}\right) = \frac{k_{c_{avg}} A}{\bar{u}_x S}$$

$$c_{A_0} = 0 \quad \text{and} \quad c_{A_i} = 0.0034 \text{ g/cm}^3$$

$$S = \frac{\pi D^2}{4} = \frac{(3.14)(5.23)^2}{4} = 21.5 \text{ cm}^2 \quad \text{and}$$

$$A = \pi D x = (3.14)(5.23)(32) = 526 \text{ cm}^2$$

$$\ln\left(\frac{0.0034}{0.0034 - \bar{c}_{A_x}}\right) = \frac{(7.7 \times 10^{-5})(526)}{(0.170)(21.5)} = 0.0111$$

$$\bar{c}_{A_x} = 0.0034 - \frac{0.0034}{e^{0.0111}} = 0.000038 \text{ g/cm}^3$$

Thus, the concentration of benzoic acid in the water leaving the cast tube is far from saturation.

3.5 MASS TRANSFER IN TURBULENT FLOW

In the two previous sections, diffusion in stagnant media and in laminar flow were considered. For both cases, Fick's law can be applied to obtain rates of mass transfer. A more common occurrence in engineering is turbulent flow, which is accompanied by much higher transport rates, but for which theory is still under development and the estimation of mass-transfer rates relies more on empirical correlations of experimental data and analogies with heat and momentum transfer. A summary of the dimensionless groups used in these correlations and the analogies is given in Table 3.13.

As shown by the famous dye experiment of Osborne Reynolds [50] in 1883, a fluid in laminar flow moves parallel to the solid boundaries in streamline patterns. Every particle of fluid moves with the same velocity along a streamline and there are no fluid velocity components normal to these streamlines. For a Newtonian fluid in laminar flow, the momentum transfer, heat transfer, and mass transfer are by molecular transport, governed by Newton's law of viscosity, Fourier's law of heat conduction, and Fick's law of molecular diffusion, respectively.

In turbulent flow, the rates of momentum, heat, and mass transfer are orders of magnitude greater than for molecular transport. This occurs because streamlines no longer exist and particles or eddies of fluid, which are large compared to the mean free path of the molecules in the fluid, mix with each other by moving from one region to another in fluctuating motion. This eddy mixing by velocity fluctuations occurs not only in the direction of flow but also in directions normal to flow, with the latter being of more interest. Momentum, heat, and mass transfer now occur by two parallel mechanisms: (1) molecular motion, which is slow; and (2) turbulent or eddy motion, which is rapid except near a solid surface, where the flow velocity accompanying turbulence decreases to zero. Mass transfer by bulk flow may also occur as given by (3-1).

In 1877, Boussinesq [51] modified Newton's law of viscosity to account for eddy motion. Analogous expressions were subsequently developed for turbulent-flow heat and mass transfer. For flow in the x-direction and transport in the z-direction normal to flow, these expressions are written in the following forms in the absence of bulk flow in the z-direction:

$$\tau_{zx} = -(\mu + \mu_t)\frac{du_x}{dz} \tag{3-151}$$

$$q_z = -(k + k_t)\frac{dT}{dz} \tag{3-152}$$

$$N_{A_z} = -(D_{AB} + D_t)\frac{dc_A}{dz} \tag{3-153}$$

where the double subscript, zx, on the shear stress, τ, stands for x-momentum in the z-direction. The molecular contributions, μ, k, and D_{AB}, are molecular properties of the fluid and depend on chemical composition, temperature, and pressure; the turbulent contributions, μ_t, k_t, and D_t, depend on the

Table 3.13 Some Useful Dimensionless Groups

Name	Formula	Meaning	Analogy
	Fluid Mechanics		
Drag Coefficient	$C_D = \dfrac{2F_D}{Au^2\rho}$	$\dfrac{\text{Drag force}}{\text{Projected area} \times \text{Velocity head}}$	
Fanning Friction Factor	$f = \dfrac{\Delta P}{L}\dfrac{D}{2\bar{u}^2\rho}$	$\dfrac{\text{Pipe wall shear stress}}{\text{Velocity head}}$	
Froude Number	$N_{\text{Fr}} = \dfrac{\bar{u}^2}{gL}$	$\dfrac{\text{Inertial force}}{\text{Gravitational force}}$	
Reynolds Number	$N_{\text{Re}} = \dfrac{L\bar{u}\rho}{\mu} = \dfrac{L\bar{u}}{\nu} = \dfrac{LG}{\mu}$	$\dfrac{\text{Inertial force}}{\text{Viscous force}}$	
Weber Number	$N_{\text{We}} = \dfrac{\bar{u}^2\rho L}{\sigma}$	$\dfrac{\text{Inertial force}}{\text{Surface-tension force}}$	
	Heat Transfer		
j-Factor for Heat Transfer	$j_H = N_{\text{St}_\text{H}}(N_{\text{Pr}})^{2/3}$		j_M
Nusselt Number	$N_{\text{Nu}} = \dfrac{hL}{k}$	$\dfrac{\text{Convective heat transfer}}{\text{Conductive heat transfer}}$	N_{Sh}
Peclet Number for Heat Transfer	$N_{\text{Pe}_\text{H}} = N_{\text{Re}}N_{\text{Pr}} = \dfrac{L\bar{u}\rho C_P}{k}$	$\dfrac{\text{Bulk transfer of heat}}{\text{Conductive heat transfer}}$	N_{Pe_M}
Prandtl Number	$N_{\text{Pr}} = \dfrac{C_P\mu}{k} = \dfrac{\nu}{\alpha}$	$\dfrac{\text{Momentum diffusivity}}{\text{Thermal diffusivity}}$	N_{Sc}
Stanton Number for Heat Transfer	$N_{\text{St}_\text{H}} = \dfrac{N_{\text{Nu}}}{N_{\text{Re}}N_{\text{Pr}}} = \dfrac{h}{C_P G}$	$\dfrac{\text{Heat transfer}}{\text{Thermal capacity}}$	N_{St_M}
	Mass Transfer		
j-Factor for Mass Transfer	$j_M = N_{\text{St}_\text{M}}(N_{\text{Sc}})^{2/3}$		j_H
Lewis Number	$N_{\text{Le}} = \dfrac{N_{\text{Sc}}}{N_{\text{Pr}}} = \dfrac{k}{\rho C_P D_{\text{AB}}} = \dfrac{\alpha}{D_{\text{AB}}}$	$\dfrac{\text{Thermal diffusivity}}{\text{Mass diffusivity}}$	
Peclet Number for Mass Transfer	$N_{\text{Pe}_\text{M}} = N_{\text{Re}}N_{\text{Sc}} = \dfrac{L\bar{u}}{D_{\text{AB}}}$	$\dfrac{\text{Bulk transfer of mass}}{\text{Molecular diffusion}}$	N_{Pe_H}
Schmidt Number	$N_{\text{Sc}} = \dfrac{\mu}{\rho D_{\text{AB}}} = \dfrac{\nu}{D_{\text{AB}}}$	$\dfrac{\text{Momentum diffusivity}}{\text{Mass diffusivity}}$	N_{Pr}
Sherwood Number	$N_{\text{Sh}} = \dfrac{k_c L}{D_{\text{AB}}}$	$\dfrac{\text{Convective mass transfer}}{\text{Molecular diffusion}}$	N_{Nu}
Stanton Number for Mass Transfer	$N_{\text{St}_\text{M}} = \dfrac{N_{\text{Sh}}}{N_{\text{Re}}N_{\text{Sc}}} = \dfrac{k_c}{\bar{u}\rho}$	$\dfrac{\text{Mass transfer}}{\text{Mass capacity}}$	N_{St_H}

L = characteristic length G = mass velocity = $\overline{u}\rho$

Subscripts: M = mass transfer H = heat transfer

mean fluid velocity in the direction of flow and on position in the fluid with respect to the solid boundaries.

In 1925, in an attempt to quantify turbulent transport, Prandtl [52] developed an expression for μ_t in terms of an eddy mixing length, l, which is a function of position. The eddy mixing length is a measure of the average distance that an eddy travels before it loses its identity and mingles with other eddies. The mixing length is analogous to the mean free path of gas molecules, which is the average distance a molecule travels before it collides with another molecule. By analogy, the same mixing length is valid for turbulent-flow heat transfer and mass transfer. To use this analogy, (3-151) to (3-153) are rewritten in diffusivity form:

$$\frac{\tau_{zx}}{\rho} = -(\nu + \epsilon_M)\frac{du_x}{dz} \tag{3-154}$$

$$\frac{q_z}{C_P\rho} = -(\alpha + \epsilon_H)\frac{dT}{dz} \tag{3-155}$$

$$N_{\text{A}_z} = -(D_{\text{AB}} + \epsilon_D)\frac{dc_{\text{A}}}{dz} \tag{3-156}$$

where ϵ_M, ϵ_H, are ϵ_D are momentum, heat, and mass eddy diffusivities, respectively; ν is the momentum diffusivity (kinematic viscosity), μ/ρ; and α is the thermal diffusivity, $k/\rho C_P$. As a first approximation, the three eddy diffusivities may be assumed equal. This assumption is reasonably valid for ϵ_H and ϵ_D, but experimental data indicate that $\epsilon_M/\epsilon_H = \epsilon_M/\epsilon_D$ is sometimes less than 1.0 and as low as 0.5 for turbulence in a free jet.

Reynolds Analogy

If (3-154) to (3-156) are applied at a solid boundary, they can be used to determine transport fluxes based on transport coefficients, with driving forces from the wall, i, at $z = 0$, to the bulk fluid, designated with an overbar, $^-$:

$$\frac{\tau_{zx}}{\bar{u}_x} = -(\nu + \epsilon_M)\left.\frac{d(\rho u_x/\bar{u}_x)}{dz}\right|_{z=0} = \frac{f\rho}{2}\bar{u}_x \tag{3-157}$$

$$q_z = -(\alpha + \epsilon_H)\left.\frac{d(\rho C_P T)}{dz}\right|_{z=0} = h(T_i - \bar{T}) \tag{3-158}$$

$$N_{A_z} = -(D_{AB} + \epsilon_D)\left.\frac{dc_A}{dz}\right|_{z=0} = k_c(c_{A_i} - \bar{c}_A) \tag{3-159}$$

We define dimensionless velocity, temperature, and solute concentration by

$$\theta = \frac{u_x}{\bar{u}_x} = \frac{T_i - T}{T_i - \bar{T}} = \frac{c_{A_i} - c_A}{c_{A_i} - \bar{c}_A} \tag{3-160}$$

If (3-160) is substituted into (3-157) to (3-159),

$$\left.\frac{\partial\theta}{\partial z}\right|_{z=0} = \frac{f\bar{u}_x}{2(\nu + \epsilon_M)} = \frac{h}{\rho C_P(\alpha + \epsilon_H)} = \frac{k_c}{(D_{AB} + \epsilon_D)} \tag{3-161}$$

This equation defines the analogies among momentum, heat, and mass transfer. Assuming that the three eddy diffusivities are equal and that the molecular diffusivities are either everywhere negligible or equal,

$$\frac{f}{2} = \frac{h}{\rho C_P \bar{u}_x} = \frac{k_c}{\bar{u}_x} \tag{3-162}$$

Equation (3-162) defines the Stanton number for heat transfer,

$$N_{St_H} = \frac{h}{\rho C_P \bar{u}_x} = \frac{h}{GC_P} \tag{3-163}$$

where G = mass velocity $= \bar{u}_x\rho$, and the Stanton number for mass transfer,

$$N_{St_M} = \frac{k_c}{\bar{u}_x} = \frac{k_c\rho}{G} \tag{3-164}$$

both of which are included in Table 3.13.

Equation (3-162) is referred to as the Reynolds analogy. It can be used to estimate values of heat and mass transfer coefficients from experimental measurements of the Fanning friction factor for turbulent flow, but only when $N_{Pr} = N_{Sc} = 1$. Thus, the Reynolds analogy has limited practical value and is rarely applied in practice. Reynolds postulated the existence of the analogy in 1874 [53] and derived it in 1883 [50].

Chilton–Colburn Analogy

A widely used extension of the Reynolds analogy to Prandtl and Schmidt numbers other than 1 was presented by Colburn [54] for heat transfer and by Chilton and Colburn [55] for mass transfer. They showed that the Reynolds analogy for turbulent flow could be corrected for differences in velocity, temperature, and concentration distributions by incorporating N_{Pr} and N_{Sc} into (3-162) to define the following three Chilton–Colburn j-factors, included in Table 3.13.

$$j_M \equiv \frac{f}{2} = j_H \equiv \frac{h}{GC_P}(N_{Pr})^{2/3} = j_D \equiv \frac{k_c\rho}{G}(N_{Sc})^{2/3} \tag{3-165}$$

Equation (3-165) is the Chilton–Colburn analogy or the Colburn analogy for estimating average transport coefficients for turbulent flow. When $N_{Pr} = N_{Sc} = 1$, (3-165) reduces to (3-162).

In general, j-factors are uniquely determined by the geometric configuration and the Reynolds number. Based on the analysis, over many years, of experimental data on momentum, heat, and mass transfer, the following representative correlations have been developed for turbulent transport to or from smooth surfaces. Other correlations are presented in other chapters. In general, these correlations are reasonably accurate for N_{Pr} and N_{Sc} in the range of 0.5 to 10, but should be used with caution outside this range.

1. Flow through a straight, circular tube of inside diameter D:

$$j_M = j_H = j_D = 0.023(N_{Re})^{-0.2} \quad \text{for} \quad 10{,}000 < N_{Re} = DG/\mu < 1{,}000{,}000 \tag{3-166}$$

2. Average transport coefficients for flow across a flat plate of length L:

$$j_M = j_H = j_D = 0.037(N_{Re})^{-0.2} \quad \text{for} \quad 5 \times 10^5 < N_{Re} = Lu_o\rho/\mu < 5 \times 10^8 \tag{3-167}$$

3. Average transport coefficients for flow normal to a long, circular cylinder of diameter D, where the drag coefficient includes both form drag and skin friction, but only the skin friction contribution applies to the analogy:

$$(j_M)_{\text{skin friction}} = j_H = j_D = 0.193(N_{Re})^{-0.382} \quad \text{for} \quad 4{,}000 < N_{Re} < 40{,}000 \tag{3-168}$$

$$(j_M)_{\text{skin friction}} = j_H = j_D = 0.0266(N_{Re})^{-0.195} \quad \text{for} \quad 40{,}000 < N_{Re} < 250{,}000 \tag{3-169}$$

with $$N_{Re} = \frac{DG}{\mu}$$

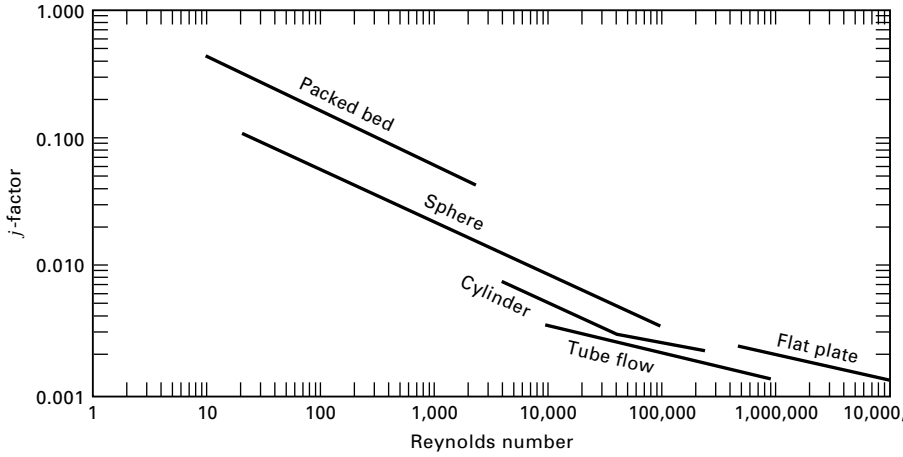

Figure 3.17 Chilton–Colburn j-factor correlations.

4. Average transport coefficients for flow past a single sphere of diameter D:

$$(j_M)_{\text{skin friction}} = j_H = j_D = 0.37(N_{\text{Re}})^{-0.4}$$
$$\text{for} \quad 20 < N_{\text{Re}} = \frac{DG}{\mu} < 100{,}000 \tag{3-170}$$

5. Average transport coefficients for flow through beds packed with spherical particles of uniform size D_P:

$$j_H = j_D = 1.17(N_{\text{Re}})^{-0.415}$$
$$\text{for} \quad 10 < N_{\text{Re}} = \frac{D_P G}{\mu} < 2{,}500 \tag{3-171}$$

The above correlations are plotted in Figure 3.17, where the curves do not coincide because of the differing definitions of the Reynolds number. However, the curves are not widely separated. When using the correlations in the presence of appreciable temperature and/or composition differences, Chilton and Colburn recommend that N_{Pr} and N_{Sc} be evaluated at the average conditions from the surface to the bulk stream.

Other Analogies

New turbulence theories have led to improvements and extensions of the Reynolds analogy, resulting in expressions for the Fanning friction factor and the Stanton numbers for heat and mass transfer that are less empirical than the Chilton–Colburn analogy. The first major improvement was by Prandtl [56] in 1910, who divided the flow into two regions: (1) a thin laminar-flow sublayer of thickness δ next to the wall boundary, where only molecular transport occurs; and (2) a turbulent region dominated by eddy transport, with $\epsilon_M = \epsilon_H = \epsilon_D$.

Further important theoretical improvements to the Reynolds analogy were made by von Karman, Martinelli, and Deissler, as discussed in detail by Knudsen and Katz [47]. The first two investigators inserted a buffer zone between the laminar sublayer and turbulent core. Deissler gradually reduced the eddy diffusivities as the wall was approached.

Other improvements were made by van Driest [64], who used a modified form of the Prandtl mixing length, Reichardt [65], who eliminated the zone concept by allowing the eddy diffusivities to decrease continuously from a maximum to zero at the wall, and Friend and Metzner [57], who modified the approach of Reichardt to obtain improved accuracy at very high Prandtl and Schmidt numbers (to 3,000). Their results for turbulent flow through a straight, circular tube are

$$N_{\text{St}_\text{H}} = \frac{f/2}{1.20 + 11.8\sqrt{f/2}(N_{\text{Pr}} - 1)(N_{\text{Pr}})^{-1/3}} \tag{3-172}$$

$$N_{\text{St}_\text{M}} = \frac{f/2}{1.20 + 11.8\sqrt{f/2}(N_{\text{Sc}} - 1)(N_{\text{Sc}})^{-1/3}} \tag{3-173}$$

Over a wide range of Reynolds number (10,000–10,000,000), the Fanning friction factor is estimated from the explicit empirical correlation of Drew, Koo, and McAdams [66],

$$f = 0.00140 + 0.125(N_{\text{Re}})^{-0.32} \tag{3-174}$$

which is in excellent agreement with the experimental data of Nikuradse [67] and is preferred over (3-165) with (3-166), which is valid only to $N_{\text{Re}} = 1{,}000{,}000$. For two- and three-dimensional turbulent-flow problems, some success has been achieved with the κ (kinetic energy of turbulence)–ϵ (rate of dissipation) model of Launder and Spalding [68], which is widely used in computational fluid dynamics (CFD) computer programs.

Theoretical Analogy of Churchill and Zajic

An alternative to (3-151) to (3-153) or the equivalent diffusivity forms of (3-154) to (3-156) for the development of transport equations for turbulent flow is to start with the time-averaged equations of Newton, Fourier, and Fick. For example, let us derive a form of Newton's law of viscosity for molecular and turbulent transport of momentum in parallel. In a turbulent-flow field in the axial x-direction, instantaneous velocity components, u_x and u_z, are

$$u_x = \bar{u}_x + u'_x$$
$$u_z = u'_z$$

where the "overbarred" component is the time-averaged (mean) local velocity and the primed component is the local fluctuating component that denotes instantaneous deviation from the local mean value. The mean velocity in the perpendicular z-direction is zero. The mean local velocity in the x-direction over a long period Θ of time θ is given by

$$\bar{u}_x = \frac{1}{\Theta}\int_0^{\Theta} u_x d\theta = \frac{1}{\Theta}\int_0^{\Theta} (\bar{u}_x + u'_x)\, d\theta \qquad (3\text{-}175)$$

The time-averaged fluctuating components u'_x and u'_z equal zero.

The local instantaneous rate of momentum transfer by turbulence in the z-direction of x-direction turbulent momentum per unit area at constant density is

$$\rho u'_z(\bar{u}_x + u'_x) \qquad (3\text{-}176)$$

The time-average of this turbulent momentum transfer is equal to the turbulent component of the shear stress, τ_{zx_t},

$$\begin{aligned}\tau_{zx_t} &= \frac{\rho}{\Theta}\int_0^{\Theta} u'_z(\bar{u}_x + u'_x)\, d\theta \\ &= \frac{\rho}{\Theta}\left[\int_0^{\Theta} u'_z(\bar{u}_x)\, d\theta + \int_0^{\Theta} u'_z(u'_x)\, d\theta\right]\end{aligned} \qquad (3\text{-}177)$$

Because the time-average of the first term is zero, (3-177) reduces to

$$\tau_{zx_t} = \rho(\overline{u'_z u'_x}) \qquad (3\text{-}178)$$

which is referred to as a Reynolds stress. Combining (3-178) with the molecular component of momentum transfer gives the turbulent-flow form of Newton's law of viscosity,

$$\tau_{zx} = -\mu\frac{du_x}{dz} + \rho(\overline{u'_z u'_x}) \qquad (3\text{-}179)$$

If (3-179) is compared to (3-151), it is seen that an alternative approach to turbulence is to develop a correlating equation for the Reynolds stress, $(\overline{u'_z u'_x})$, first introduced by Churchill and Chan [73], rather than an expression for a turbulent viscosity μ_t. This stress, which is a complex function of position and rate of flow, has been correlated quite accurately for fully developed turbulent flow in a straight, circular tube by Heng, Chan, and Churchill [69]. In generalized form, with a the radius of the tube and $y = (a - z)$ the distance from the inside wall to the center of the tube, their equation is

$$\begin{aligned}(\overline{u'_z u'_x})^{++} = \Bigg(&\left[0.7\left(\frac{y^+}{10}\right)^3\right]^{-8/7} + \left|\exp\left\{\frac{-1}{0.436y^+}\right\}\right. \\ &\left. - \frac{1}{0.436a^+}\left(1 + \frac{6.95y^+}{a^+}\right)\right|^{-8/7}\Bigg)^{-7/8}\end{aligned} \qquad (3\text{-}180)$$

where

$$\begin{aligned}(\overline{u'_z u'_x})^{++} &= -\rho\overline{u'_z u'_x}/\tau \\ a^+ &= a(\tau_w\rho)^{1/2}/\mu \\ y^+ &= y(\tau_w\rho)^{1/2}/\mu\end{aligned}$$

Equation (3-180) is a highly accurate quantitative representation of turbulent flow because it is based on experimental data and numerical simulations described by Churchill and Zajic [70] and in considerable detail by Churchill [71]. From (3-142) and (3-143), the shear stress at the wall, τ_w, is related to the Fanning friction factor by

$$f = \frac{2\tau_w}{\rho\bar{u}_x^2} \qquad (3\text{-}181)$$

where $\bar{u}_x$ is the flow-average velocity in the axial direction. Combining (3-179) with (3-181) and performing the required integrations, both numerically and analytically, lead to the following implicit equation for the Fanning friction factor as a function of the Reynolds number, $N_{\mathrm{Re}} = 2a\bar{u}_x\rho/\mu$:

$$\begin{aligned}\left(\frac{2}{f}\right)^{1/2} = 3.2 &- 227\frac{\left(\frac{2}{f}\right)^{1/2}}{\frac{N_{\mathrm{Re}}}{2}} + 2500\left[\frac{\left(\frac{2}{f}\right)^{1/2}}{\frac{N_{\mathrm{Re}}}{2}}\right]^2 \\ &+ \frac{1}{0.436}\ln\left[\frac{\frac{N_{\mathrm{Re}}}{2}}{\left(\frac{2}{f}\right)^{1/2}}\right]\end{aligned} \qquad (3\text{-}182)$$

This equation is in excellent agreement with experimental data over a Reynolds number range of 4,000–3,000,000 and can probably be used to a Reynolds number of 100,000,000. Table 3.14 presents a comparison of the Churchill–Zajic equation, (3-182), with (3-174) of Drew et al. and (3-166) of Chilton and Colburn. Equation (3-174) gives satisfactory agreement for Reynolds numbers from 10,000 to 10,000,000, while (3-166) is useful only from 100,000 to 1,000,000.

Churchill and Zajic [70] show that if the equation for the conservation of energy is time averaged, a turbulent-flow form of Fourier's law of conduction can be obtained with the fluctuation term $(\overline{u'_z T'})$. Similar time averaging leads to a turbulent-flow form of Fick's law of diffusion with $(\overline{u'_z c'_{\mathrm{A}}})$. To extend (3-180) and (3-182) to obtain an expression for the Nusselt number for turbulent-flow convective heat transfer in a straight, circular tube, Churchill and Zajic employ an analogy that is free of empircism, but not exact. The result

Table 3.14 Comparison of Fanning Friction Factors for Fully Developed Turbulent Flow in a Smooth, Straight Circular Tube

N_{Re}	f, Drew et al. (3-174)	f, Chilton–Colburn (3-166)	f, Churchill–Zajic (3-182)
10,000	0.007960	0.007291	0.008087
100,000	0.004540	0.004600	0.004559
1,000,000	0.002903	0.002902	0.002998
10,000,000	0.002119	0.001831	0.002119
100,000,000	0.001744	0.001155	0.001573

for Prandtl numbers greater than 1 is

$$N_{\mathrm{Nu}} = \frac{1}{\left(\dfrac{N_{\mathrm{Pr}_t}}{N_{\mathrm{Pr}}}\right)\dfrac{1}{N_{\mathrm{Nu}_1}} + \left[1 - \left(\dfrac{N_{\mathrm{Pr}_t}}{N_{\mathrm{Pr}}}\right)^{2/3}\right]\dfrac{1}{N_{\mathrm{Nu}_\infty}}} \tag{3-183}$$

where, from Yu, Ozoe, and Churchill [72],

$$N_{\mathrm{Pr}_t} = \text{turbulent Prandtl number} = 0.85 + \frac{0.015}{N_{\mathrm{Pr}}} \tag{3-184}$$

which replaces $(\overline{u'_z T'})$, as introduced by Churchill [74],

$$\begin{aligned} N_{\mathrm{Nu}_1} &= \text{Nusselt number for } (N_{\mathrm{Pr}} = N_{\mathrm{Pr}_t}) \\ &= \frac{N_{\mathrm{Re}}\left(\dfrac{f}{2}\right)}{1 + 145\left(\dfrac{2}{f}\right)^{-5/4}} \end{aligned} \tag{3-185}$$

$$\begin{aligned} N_{\mathrm{Nu}_\infty} &= \text{Nusselt number for } (N_{\mathrm{Pr}} = \infty) \\ &= 0.07343\left(\frac{N_{\mathrm{Pr}}}{N_{\mathrm{Pr}_t}}\right)^{1/3} N_{\mathrm{Re}}\left(\frac{f}{2}\right)^{1/2} \end{aligned} \tag{3-186}$$

The accuracy of (3-183) is due to (3-185) and (3-186), which are known from theoretical considerations. Although (3-184) is somewhat uncertain, its effect is negligible.

A comparison of the Churchill et al. correlation of (3-183) with the Nusselt forms of (3-172) of Friend and Metzner and (3-166) of Chilton and Colburn, where from Table 3.13, $N_{\mathrm{Nu}} = N_{\mathrm{St}} N_{\mathrm{Re}} N_{\mathrm{Pr}}$, is given in Table 3.15 for a wide range of Reynolds number and Prandtl numbers of 1 and 1,000.

In Table 3.15, at a Prandtl number of 1, which is typical of low-viscosity liquids and close to that of most gases, the Chilton–Colburn correlation, which is widely used, is within 10% of the more theoretically based Churchill–Zajic equation for Reynolds numbers up to 1,000,000. However, beyond that, serious deviations occur (25% at $N_{\mathrm{Re}} = 10{,}000{,}000$ and almost 50% at $N_{\mathrm{Re}} = 100{,}000{,}000$). Deviations of the Friend–Metzner correlation from the Churchill–Zajic equation vary from about 15% to 30% over the entire range of Reynolds number in Table 3.15. At all Reynolds numbers, the Churchill–Zajic equation predicts higher Nusselt numbers and, therefore, higher heat-transfer coefficients.

At a Prandtl number of 1,000, which is typical of high-viscosity liquids, the Friend–Metzner correlation is in fairly close agreement with the Churchill–Zajic equation, predicting values from 6 to 13% higher. The Chilton–Colburn correlation is seriously in error over the entire range of Reynolds number, predicting values ranging from 74 to 27% of those from the Churchill–Zajic equation as the Reynolds number increases. It is clear that the Chilton–Colburn correlation should not be used at high Prandtl numbers for heat transfer or (by analogy) at high Schmidt numbers for mass transfer.

The Churchill–Zajic equation for predicting the Nusselt number provides an effective power dependence on the Reynolds number as the Reynolds number increases. This is in contrast to the typically cited constant exponent of 0.8, as in the Chilton–Colburn correlation. For the Churchill–Zajic equation, at a Prandtl number of 1, the exponent increases with Reynolds number from 0.79 to 0.88; at a Prandtl number of 1,000, the exponent increases from 0.87 to 0.93.

Extension of the Churchill–Zajic equation to low Prandtl numbers, typical of molten metals, and to other geometries, such as parallel plates, is discussed by Churchill [71], who also considers the important effect of boundary conditions

Table 3.15 Comparison of Nusselt Numbers for Fully Developed Turbulent Flow in a Smooth, Straight Circular Tube

Prandtl number, $N_{\mathrm{Pr}} = 1$			
N_{Re}	N_{Nu}, Friend–Metzner (3-172)	N_{Nu}, Chilton–Colburn (3-166)	N_{Nu}, Churchill–Zajic (3-183)
10,000	33.2	36.5	37.8
100,000	189	230	232
1,000,000	1210	1450	1580
10,000,000	8830	9160	11400
100,000,000	72700	57800	86000
Prandtl number, $N_{\mathrm{Pr}} = 1000$			
N_{Re}	N_{Nu}, Friend–Metzner (3-172)	N_{Nu}, Chilton–Colburn (3-166)	N_{Nu}, Churchill–Zajic (3-183)
10,000	527	365	491
100,000	3960	2300	3680
1,000,000	31500	14500	29800
10,000,000	267800	91600	249000
100,000,000	2420000	578000	2140000

(e.g., constant wall temperature and uniform heat flux) at low-to-moderate Prandtl numbers.

For calculation of convective mass-transfer coefficients, k_c, for turbulent flow of gases and liquids in straight, smooth, circular tubes, it is recommended that the Churchill–Zajic equation be employed by applying the analogy between heat and mass transfer. Thus, as illustrated in the following example, in (3-183) to (3-186), from Table 3.13, the Sherwood number, N_{Sh}, is substituted for the Nusselt number, N_{Nu}; and the Schmidt number, N_{Sc}, is substituted for the Prandtl number, N_{Pr}.

EXAMPLE 3.16

Linton and Sherwood [49] conducted experiments on the dissolving of cast tubes of cinnamic acid (A) into water (B) flowing through the tubes in turbulent flow. In one run, with a 5.23-cm-i.d. tube, $N_{\mathrm{Re}} = 35{,}800$, and $N_{\mathrm{Sc}} = 1{,}450$, they measured a Stanton number for mass transfer, $N_{\mathrm{St_M}}$, of 0.0000351. Compare this experimental value with predictions by the Reynolds, Chilton–Colburn, and Friend–Metzner analogies, and by the more theoretically-based Churchill–Zajic equation.

SOLUTION

From either (3-174) or (3-182), the Fanning friction factor is 0.00576.

Reynolds analogy:

From (3-162), $N_{\mathrm{St_M}} = \frac{f}{2} = 0.00576/2 = 0.00288$, which, as expected, is in poor agreement with the experimental value because the effect of Schmidt number is ignored.

Chilton–Colburn analogy:

From (3-165),

$$N_{\mathrm{St_M}} = \left(\frac{f}{2}\right) \Big/ (N_{\mathrm{Sc}})^{2/3} = \left(\frac{0.00576}{2}\right) \Big/ (1450)^{2/3} = 0.0000225,$$

which is 64% of the experimental value.

Friend–Metzner analogy:

From (3-173), $N_{\mathrm{St_M}} = 0.0000350$, which is almost identical to the experimental value.

Churchill–Zajic equation:

Using mass-transfer analogs,

$$\text{(3-184) gives } N_{\mathrm{Sc}_t} = 0.850$$
$$\text{(3-185) gives } N_{\mathrm{Sh}_1} = 94$$
$$\text{(3-186) gives } N_{\mathrm{Sh}_\infty} = 1686$$
$$\text{(3-183) gives } N_{\mathrm{Sh}} = 1680$$

From Table 3.13,

$$N_{\mathrm{St_M}} = \frac{N_{\mathrm{Sh}}}{N_{\mathrm{Re}} N_{\mathrm{Sc}}} = \frac{1680}{(35800)(1450)} = 0.0000324,$$

which is an acceptable 92% of the experimental value.

3.6 MODELS FOR MASS TRANSFER AT A FLUID–FLUID INTERFACE

In the three previous sections, diffusion and mass transfer within solids and fluids were considered, where the interface was a smooth solid surface. Of greater interest in separation processes is mass transfer across an interface between a gas and a liquid or between two liquid phases. Such interfaces exist in absorption, distillation, extraction, and stripping. At fluid–fluid interfaces, turbulence may persist to the interface. The following theoretical models have been developed to describe mass transfer between a fluid and such an interface.

Film Theory

A simple theoretical model for turbulent mass transfer to or from a fluid-phase boundary was suggested in 1904 by Nernst [58], who postulated that the entire resistance to mass transfer in a given turbulent phase is in a thin, stagnant region of that phase at the interface, called a film. This film is similar to the laminar sublayer that forms when a fluid flows in the turbulent regime parallel to a flat plate. This is shown schematically in Figure 3.18a for the case of a gas–liquid interface, where the gas is pure component A, which diffuses into nonvolatile liquid B. Thus, a process of absorption of A into liquid B takes place, without desorption of B into

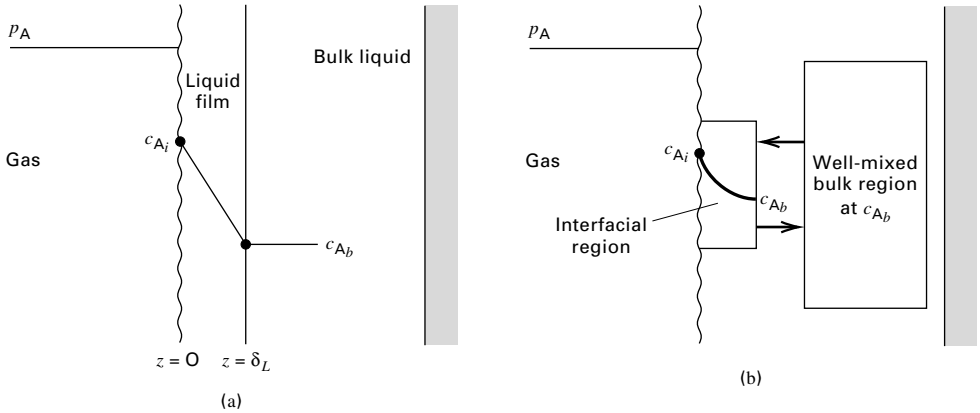

Figure 3.18 Theories for mass transfer from a fluid–fluid interface into a liquid: (a) film theory; (b) penetration and surface-renewal theories.

gaseous A. Because the gas is pure A at total pressure $P = p_A$, there is no resistance to mass transfer in the gas phase. At the gas–liquid interface, phase equilibrium is assumed so the concentration of A, c_{A_i}, is related to the partial pressure of A, p_A, by some form of Henry's law, for example, $c_{A_i} = H_A p_A$. In the thin, stagnant liquid film of thickness δ, molecular diffusion only occurs with a driving force of $c_{A_i} - c_{A_b}$. Since the film is assumed to be very thin, all of the diffusing A passes through the film and into the bulk liquid. If, in addition, bulk flow of A is neglected, the concentration gradient is linear as in Figure 3.18a. Accordingly, Fick's first law, (3-3a), for the diffusion flux integrates to

$$J_A = \frac{D_{AB}}{\delta}(c_{A_i} - c_{A_b}) = \frac{cD_{AB}}{\delta}(x_{A_i} - x_{A_b}) \qquad (3\text{-}187)$$

If the liquid phase is dilute in A, the bulk-flow effect can be neglected and (3-187) applies to the total flux:

$$N_A = \frac{D_{AB}}{\delta}(c_{A_i} - c_{A_b}) = \frac{cD_{AB}}{\delta}(x_{A_i} - x_{A_b}) \qquad (3\text{-}188)$$

If the bulk-flow effect is not negligible, then, from (3-31),

$$N_A = \frac{cD_{AB}}{\delta}\ln\left[\frac{1 - x_{A_b}}{1 - x_{A_i}}\right] = \frac{cD_{AB}}{\delta(1 - x_A)_{LM}}(x_{A_i} - x_{A_b}) \qquad (3\text{-}189)$$

where

$$(1 - x_A)_{LM} = \frac{x_{A_i} - x_{A_b}}{\ln[(1 - x_{A_b})/(1 - x_{A_i})]} = (x_B)_{LM} \qquad (3\text{-}190)$$

In practice, the ratios D_{AB}/δ in (3-188) and $D_{AB}/\delta(1 - x_A)_{LM}$ in (3-189) are replaced by mass transfer coefficients k_c and k'_c, respectively, because the film thickness, δ, which depends on the flow conditions, is not known and the subscript, c, refers to a concentration driving force.

The film theory, which is easy to understand and apply, is often criticized because it appears to predict that the rate of mass transfer is directly proportional to the molecular diffusivity. This dependency is at odds with experimental data, which indicate a dependency of D^n, where n ranges from about 0.5 to 0.75. However, if D_{AB}/δ is replaced with k_c, which is then estimated from the Chilton–Colburn analogy, Eq. (3-165), we obtain k_c proportional to $D_{AB}^{2/3}$, which is in better agreement with experimental data. In effect, δ depends on D_{AB} (or N_{Sc}). Regardless of whether the criticism of the film theory is valid, the theory has been and continues to be widely used in the design of mass-transfer separation equipment.

EXAMPLE 3.17

Sulfur dioxide is absorbed from air into water in a packed absorption tower. At a certain location in the tower, the mass-transfer flux is 0.0270 kmol SO_2/m^2-h and the liquid-phase mole fractions are 0.0025 and 0.0003, respectively, at the two-phase interface and in the bulk liquid. If the diffusivity of SO_2 in water is 1.7×10^{-5} cm^2/s, determine the mass-transfer coefficient, k_c, and the film thickness, neglecting the bulk-flow effect.

SOLUTION

$$N_{SO_2} = \frac{0.027(1{,}000)}{(3{,}600)(100)^2} = 7.5 \times 10^{-7}\,\frac{\text{mol}}{\text{cm}^2\text{-s}}$$

For dilute conditions, the concentration of water is

$$c = \frac{1}{18.02} = 5.55 \times 10^{-2}\ \text{mol/cm}^3$$

From (3-188),

$$k_c = \frac{D_{AB}}{\delta} = \frac{N_A}{c(x_{A_i} - x_{A_b})} = \frac{7.5 \times 10^{-7}}{5.55 \times 10^{-2}(0.0025 - 0.0003)} = 6.14 \times 10^{-3}\ \text{cm/s}$$

Therefore,

$$\delta = \frac{D_{AB}}{k_c} = \frac{1.7 \times 10^{-5}}{6.14 \times 10^{-3}} = 0.0028\ \text{cm}$$

which is very small and typical of turbulent-flow mass-transfer processes.

Penetration Theory

A more realistic physical model of mass transfer from a fluid–fluid interface into a bulk liquid stream is provided by the penetration theory of Higbie [59], shown schematically in Figure 3.18b. The stagnant-film concept is replaced by Boussinesq eddies that, during a cycle, (1) move from the bulk to the interface; (2) stay at the interface for a short, fixed period of time during which they remain static so that molecular diffusion takes place in a direction normal to the interface; and (3) leave the interface to mix with the bulk stream. When an eddy moves to the interface, it replaces another static eddy. Thus, the eddies are alternately static and moving. Turbulence extends to the interface.

In the penetration theory, unsteady-state diffusion takes place at the interface during the time the eddy is static. This process is governed by Fick's second law, (3-68), with boundary conditions

$$c_A = c_{A_b} \quad \text{at} \quad t = 0 \quad \text{for} \quad 0 \le z \le \infty;$$
$$c_A = c_{A_i} \quad \text{at} \quad z = 0 \quad \text{for} \quad t > 0; \quad \text{and}$$
$$c_A = c_{A_b} \quad \text{at} \quad z = \infty \quad \text{for} \quad t > 0$$

These are the same boundary conditions as in unsteady-state diffusion in a semi-infinite medium. Thus, the solution can be written by a rearrangement of (3-75):

$$\frac{c_{A_i} - c_A}{c_{A_i} - c_{A_b}} = \text{erf}\left(\frac{z}{2\sqrt{D_{AB}t_c}}\right) \qquad (3\text{-}191)$$

where t_c = "contact time" of the static eddy at the interface during one cycle. The corresponding average mass-transfer flux of A in the absence of bulk flow is given by the

following form of (3-79):

$$N_A = 2\sqrt{\frac{D_{AB}}{\pi t_c}}(c_{A_i} - c_{A_b}) \tag{3-192}$$

or

$$N_A = k_c(c_{A_i} - c_{A_b}) \tag{3-193}$$

Thus, the penetration theory gives

$$k_c = 2\sqrt{\frac{D_{AB}}{\pi t_c}} \tag{3-194}$$

which predicts that k_c is proportional to the square root of the molecular diffusivity, which is at the lower limit of experimental data.

The penetration theory is most useful when mass transfer involves bubbles or droplets, or flow over random packing. For bubbles, the contact time, t_c, of the liquid surrounding the bubble is taken as the ratio of bubble diameter to bubble-rise velocity. For example, an air bubble of 0.4-cm diameter rises through water at a velocity of about 20 cm/s. Thus, the estimated contact time, t_c, is $0.4/20 = 0.02$ s. For a liquid spray, where no circulation of liquid occurs inside the droplets, the contact time is the total time for the droplets to fall through the gas. For a packed tower, where the liquid flows as a film over particles of random packing, mixing can be assumed to occur each time the liquid film passes from one piece of packing to another. Resulting contact times are of the order of about 1 s. In the absence of any method of estimating the contact time, the liquid-phase mass-transfer coefficient is sometimes correlated by an empirical expression consistent with the 0.5 exponent on D_{AB}, given by (3-194) with the contact time replaced by a function of geometry and the liquid velocity, density, and viscosity.

EXAMPLE 3.18

For the conditions of Example 3.17, estimate the contact time for Higbie's penetration theory.

SOLUTION

From Example 3.17, $k_c = 6.14 \times 10^{-3}$ cm/s and $D_{AB} = 1.7 \times 10^{-5}$ cm^2/s. From a rearrangement of (3-194),

$$t_c = \frac{4D_{AB}}{\pi k_c^2} = \frac{4(1.7 \times 10^{-5})}{3.14(6.14 \times 10^{-3})^2} = 0.57 \text{ s}$$

Surface-Renewal Theory

The penetration theory is not satisfying because the assumption of a constant contact time for all eddies that temporarily reside at the surface is not reasonable, especially for stirred tanks, contactors with random packings, and bubble and spray columns where the bubbles and droplets cover a wide range of sizes. In 1951, Danckwerts [60] suggested an improvement to the penetration theory that involves the replacement of the constant eddy contact time with the assumption of a residence-time distribution, wherein the probability of an eddy at the surface being replaced by a fresh eddy is independent of the age of the surface eddy.

Following the Levenspiel [61] treatment of residence-time distribution, let $F(t)$ be the fraction of eddies with a contact time of less than t. For $t = 0$, $F\{t\} = 0$, and $F\{t\}$ approaches 1 as t goes to infinity. A plot of $F\{t\}$ versus t, as shown in Figure 3.19, is referred to as a residence-time or age distribution. If $F\{t\}$ is differentiated with respect to t, we obtain another function:

$$\phi\{t\} = dF\{t\}/dt$$

where $\phi\{t\}dt =$ the probability that a given surface eddy will have a residence time t. The sum of probabilities is

$$\int_0^\infty \phi\{t\}\, dt = 1 \tag{3-195}$$

Typical plots of $F\{t\}$ and $\phi\{t\}$ are shown in Figure 3.19, where it is seen that $\phi\{t\}$ is similar to a normal probability curve.

For steady-state flow in and out of a well-mixed vessel, Levenspiel shows that

$$F\{t\} = 1 - e^{-t/\bar{t}} \tag{3-196}$$

where $\bar{t}$ is the average residence time. This function forms the basis, in reaction engineering, of the ideal model of a continuous, stirred-tank reactor (CSTR). Danckwerts selected the same model for his surface-renewal theory, using the corresponding $\phi\{t\}$ function:

$$\phi\{t\} = se^{-st} \tag{3-197}$$

where $s = 1/\bar{t} =$ fractional rate of surface renewal. As shown in Example 3.19 below, plots of (3-196) and (3-197) are much different from those in Figure 3.19.

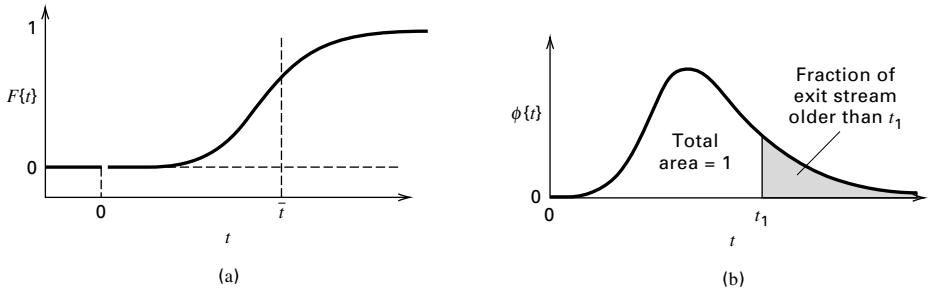

Figure 3.19 Residence-time distribution plots: (a) typical F curve; (b) typical age distribution.
[Adapted from O. Levenspiel, *Chemical Reaction Engineering,* 2nd ed., John Wiley and Sons, New York (1972).]

The instantaneous mass-transfer rate for an eddy with an age t is given by (3-192) for the penetration theory in flux form as

$$N_{A_t} = \sqrt{\frac{D_{AB}}{\pi t}}(c_{A_i} - c_{A_b}) \tag{3-198}$$

The integrated average rate is

$$(N_A)_{avg} = \int_0^\infty \phi\{t\} N_{A_t}\, dt \tag{3-199}$$

Combining (3-197), (3-198), and (3-199), and integrating:

$$(N_A)_{avg} = \sqrt{D_{AB}s}(c_{A_i} - c_{A_b}) \tag{3-200}$$

Thus,

$$k_c = \sqrt{D_{AB}s} \tag{3-201}$$

The more reasonable surface-renewal theory predicts the same dependency of the mass-transfer coefficient on molecular diffusivity as the penetration theory. Unfortunately, s, the fractional rate of surface renewal, is as elusive a parameter as the constant contact time, t_c.

EXAMPLE 3.19

For the conditions of Example 3.17, estimate the fractional rate of surface renewal, s, for Danckwert's theory and determine the residence time and probability distributions.

SOLUTION

From Example 3.17,

$$k_c = 6.14 \times 10^{-3} \text{ cm/s} \quad \text{and} \quad D_{AB} = 1.7 \times 10^{-5} \text{ cm}^2/\text{s}$$

From (3-201),

$$s = \frac{k_c^2}{D_{AB}} = \frac{(6.14 \times 10^{-3})^2}{1.7 \times 10^{-5}} = 2.22\,\text{s}^{-1}$$

Thus, the average residence time of an eddy at the surface is $1/2.22 = 0.45$ s.

From (3-197),

$$\phi\{t\} = 2.22e^{-2.22t} \tag{1}$$

From (3-196), the residence-time distribution is given by

$$F\{t\} = 1 - e^{-t/0.45}, \tag{2}$$

where t is in seconds. Equations (1) and (2) are plotted in Figure 3.20. These curves are much different from the curves of Figure 3.19.

Film-Penetration Theory

Toor and Marchello [62], in 1958, combined features of the film, penetration, and surface-renewal theories to develop a film-penetration model, which predicts a dependency of the mass-transfer coefficient k_c, on the diffusivity, that varies from $\sqrt{D_{AB}}$ to D_{AB}. Their theory assumes that the entire resistance to mass transfer resides in a film of fixed thickness δ. Eddies move to and from the bulk fluid and this film. Age distributions for time spent in the film are of the Higbie or Danckwerts type.

Fick's second law, (3-68), still applies, but the boundary conditions are now

$$\begin{aligned} &c_A = c_{A_b} \quad \text{at} \quad t = 0 \quad \text{for} \quad 0 \le z \le \infty, \\ &c_A = c_{A_i} \quad \text{at} \quad z = 0 \quad \text{for} \quad t > 0; \quad \text{and} \\ &c_A = c_{A_b} \quad \text{at} \quad z = \delta \quad \text{for} \quad t > 0 \end{aligned}$$

Infinite-series solutions are obtained by the method of Laplace transforms. The rate of mass transfer is then obtained in the usual manner by applying Fick's first law (3-117) at the fluid–fluid interface. For small t, the solution, given as

$$N_{A_t} = (c_{A_i} - c_{A_b})\left(\frac{D_{AB}}{\pi t}\right)^{1/2}\left[1 + 2\sum_{n=1}^{\infty}\exp\left(-\frac{n^2\delta^2}{D_{AB}t}\right)\right] \tag{3-202}$$

converges rapidly. For large t,

$$N_{A_t} = (c_{A_i} - c_{A_b})\left(\frac{D_{AB}}{\delta}\right) \times \left[1 + 2\sum_{n=1}^{\infty}\exp\left(-n^2\pi^2\frac{D_{AB}t}{\delta^2}\right)\right] \tag{3-203}$$

Equation (3-199) with $\phi\{t\}$ from (3-197) can then be used to obtain average rates of mass transfer. Again, we can write two equivalent series solutions, which converge

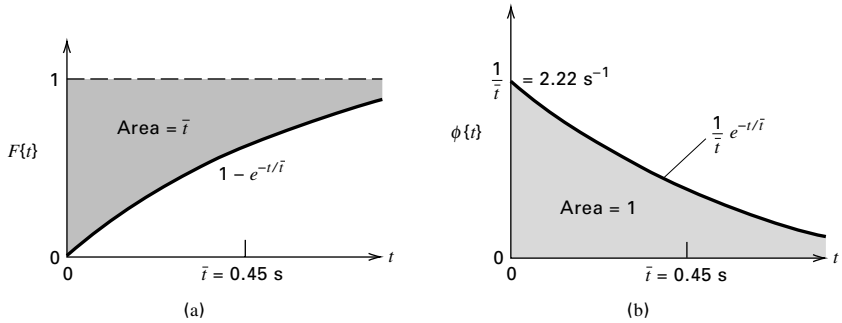

Figure 3.20 Age distribution curves for Example 3.19: (a) F curve; (b) $\phi\{t\}$ curve.

at different rates. Equations (3-202) and (3-203) become, respectively,

$$N_{A_{avg}} = k_c(c_{A_i} - c_{A_b}) = (c_{A_i} - c_{A_b})(sD_{AB})^{1/2} \times \left[1 + 2\sum_{n=1}^{\infty} \exp\left(-2n\delta\sqrt{\frac{s}{D_{AB}}}\right)\right] \quad (3\text{-}204)$$

$$N_{A_{avg}} = k_c(c_{A_i} - c_{A_b}) = (c_{A_i} - c_{A_b})\left(\frac{D_{AB}}{\delta}\right) \times \left[1 + 2\sum_{n=1}^{\infty} \frac{1}{1 + n^2\pi^2\dfrac{D_{AB}}{s\delta^2}}\right] \quad (3\text{-}205)$$

In the limit, for a high rate of surface renewal, $s\delta^2/D_{AB}$, (3-204) reduces to the surface-renewal theory, (3-200). For low rates of renewal, (3-205) reduces to the film theory, (3-188). At conditions in between, k_c is proportional to D_{AB}^n, where n is in the range of 0.5–1.0. The application of the film-penetration theory is difficult because of lack of data for δ and s, but the predicted effect of molecular diffusivity brackets experimental data.

3.7 TWO-FILM THEORY AND OVERALL MASS-TRANSFER COEFFICIENTS

Separation processes that involve contacting two fluid phases require consideration of mass-transfer resistances in both phases. In 1923, Whitman [63] suggested an extension of the film theory to two fluid films in series. Each film presents a resistance to mass transfer, but concentrations in the two fluids at the interface are assumed to be in phase equilibrium. That is, there is no additional interfacial resistance to mass transfer. This concept has found extensive application in modeling of steady-state, gas–liquid, and liquid–liquid separation processes.

The assumption of phase equilibrium at the phase interface, while widely used, may not be valid when gradients of interfacial tension are established during mass transfer between two fluids. These gradients give rise to interfacial turbulence resulting, most often, in considerably increased mass-transfer coefficients. This phenomenon, referred to as the *Marangoni effect,* is discussed in some detail by Bird, Stewart, and Lightfoot [28], who cite additional references. The effect can occur at both vapor–liquid and liquid–liquid interfaces, with the latter receiving the most attention. By adding surfactants, which tend to concentrate at the interface, the Marangoni effect may be reduced because of stabilization of the interface, even to the extent that an interfacial mass-transfer resistance may result, causing the overall mass-transfer coefficient to be reduced. In this book, unless otherwise indicated, the Marangoni effect will be ignored and phase equilibrium will always be assumed at the phase interface.

Gas–Liquid Case

Consider the steady-state mass transfer of A from a gas phase, across an interface, into a liquid phase. It could be postulated, as shown in Figure 3.21a, that a thin gas film exists on one side of the interface and a thin liquid film exists on the other side, with the controlling factors being molecular diffusion through each film. However, this postulation is not necessary, because instead of writing

$$N_A = \frac{(D_{AB})_G}{\delta_G}(c_{A_b} - c_{A_i})_G = \frac{(D_{AB})_L}{\delta_L}(c_{A_i} - c_{A_b})_L \quad (3\text{-}206)$$

we can express the rate of mass transfer in terms of mass-transfer coefficients determined from any suitable theory, with the concentration gradients visualized more realistically as in Figure 3.21b. In addition, we can use any number of different mass-transfer coefficients, depending on the selection of the driving force for mass transfer. For the gas phase, under dilute or equimolar counter diffusion (EMD) conditions, we write the mass-transfer rate in terms of partial pressures:

$$N_A = k_p(p_{A_b} - p_{A_i}) \quad (3\text{-}207)$$

where k_p is a gas-phase mass-transfer coefficient based on a partial-pressure driving force.

For the liquid phase, we use molar concentrations:

$$N_A = k_c(c_{A_i} - c_{A_b}) \quad (3\text{-}208)$$

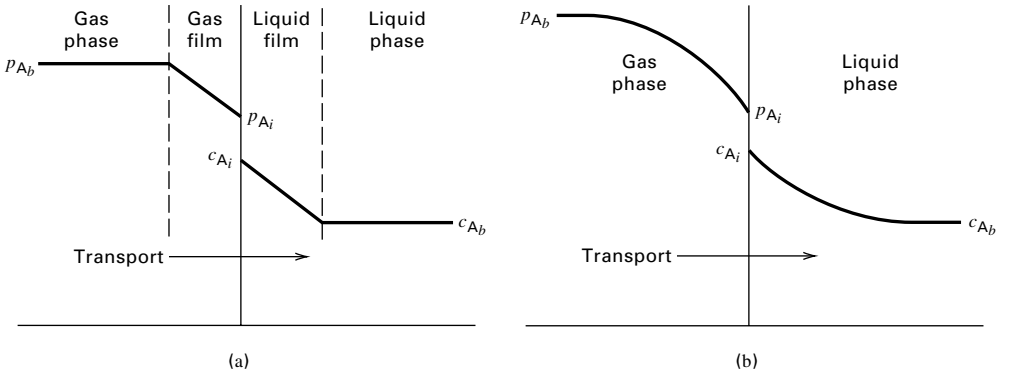

Figure 3.21 Concentration gradients for two-resistance theory: (a) film theory; (b) more realistic gradients.

At the phase interface, c_{A_i} and p_{A_i} are assumed to be in phase equilibrium. Applying a version of Henry's law different from that in Table 2.3,[1]

$$c_{A_i} = H_A p_{A_i} \tag{3-209}$$

Equations (3-207) to (3-209) are a commonly used combination for vapor–liquid mass transfer. Computations of mass-transfer rates are generally made from a knowledge of bulk concentrations, which in this case are p_{A_b} and c_{A_b}. To obtain an expression for N_A in terms of an overall driving force for mass transfer, (3-207) to (3-209) are combined in the following manner to eliminate the interfacial concentrations, c_{A_i} and p_{A_i}. Solve (3-207) for p_{A_i}:

$$p_{A_i} = p_{A_b} - \frac{N_A}{k_p} \tag{3-210}$$

Solve (3-208) for c_{A_i}:

$$c_{A_i} = c_{A_b} + \frac{N_A}{k_c} \tag{3-211}$$

Combine (3-211) with (3-209) to eliminate c_{A_i} and combine the result with (3-210) to eliminate p_{A_i} to give

$$N_A = \frac{p_{A_b} H_A - c_{A_b}}{(H_A/k_p) + (1/k_c)} \tag{3-212}$$

It is customary to define: (1) a fictitious liquid-phase concentration $c_A^* = p_{A_b} H_A$, which is the concentration that would be in equilibrium with the partial pressure in the bulk gas; and (2) an overall mass-transfer coefficient, K_L. Thus, (3-212) is rewritten as

$$N_A = K_L(c_A^* - c_{A_b}) = \frac{(c_A^* - c_{A_b})}{(H_A/k_p) + (1/k_c)} \tag{3-213}$$

where

$$\frac{1}{K_L} = \frac{H_A}{k_p} + \frac{1}{k_c} \tag{3-214}$$

in which K_L is the overall mass-transfer coefficient based on the liquid phase. The quantities H_A/k_p and $1/k_c$ are measures of the mass-transfer resistances of the gas phase and the liquid phase, respectively. When $1/k_c >> H_A/k_p$, (3-214) becomes

$$N_A = k_c(c_A^* - c_{A_b}) \tag{3-215}$$

Since resistance in the gas phase is then negligible, the gas-phase driving force is $p_{A_b} - p_{A_i} \approx 0$ and $p_{A_b} \approx p_{A_i}$.

[1]Many different forms of Henry's law are found in the literature. They include

$$p_A = H_A x_A, \quad p_A = \frac{c_A}{H_A}, \quad \text{and} \quad y_A = H_A x_A$$

When a Henry's-law constant, H_A, is given without citing the equation that defines it, the defining equation can be determined from the units of the constant. For example, if the constant has the units of atm or atm/mole fraction, Henry's law is given by $p_A = H_A x_A$. If the units are mol/L-mmHg, Henry's law is $p_A = \frac{c_A}{H_A}$.

Alternatively, (3-207) to (3-209) can be combined to define an overall mass-transfer coefficient, K_G, based on the gas phase. The result is

$$N_A = \frac{p_{A_b} - c_{A_b}/H_A}{(1/k_p) + (1/H_A k_c)} \tag{3-216}$$

In this case, it is customary to define: (1) a fictitious gas-phase partial pressure $p_A^* = c_{A_b}/H_A$, which is the partial pressure that would be in equilibrium with the bulk liquid; and (2) an overall mass-transfer coefficient for the gas phase, K_G, based on a partial-pressure driving force. Thus, (3-216) can be rewritten as

$$N_A = K_G(p_{A_b} - p_A^*) = \frac{(p_{A_b} - p_A^*)}{(1/k_p) + (1/H_A k_c)} \tag{3-217}$$

where

$$\frac{1}{K_G} = \frac{1}{k_p} + \frac{1}{H_A k_c} \tag{3-218}$$

In this, the resistances are $1/k_p$ and $1/(H_A k_c)$. When $1/k_p >> 1/H_A k_c$,

$$N_A = k_p(p_{A_b} - p_A^*) \tag{3-219}$$

Since the resistance in the liquid phase is then negligible, the liquid-phase driving force is $c_{A_i} - c_{A_b} \approx 0$ and $c_{A_i} \approx c_{A_b}$.

The choice between using (3-213) or (3-217) is arbitrary, but is usually made on the basis of which phase has the largest mass-transfer resistance; if the liquid, use (3-213); if the gas, use (3-217). Another common combination for vapor–liquid mass transfer uses mole fraction-driving forces, which define another set of mass-transfer coefficients:

$$N_A = k_y(y_{A_b} - y_{A_i}) = k_x(x_{A_i} - x_{A_b}) \tag{3-220}$$

In this case, phase equilibrium at the interface can be expressed in terms of the K-value for vapor–liquid equilibrium. Thus,

$$K_A = y_{A_i}/x_{A_i} \tag{3-221}$$

Combining (3-220) and (3-221) to eliminate y_{A_i} and x_{A_i},

$$N_A = \frac{y_{A_b} - x_{A_b}}{(1/K_A k_y) + (1/k_x)} \tag{3-222}$$

This time we define fictitious concentration quantities and overall mass-transfer coefficients for mole-fraction driving forces. Thus, $x_A^* = y_{A_b}/K_A$ and $y_A^* = K_A x_{A_b}$. If the two values of K_A are equal, we obtain

$$N_A = K_x(x_A^* - x_{A_b}) = \frac{x_A^* - x_{A_b}}{(1/K_A k_y) + (1/k_x)} \tag{3-223}$$

and

$$N_A = K_y(y_{A_b} - y_A^*) = \frac{y_{A_b} - y_A^*}{(1/k_y) + (K_A/k_x)} \tag{3-224}$$

where K_x and K_y are overall mass-transfer coefficients based on mole-fraction driving forces with

$$\frac{1}{K_x} = \frac{1}{K_A k_y} + \frac{1}{k_x} \tag{3-225}$$

and

$$\frac{1}{K_y} = \frac{1}{k_y} + \frac{K_A}{k_x} \tag{3-226}$$

When using correlations to estimate mass-transfer coefficients for use in the above equations, it is important to determine which coefficient (k_p, k_c, k_y, or k_x) is correlated. This can usually be done by checking the units or the form of the Sherwood or Stanton numbers. Coefficients correlated by the Chilton–Colburn analogy are k_c for either the liquid or gas phase. The different coefficients are related by the following expressions, which are summarized in Table 3.16.

Liquid phase:

$$k_x = k_c c = k_c \left(\frac{\rho_L}{M}\right) \tag{3-227}$$

Ideal-gas phase:

$$k_y = k_p P = (k_c)_g \frac{P}{RT} = (k_c)_g c = (k_c)_g \left(\frac{\rho_G}{M}\right) \tag{3-228}$$

Typical units are

	SI	American Engineering
k_c	m/s	ft/h
k_p	kmol/s-m^2-kPa	lbmol/h-ft^2-atm
k_y, k_x	kmol/s-m^2	lbmol/h-ft^2

When unimolecular diffusion (UMD) occurs under nondilute conditions, the effect of bulk flow must be included in the above equations. For binary mixtures, one method for doing this is to define modified mass-transfer coefficients, designated with a prime, as follows.

Table 3.16 Relationships among Mass-Transfer Coefficients

Equimolar Counterdiffusion (EMD):

Gases: $N_A = k_y \Delta y_A = k_c \Delta c_A = k_p \Delta p_A$

$k_y = k_c \dfrac{P}{RT} = k_p P$ if ideal gas

Liquids: $N_A = k_x \Delta x_A = k_c \Delta c_A$

$k_x = k_c c$, where c = total molar concentration (A + B)

Unimolecular Diffusion (UMD):

Gases: Same equations as for EMD with k replaced by $k' = \dfrac{k}{(y_B)_{LM}}$

Liquids: Same equations as for EMD with k replaced by $k' = \dfrac{k}{(x_B)_{LM}}$

When using concentration units for both phases, it is convenient to use:

$k_G(\Delta c_G) = k_c(\Delta c)$ for the gas phase

$k_L(\Delta c_L) = k_c(\Delta c)$ for the liquid phase

For the liquid phase, using k_c or k_x,

$$k' = \frac{k}{(1 - x_A)_{LM}} = \frac{k}{(x_B)_{LM}} \tag{3-229}$$

For the gas phase, using k_p, k_y, or k_c,

$$k' = \frac{k}{(1 - y_A)_{LM}} = \frac{k}{(y_B)_{LM}} \tag{3-230}$$

The expressions for k' are most readily used when the mass-transfer rate is controlled mainly by one of the two resistances. Experimental mass-transfer coefficient data reported in the literature are generally correlated in terms of k rather than k'. Mass-transfer coefficients estimated from the Chilton–Colburn analogy [e.g., equations (3-166) to (3-171)] are k_c, not k'_c.

Liquid–Liquid Case

For mass transfer across two liquid phases, equilibrium is again assumed at the interface. Denoting the two phases by $L^{(1)}$ and $L^{(2)}$, (3-223) and (3-224) can be rewritten as

$$N_A = K_x^{(2)}\left(x_A^{(2)*} - x_{A_b}^{(2)}\right) = \frac{x_A^{(2)*} - x_{A_b}^{(2)}}{(1/K_{D_A}k_x^{(1)}) + (1/k_x^{(2)})} \tag{3-231}$$

and

$$N_A = K_x^{(1)}\left(x_{A_b}^{(1)} - x_A^{(1)*}\right) = \frac{x_{A_b}^{(1)} - x_A^{(1)*}}{(1/k_x^{(1)}) + (K_{D_A}/k_x^{(2)})} \tag{3-232}$$

where

$$K_{D_A} = \frac{x_{A_i}^{(1)}}{x_{A_i}^{(2)}} \tag{3-233}$$

Case of Large Driving Forces for Mass Transfer

When large driving forces exist for mass transfer, phase equilibria ratios such as H_A, K_A, and K_{D_A} may not be constant across the two phases. This occurs particularly when one or both phases are not dilute with respect to the diffusing solute, A. In that case, expressions for the mass-transfer flux must be revised.

For example, if mole-fraction driving forces are used, we write, from (3-220) and (3-224),

$$N_A = k_y(y_{A_b} - y_{A_i}) = K_y(y_{A_b} - y_A^*) \tag{3-234}$$

Thus,

$$\frac{1}{K_y} = \frac{y_{A_b} - y_A^*}{k_y(y_{A_b} - y_{A_i})} \tag{3-235}$$

or

$$\frac{1}{K_y} = \frac{(y_{A_b} - y_{A_i}) + (y_{A_i} - y_A^*)}{k_y(y_{A_b} - y_{A_i})} = \frac{1}{k_y} + \frac{1}{k_y}\left(\frac{y_{A_i} - y_A^*}{y_{A_b} - y_{A_i}}\right) \tag{3-236}$$

From (3-220),

$$\frac{k_x}{k_y} = \frac{(y_{A_b} - y_{A_i})}{(x_{A_i} - x_{A_b})} \tag{3-237}$$

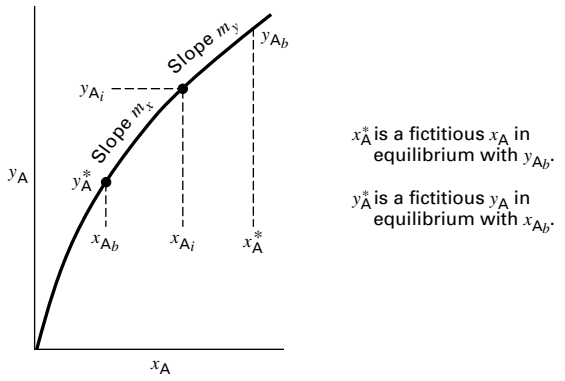

Figure 3.22 Curved equilibrium line.

Combining (3-234) and (3-237),

$$\frac{1}{K_y} = \frac{1}{k_y} + \frac{1}{k_x}\left(\frac{y_{A_i} - y_A^*}{x_{A_i} - x_{A_b}}\right) \tag{3-238}$$

In a similar manner,

$$\frac{1}{K_x} = \frac{1}{k_x} + \frac{1}{k_y}\left(\frac{x_A^* - x_{A_i}}{y_{A_b} - y_{A_i}}\right) \tag{3-239}$$

A typical curved equilibrium line is shown in Figure 3.22 with representative values of y_{A_b}, y_{A_i}, y_A^*, x_A^*, x_{A_i}, and x_{A_b} indicated. Because the line is curved, the vapor–liquid equilibrium ratio, $K_A = y_A/x_A$, is not constant across the two phases. As shown, the slope of the curve and thus, K_A, decreases with increasing concentration of A. Denote two slopes of the equilibrium line by

$$m_x = \left(\frac{y_{A_i} - y_A^*}{x_{A_i} - x_{A_b}}\right) \tag{3-240}$$

and

$$m_y = \left(\frac{y_{A_b} - y_{A_i}}{x_A^* - x_{A_i}}\right) \tag{3-241}$$

Substituting (3-240) and (3-241) into (3-238) and (3-239), respectively, gives

$$\frac{1}{K_y} = \frac{1}{k_y} + \frac{m_x}{k_x} \tag{3-242}$$

and

$$\frac{1}{K_x} = \frac{1}{k_x} + \frac{1}{m_y k_y} \tag{3-243}$$

EXAMPLE 3.20

Sulfur dioxide (A) is absorbed into water in a packed column. At a certain location, the bulk conditions are 50°C, 2 atm, $y_{A_b} = 0.085$, and $x_{A_b} = 0.001$. Equilibrium data for SO_2 between air and water at 50°C are

p_{SO_2}, atm	c_{SO_2}, lbmol/ft^3
0.0382	0.00193
0.0606	0.00290
0.1092	0.00483
0.1700	0.00676

Experimental values of the mass transfer coefficients are as follows.

Liquid phase: $k_c = 0.18$ m/h

Gas phase: $k_p = 0.040 \dfrac{\text{kmol}}{\text{h-m}^2\text{-kPa}}$

Using mole-fraction driving forces, compute the mass-transfer flux by:

(a) Assuming an average Henry's-law constant and a negligible bulk-flow effect.

(b) Utilizing the actual curved equilibrium line and assuming a negligible bulk-flow effect.

(c) Utilizing the actual curved equilibrium line and taking into account the bulk-flow effect.

In addition,

(d) Determine the relative magnitude of the two resistances and the values of the mole fractions at the interface from the results of part (c).

SOLUTION

The equilibrium data are converted to mole fractions by assuming Dalton's law, $y_A = p_A/P$, for the gas and using $x_A = c_A/c$ for the liquid. The concentration of the liquid is close to that of pure water or 3.43 lbmol/ft^3 or 55.0 kmol/m^3. Thus, the mole fractions at equilibrium are:

y_{SO_2}	x_{SO_2}
0.0191	0.000563
0.0303	0.000846
0.0546	0.001408
0.0850	0.001971

These data are fitted with average and maximum absolute deviations of 0.91% and 1.16%, respectively, by the quadratic equation

$$y_{SO_2} = 29.74x_{SO_2} + 6{,}733x_{SO_2}^2 \tag{1}$$

Thus, differentiating, the slope of the equilibrium curve is given by

$$m = \frac{dy}{dx} = 29.74 + 13{,}466x_{SO_2} \tag{2}$$

The given mass-transfer coefficients can be converted to k_x and k_y by (3-227) and (3-228):

$$k_x = k_c c = 0.18(55.0) = 9.9 \frac{\text{kmol}}{\text{h-m}^2}$$

$$k_y = k_p P = 0.040(2)(101.3) = 8.1 \frac{\text{kmol}}{\text{h-m}^2}.$$

(a) From (1) for $x_{A_b} = 0.001$, $y_A^* = 29.74(0.001) + 6{,}733(0.001)^2 = 0.0365$. From (1), for $y_{A_b} = 0.085$, we solve the quadratic equation to obtain $x_A^* = 0.001975$.

The average slope in this range is

$$m = \frac{0.085 - 0.0365}{0.001975 - 0.001} = 49.7\,.$$

From an examination of (3-242) and (3-243), the liquid-phase resistance is controlling because the term in k_x is much larger than the term in k_y. Therefore, from (3-243), using $m = m_x$,

$$\frac{1}{K_x} = \frac{1}{9.9} + \frac{1}{49.7(8.1)} = 0.1010 + 0.0025 = 0.1035$$

$$\text{or} \quad K_x = 9.66\,\frac{\text{kmol}}{\text{h-m}^2}$$

From (3-223),

$$N_\text{A} = 9.66(0.001975 - 0.001) = 0.00942\,\frac{\text{kmol}}{\text{h-m}^2}\,.$$

(b) From part (a), the gas-phase resistance is almost negligible. Therefore, $y_{\text{A}_i} \approx y_{\text{A}_b}$ and $x_{\text{A}_i} \approx x^*_\text{A}$.

From (3-241), the slope m_y must, therefore, be taken at the point $y_{\text{A}_b} = 0.085$ and $x^*_\text{A} = 0.001975$ on the equilibrium line.

From (2), $m_y = 29.74 + 13{,}466(0.001975) = 56.3$. From (3-243),

$$K_x = \frac{1}{(1/9.9) + [1/(56.3)(8.1)]} = 9.69\,\frac{\text{kmol}}{\text{h-m}^2},$$

giving $N_\text{A} = 0.00945$ kmol/h-m^2. This is only a slight change from part (a).

(c) We now correct for bulk flow. From the results of parts (a) and (b), we have

$$y_{\text{A}_b} = 0.085,\ y_{\text{A}_i} = 0.085,\ x_{\text{A}_i} = 0.1975,\ x_{\text{A}_b} = 0.001$$

$$(y_\text{B})_\text{LM} = 1.0 - 0.085 = 0.915 \text{ and } (x_\text{B})_\text{LM} \approx 0.9986$$

From (3-229),

$$k'_x = \frac{9.9}{0.9986} = 9.9\,\frac{\text{kmol}}{\text{h-m}^2} \text{ and } k'_y = \frac{8.1}{0.915} = 8.85\,\frac{\text{kmol}}{\text{h-m}^2}$$

From (3-243),

$$K_x = \frac{1}{(1/9.9) + [1/56.3(8.85)]} = 9.71\,\frac{\text{kmol}}{\text{h-m}^2}$$

From (3-223),

$$N_\text{A} = 9.71(0.001975 - 0.001) = 0.00947\,\frac{\text{kmol}}{\text{h-m}^2}$$

which is only a very slight change from parts (a) and (b), where the bulk-flow effect was ignored. The effect is very small because here it is important only in the gas phase; but the liquid-phase resistance is controlling.

(d) The relative magnitude of the mass-transfer resistances can be written as

$$\frac{1/m_y k'_y}{1/k'_x} = \frac{1/(56.3)(8.85)}{1/9.9} = 0.02$$

Thus, the gas-phase resistance is only 2% of the liquid-phase resistance. The interface vapor mole fraction can be obtained from (3-223), after accounting for the bulk-flow effect:

$$y_{\text{A}_i} = y_{\text{A}_b} - \frac{N_\text{A}}{k'_y} = 0.085 - \frac{0.00947}{8.85} = 0.084$$

Similarly,

$$x_{\text{A}_i} = \frac{N_\text{A}}{k'_x} + x_{\text{A}_b} = \frac{0.00947}{9.9} + 0.001 = 0.00196$$

SUMMARY

1. Mass transfer is the net movement of a component in a mixture from one region to another region of different concentration, often between two phases across an interface. Mass transfer occurs by molecular diffusion, eddy diffusion, and bulk flow. Molecular diffusion occurs by a number of different driving forces, including concentration (the most important), pressure, temperature, and external force fields.

2. Fick's first law for steady-state conditions states that the mass-transfer flux by ordinary molecular diffusion is equal to the product of the diffusion coefficient (diffusivity) and the negative of the concentration gradient.

3. Two limiting cases of mass transfer are equimolar counterdiffusion (EMD) and unimolecular diffusion (UMD). The former is also a good approximation for dilute conditions. The latter must include the bulk-flow effect.

4. When experimental data are not available, diffusivities in gas and liquid mixtures can be estimated. Diffusivities in solids, including porous solids, crystalline solids, metals, glass, ceramics, polymers, and cellular solids, are best measured. For some solids—for example, wood—diffusivity is an anisotropic property.

5. Diffusivity values vary by orders of magnitude. Typical values are 0.10, 1×10^{-5}, and 1×10^{-9} cm^2/s for ordinary molecular diffusion of a solute in a gas, liquid, and solid, respectively.

6. Fick's second law for unsteady-state diffusion is readily applied to semi-infinite and finite stagnant media, including certain anisotropic materials.

7. Molecular diffusion under laminar-flow conditions can be determined from Fick's first and second laws, provided that velocity profiles are available. Common cases include falling liquid-film flow, boundary-layer flow on a flat plate, and fully developed flow in a straight, circular tube. Results are often expressed in terms of a mass-transfer coefficient embedded in a dimensionless group called the Sherwood number. The mass-transfer flux is given by the product of the mass-transfer coefficient and a concentration driving force.

8. Mass transfer in turbulent flow is often predicted by analogy to heat transfer. Of particular importance is the Chilton–Colburn analogy, which utilizes empirical j-factor correlations and the dimensionless Stanton number for mass transfer. A more accurate equation by Churchill and Zajic should be used for flow in tubes, particularly at high Schmidt and Reynolds numbers.

9. A number of models have been developed for mass transfer across a two-fluid interface and into a liquid. These include the film theory, penetration theory, surface-renewal theory, and the film-penetration theory. These theories predict mass-transfer coefficients that are proportional to the diffusivity raised to an exponent that varies from 0.5 to 1.0. Most experimental data provide exponents ranging from 0.5 to 0.75.

10. The two-film theory of Whitman (more properly referred to as a two-resistance theory) is widely used to predict the mass-transfer flux from one fluid phase, across an interface, and into another fluid phase, assuming equilibrium at the interface. One resistance is often controlling. The theory defines an overall mass-transfer coefficient that is determined from the separate coefficients for each of the two phases and the equilibrium relationship at the interface.

REFERENCES

1. TAYLOR, R., and R. KRISHNA, *Multicomponent Mass Transfer,* John Wiley and Sons, New York (1993).
2. POLING, B.E., J.M. PRAUSNITZ, and J.P. O'CONNELL, *The Properties of Liquids and Gases,* 5th ed., McGraw-Hill, New York (2001).
3. FULLER, E.N., P.D. SCHETTLER, and J.C. GIDDINGS, *Ind. Eng. Chem.,* **58** (5), 18–27 (1966).
4. TAKAHASHI, S., *J. Chem. Eng. Jpn.*, **7,** 417–420 (1974).
5. SLATTERY, J.C., M.S. thesis, University of Wisconsin, Madison (1955).
6. WILKE, C.R., and P. CHANG, *AIChE J.,* **1,** 264–270 (1955).
7. HAYDUK, W., and B.S. MINHAS, *Can. J. Chem. Eng.,* **60,** 295–299 (1982).
8. QUAYLE, O.R., *Chem. Rev.,* **53,** 439–589 (1953).
9. VIGNES, A., *Ind. Eng. Chem. Fundam.,* **5,** 189–199 (1966).
10. SORBER, H.A., *Handbook of Biochemistry, Selected Data for Molecular Biology,* 2nd ed., Chemical Rubber Co., Cleveland, OH (1970).
11. GEANKOPLIS, C.J., *Transport Processes and Separation Process Principles,* 4th ed., Prentice-Hall, Upper Saddle River, NJ (2003).
12. FRIEDMAN, L., and E.O. KRAEMER, *J. Am. Chem. Soc.,* **52,** 1298–1304, 1305–1310, 1311–1314 (1930).
13. BOUCHER, D.F., J.C. BRIER, and J.O. OSBURN, *Trans. AIChE,* **38,** 967–993 (1942).
14. BARRER, R.M., *Diffusion in and through Solids,* Oxford University Press, London (1951).
15. SWETS, D.E., R.W. LEE, and R.C. FRANK, *J. Chem. Phys.,* **34,** 17–22 (1961).
16. LEE, R. W., *J. Chem, Phys.,* **38,** 44–455 (1963).
17. WILLIAMS, E.L., *J. Am. Ceram. Soc.,* **48,** 190–194 (1965).
18. SUCOV, E.W., *J. Am. Ceram. Soc.,* **46,** 14–20 (1963).
19. KINGERY, W.D., H.K. BOWEN, and D.R. UHLMANN, *Introduction to Ceramics,* 2nd ed., John Wiley and Sons, New York (1976).
20. FERRY, J.D., *Viscoelastic Properties of Polymers,* John Wiley and Sons, New York (1980).
21. RHEE, C.K., and J.D. FERRY, *J. Appl. Polym. Sci.*, **21,** 467–476 (1977).
22. BRANDRUP, J., and E.H. IMMERGUT, Eds., *Polymer Handbook,* 3rd ed., John Wiley and Sons, New York (1989).
23. GIBSON, L.J., and M.F. ASHBY, *Cellular Solids, Structure and Properties,* Pergamon Press, Elmsford, NY (1988).
24. STAMM, A.J., *Wood and Cellulose Science,* Ronald Press, New York (1964).
25. SHERWOOD, T.K., *Ind. Eng. Chem.,* **21,** 12–16 (1929).
26. CARSLAW, H.S., and J.C. JAEGER, *Heat Conduction in Solids,* 2nd ed., Oxford University Press, London (1959).
27. CRANK, J., *The Mathematics of Diffusion,* Oxford University Press, London (1956).
28. BIRD, R.B., W.E. STEWART, and E.N. LIGHTFOOT, *Transport Phenomena,* 2nd ed., John Wiley and Sons, New York (2002).
29. CHURCHILL, R.V., *Operational Mathematics,* 2nd ed., McGraw-Hill, New York (1958).
30. ABRAMOWITZ, M., and I.A. STEGUN, Eds., *Handbook of Mathematical Functions,* National Bureau of Standards, Applied Mathematics Series 55, Washington, DC (1964).
31. NEWMAN, A.B., *Trans. AIChE,* **27,** 310–333 (1931).
32. GRIMLEY, S.S., *Trans. Inst. Chem. Eng.* (London), **23,** 228–235 (1948).
33. JOHNSTONE, H.F., and R.L. PIGFORD, *Trans. AIChE,* **38,** 25–51 (1942).
34. OLBRICH, W.E., and J.D. WILD, *Chem. Eng. Sci.,* **24,** 25–32 (1969).
35. CHURCHILL, S.W., *The Interpretation and Use of Rate Data: The Rate Concept,* McGraw-Hill, New York (1974).
36. CHURCHILL, S.W., and R. USAGI, *AIChE J.,* **18,** 1121–1128 (1972).
37. EMMERT, R.E., and R.L. PIGFORD, *Chem. Eng. Prog.,* **50,** 87–93 (1954).
38. PRANDTL, L., *Proc. 3rd Int. Math. Congress,* Heidelberg (1904); reprinted in *NACA Tech. Memo 452* (1928).
39. BLASIUS, H., *Z. Math Phys.,* **56,** 1–37 (1908); reprinted in *NACA Tech. Memo 1256*.
40. SCHLICHTING, H., *Boundary Layer Theory,* 4th ed., McGraw-Hill, New York (1960).
41. POHLHAUSEN, E., *Z. Angew. Math Mech.,* **1,** 252 (1921).
42. POHLHAUSEN, E., *Z. Angew. Math Mech.,* **1,** 115–121 (1921).
43. LANGHAAR, H.L., *Trans. ASME,* **64,** A-55 (1942).
44. GRAETZ, L., *Ann. d. Physik,* **25,** 337–357 (1885).
45. SELLARS, J.R., M. TRIBUS, and J.S. KLEIN, *Trans. ASME,* **78,** 441–448 (1956).
46. LEVEQUE, J., *Ann. Mines,* [12], **13,** 201, 305, 381 (1928).
47. KNUDSEN, J.G., and D.L. KATZ, *Fluid Dynamics and Heat Transfer,* McGraw-Hill, New York (1958).
48. HAUSEN, H., *Verfahrenstechnik Beih. z. Ver. Deut. Ing.,* **4,** 91 (1943).
49. LINTON, W.H. Jr., and T.K. SHERWOOD, *Chem. Eng. Prog.,* **46,** 258–264 (1950).
50. REYNOLDS, O., *Trans. Roy. Soc.* (London), **174A,** 935–982 (1883).
51. BOUSSINESQ, J., *Mem. Pre. Par. Div. Sav.,* XXIII, Paris (1877).
52. PRANDTL, L., *Z. Angew, Math Mech.,* **5,** 136 (1925); reprinted in *NACA Tech. Memo 1231* (1949).
53. REYNOLDS, O., *Proc. Manchester Lit. Phil. Soc.,* **14,** 7 (1874).
54. COLBURN, A.P., *Trans. AIChE,* **29,** 174–210 (1933).
55. CHILTON, T.H., and A.P. COLBURN, *Ind. Eng. Chem.,* **26,** 1183–1187 (1934).
56. PRANDTL, L., *Physik. Z.,* **11,** 1072 (1910).

57. FRIEND, W.L., and A.B. METZNER, *AIChE J.,* **4,** 393–402 (1958).

58. NERNST, W., *Z. Phys. Chem.,* **47,** 52 (1904).

59. HIGBIE, R., *Trans. AIChE,* **31,** 365–389 (1935).

60. DANCKWERTS, P.V., *Ind. Eng. Chem.,* **43,** 1460–1467 (1951).

61. LEVENSPIEL, O., *Chemical Reaction Engineering,* 3rd ed., John Wiley and Sons, New York (1999).

62. TOOR, H.L., and J.M. MARCHELLO, *AIChE J.,* **4,** 97–101 (1958).

63. WHITMAN, W.G., *Chem. Met. Eng.,* **29,** 146–148 (1923).

64. VAN DRIEST, E.R., *J. Aero Sci.,* 1007–1011 and 1036 (1956).

65. REICHARDT, H., *Fundamentals of Turbulent Heat Transfer,* NACA Report TM-1408 (1957).

66. DREW, T.B., E.C. KOO, and W.H. MCADAMS, *Trans. Am. Inst. Chem. Engrs.,* **28,** 56 (1933).

67. NIKURADSE, J., *VDI-Forschungsheft,* p. 361 (1933).

68. LAUNDER, B.E., and D.B. SPALDING, *Lectures in Mathematical Models of Turbulence,* Academic Press, New York (1972).

69. HENG, L., C. CHAN, and S.W. CHURCHILL, *Chem. Eng. J.,* **71,** 163 (1998).

70. CHURCHILL, S.W., and S.C. ZAJIC, *AIChE J.,* **48,** 927–940 (2002).

71. CHURCHILL, S.W., "Turbulent Flow and Convection: The Prediction of Turbulent Flow and Convection in a Round Tube," in *Advances in Heat Transfer,* J.P. Hartnett, and T.F. Irvine, Jr., Ser. Eds., Academic Press, New York, **34,** 255–361 (2001).

72. YU, B., H. OZOE, and S.W. CHURCHILL, *Chem. Eng. Sci.,* **56,** 1781 (2001).

73. CHURCHILL, S.W., and C. CHAN, *Ind. Eng. Chem. Res.,* **34,** 1332 (1995).

74. CHURCHILL, S.W., *AIChE J.,* **43,** 1125 (1997).

EXERCISES

Section 3.1

3.1 A beaker filled with an equimolar liquid mixture of ethyl alcohol and ethyl acetate evaporates at 0°C into still air at 101 kPa (1 atm) total pressure. Assuming Raoult's law applies, what will be the composition of the liquid remaining when half the original ethyl alcohol has evaporated, assuming that each component evaporates independently of the other? Also assume that the liquid is always well mixed. The following data are available:

	Vapor Pressure, kPa at 0°C	Diffusivity in Air m^2/s
Ethyl acetate (AC)	3.23	6.45×10^{-6}
Ethyl alcohol (AL)	1.62	9.29×10^{-6}

3.2 An open tank, 10 ft in diameter and containing benzene at 25°C, is exposed to air in such a manner that the surface of the liquid is covered with a stagnant air film estimated to be 0.2 in. thick. If the total pressure is 1 atm and the air temperature is 25°C, what loss of material in pounds per day occurs from this tank? The specific gravity of benzene at 60°F is 0.877. The concentration of benzene at the outside of the film is so low that it may be neglected. For benzene, the vapor pressure at 25°C is 100 torr, and the diffusivity in air is 0.08 cm^2/s.

3.3 An insulated glass tube and condenser are mounted on a reboiler containing benzene and toluene. The condenser returns liquid reflux so that it runs down the wall of the tube. At one point in the tube the temperature is 170°F, the vapor contains 30 mol% toluene, and the liquid reflux contains 40 mol% toluene. The effective thickness of the stagnant vapor film is estimated to be 0.1 in. The molar latent heats of benzene and toluene are equal. Calculate the rate at which toluene and benzene are being interchanged by equimolar countercurrent diffusion at this point in the tube in lbmol/h-ft^2.

Diffusivity of toluene in benzene = 0.2 ft^2/h.

Pressure = 1 atm total pressure (in the tube).

Vapor pressure of toluene at 170°F = 400 torr.

3.4 Air at 25°C with a dew-point temperature of 0°C flows past the open end of a vertical tube filled with liquid water maintained at 25°C. The tube has an inside diameter of 0.83 in., and the liquid level was originally 0.5 in. below the top of the tube. The diffusivity of water in air at 25°C is 0.256 cm^2/s.

(a) How long will it take for the liquid level in the tube to drop 3 in.?

(b) Make a plot of the liquid level in the tube as a function of time for this period.

3.5 Two bulbs are connected by a tube, 0.002 m in diameter and 0.20 m in length. Initially bulb 1 contains argon, and bulb 2 contains xenon. The pressure and temperature are maintained at 1 atm and 105°C, at which the diffusivity is 0.180 cm^2/s. At time $t = 0$, diffusion is allowed to occur between the two bulbs. At a later time, the argon mole fraction in the gas at end 1 of the tube is 0.75, and 0.20 at the other end. Determine at the later time:

(a) The rates and directions of mass transfer of argon and xenon

(b) The transport velocity of each species

(c) The molar average velocity of the mixture

Section 3.2

3.6 The diffusivity of toluene in air was determined experimentally by allowing liquid toluene to vaporize isothermally into air from a partially filled vertical tube 3 mm in diameter. At a temperature of 39.4°C, it took 96×10^4 s for the level of the toluene to drop from 1.9 cm below the top of the open tube to a level of 7.9 cm below the top. The density of toluene is 0.852 g/cm^3, and the vapor pressure is 57.3 torr at 39.4°C. The barometer reading was 1 atm. Calculate the diffusivity and compare it with the value predicted from (3-36). Neglect the counterdiffusion of air.

3.7 An open tube, 1 mm in diameter and 6 in. long, has pure hydrogen blowing across one end and pure nitrogen blowing across the other. The temperature is 75°C.

(a) For equimolar counterdiffusion, what will be the rate of transfer of hydrogen into the nitrogen stream (mol/s)? Estimate the diffusivity from (3-36).

(b) For part (a), plot the mole fraction of hydrogen against distance from the end of the tube past which nitrogen is blown.

3.8 Some HCl gas diffuses across a film of air 0.1 in. thick at 20°C. The partial pressure of HCl on one side of the film is 0.08 atm and it is zero on the other. Estimate the rate of diffusion, as mol HCl/s-cm^2, if the total pressure is (a) 10 atm, (b) 1 atm, (c) 0.1 atm.

The diffusivity of HCl in air at 20°C and 1 atm is 0.145 cm^2/s.

3.9 Estimate the diffusion coefficient for the gaseous binary system nitrogen (A)/toluene (B) at 25°C and 3 atm using the method of Fuller et al.

3.10 For the mixture of Example 3.3, estimate the diffusion coefficient if the pressure is increased to 100 atm using the method of Takahashi.

3.11 Estimate the diffusivity of carbon tetrachloride at 25°C in a dilute solution of: (a) Methanol, (b) Ethanol, (c) Benzene, and (d) *n*-Hexane by the method of Wilke–Chang and Hayduk–Minhas. Compare the estimated values with the following experimental observations:

Solvent	Experimental D_{AB}, cm^2/s
Methanol	1.69×10^{-5} cm^2/s at 15°C
Ethanol	1.50×10^{-5} cm^2/s at 25°C
Benzene	1.92×10^{-5} cm^2/s at 25°C
n-Hexane	3.70×10^{-5} cm^2/s at 25°C

3.12 Estimate the liquid diffusivity of benzene (A) in formic acid (B) at 25°C and infinite dilution. Compare the estimated value to that of Example 3.6 for formic acid at infinite dilution in benzene.

3.13 Estimate the liquid diffusivity of acetic acid at 25°C in a dilute solution of: (a) Benzene, (b) Acetone, (c) Ethyl acetate, and (d) Water by an appropriate method. Compare the estimated values with the following experimental values:

Solvent	Experimental D_{AB}, cm^2/s
Benzene	2.09×10^{-5} cm^2/s at 25°C
Acetone	2.92×10^{-5} cm^2/s at 25°C
Ethyl acetate	2.18×10^{-5} cm^2/s at 25°C
Water	1.19×10^{-5} cm^2/s at 20°C

3.14 Water in an open dish exposed to dry air at 25°C is found to vaporize at a constant rate of 0.04 g/h-cm^2. Assuming the water surface to be at the wet-bulb temperature of 11.0°C, calculate the effective gas-film thickness (i.e., the thickness of a stagnant air film that would offer the same resistance to vapor diffusion as is actually encountered at the water surface).

3.15 Isopropyl alcohol is undergoing mass transfer at 35°C and 2 atm under dilute conditions through water, across a phase boundary, and then through nitrogen. Based on the date given below, estimate for isopropyl alcohol:

(a) The diffusivity in water using the Wilke–Chang equation

(b) The diffusivity in nitrogen using the Fuller et al. equation

(c) The product, $D_{AB}\rho_M$, in water

(d) The product, $D_{AB}\rho_M$, in air

where ρ_M is the molar density of the mixture.

Using the above results, compare:

(e) The diffusivities in parts (a) and (b)

(f) The diffusivity-molar density products in Parts (c) and (d)

Lastly:

(g) What conclusions can you come to about molecular diffusion in the liquid phase versus the gaseous phase?

Data:

Component	T_c, °R	P_c, psia	Z_c	v_L, cm^3/mol
Nitrogen	227.3	492.9	0.289	—
Isopropyl alcohol	915	691	0.249	76.5

3.16 Experimental liquid-phase activity-coefficient data are given in Exercise 2.23 for the ethanol/benzene system at 45°C. Estimate and plot diffusion coefficients for both ethanol and benzene over the entire composition range.

3.17 Estimate the diffusion coefficient of NaOH in a 1-M aqueous solution at 25°C.

3.18 Estimate the diffusion coefficient of NaCl in a 2-M aqueous solution at 18°C. Compare your estimate with the experimental value of 1.28×10^{-5} cm^2/s.

3.19 Estimate the diffusivity of N_2 in H_2 in the pores of a catalyst at 300°C and 20 atm if the porosity is 0.45 and the tortuosity is 2.5. Assume ordinary molecular diffusion in the pores.

3.20 Gaseous hydrogen at 150 psia and 80°F is stored in a small, spherical, steel pressure vessel having an inside diameter of 4 in. and a wall thickness of 0.125 in. At these conditions, the solubility of hydrogen in steel is 0.094 lbmol/ft^3 and the diffusivity of hydrogen in steel is 3.0×10^{-9} cm^2/s. If the inner surface of the vessel remains saturated at the existing hydrogen pressure and the hydrogen partial pressure at the outer surface is assumed to be zero, estimate:

(a) The initial rate of mass transfer of hydrogen through the metal wall

(b) The initial rate of pressure decrease inside the vessel

(c) The time in hours for the pressure to decrease to 50 psia, assuming the temperature stays constant at 80°F

3.21 A polyisoprene membrane of 0.8-μm thickness is to be used to separate a mixture of methane and H_2. Using the data in Table 14.9 and the following compositions, estimate the mass-transfer flux of each of the two species.

	Partial Pressures, MPa	
	Membrane Side 1	**Membrane Side 2**
Methane	2.5	0.05
Hydrogen	2.0	0.20

Section 3.3

3.22 A 3-ft depth of stagnant water at 25°C lies on top of a 0.10-in. thickness of NaCl. At time < 0, the water is pure. At time $= 0$, the salt begins to dissolve and diffuse into the water. If the concentration of salt in the water at the solid–liquid interface is maintained at saturation (36 g NaCl/100 g H_2O) and the diffusivity of NaCl in water is 1.2×10^{-5} cm^2/s, independent of concentration, estimate, by assuming the water to act as a semi-infinite medium, the time and the concentration profile of salt in the water when

(a) 10% of the salt has dissolved

(b) 50% of the salt has dissolved

(c) 90% of the salt has dissolved

3.23 A slab of dry wood of 4-in. thickness and sealed edges is exposed to air of 40% relative humidity. Assuming that the two unsealed faces of the wood immediately jump to an equilibrium moisture content of 10 lb H_2O per 100 lb of dry wood, determine the time for the moisture to penetrate to the center of the slab (2 in. from either face). Assume a diffusivity of water in the wood as 8.3×10^{-6} cm^2/s.

3.24 A wet, clay brick measuring $2 \times 4 \times 6$ in. has an initial uniform moisture content of 12 wt%. At time $= 0$, the brick is exposed on all sides to air such that the surface moisture content is

maintained at 2 wt%. After 5 h, the average moisture content is 8 wt%. Estimate:

(a) The diffusivity of water in the clay in cm^2/s.

(b) The additional time for the average moisture content to reach 4 wt%. All moisture contents are on a dry basis.

3.25 A spherical ball of clay, 2 in. in diameter, has an initial moisture content of 10 wt%. The diffusivity of water in the clay is 5×10^{-6} cm^2/s. At time $t = 0$, the surface of the clay is brought into contact with air such that the moisture content at the surface is maintained at 3 wt%. Estimate the time for the average moisture content in the sphere to drop to 5 wt%. All moisture contents are on a dry basis.

Section 3.4

3.26 Estimate the rate of absorption of pure oxygen at 10 atm and 25°C into water flowing as a film down a vertical wall 1 m high and 6 cm in width at a Reynolds number of 50 without surface ripples. Assume the diffusivity of oxygen in water is 2.5×10^{-5} cm^2/s and that the mole fraction of oxygen in water at saturation for the above temperature and pressure is 2.3×10^{-4}.

3.27 For the conditions of Example 3.13, determine at what height from the top the average concentration of CO_2 would correspond to 50% of saturation.

3.28 Air at 1 atm flows at 2 m/s across the surface of a 2-in.-long surface that is covered with a thin film of water. If the air and water are maintained at 25°C, and the diffusivity of water in air at these conditions is 0.25 cm^2/s, estimate the mass flux for the evaporation of water at the middle of the surface assuming laminar boundary-layer flow. Is this assumption reasonable?

3.29 Air at 1 atm and 100°C flows across a thin, flat plate of naphthalene that is 1 m long, causing the plate to sublime. The Reynolds number at the trailing edge of the plate is at the upper limit for a laminar boundary layer. Estimate:

(a) The average rate of sublimation in kmol/s-m^2

(b) The local rate of sublimation at a distance of 0.5 m from the leading edge of the plate

Physical properties are given in Example 3.14.

3.30 Air at 1 atm and 100°C flows through a straight, 5-cm-diameter circular tube, cast from naphthalene, at a Reynolds number of 1,500. Air entering the tube has an established laminar-flow velocity profile. Properties are given in Example 3.14. If pressure drop through the tube is negligible, calculate the length of tube needed for the average mole fraction of naphthalene in the exiting air to be 0.005.

3.31 A spherical water drop is suspended from a fine thread in still, dry air. Show:

(a) That the Sherwood number for mass transfer from the surface of the drop into the surroundings has a value of 2 if the characteristic length is the diameter of the drop.

If the initial drop diameter is 1 mm, the air temperature is 38°C, the drop temperature is 14.4°C, and the pressure is 1 atm, calculate:

(b) The initial mass of the drop in grams.

(c) The initial rate of evaporation in grams per second.

(d) The time in seconds for the drop diameter to be reduced to 0.2 mm.

(e) The initial rate of heat transfer to the drop. If the Nusselt number is also 2, is the rate of heat transfer sufficient to supply the heat of vaporization and sensible heat of the evaporated water? If not, what will happen?

Section 3.5

3.32 Water at 25°C flows at 5 ft/s through a straight, cylindrical tube cast from benzoic acid, of 2-in. inside diameter. If the tube is 10 ft long, and fully developed, turbulent flow is assumed, estimate the average concentration of benzoic acid in the water leaving the tube. Physical properties are given in Example 3.15.

3.33 Air at 1 atm flows at a Reynolds number of 50,000 normal to a long, circular, 1-in.-diameter cylinder made of naphthalene. Using the physical properties of Example 3.14 for a temperature of 100°C, calculate the average sublimation flux in kmol/s-m^2.

3.34 For the conditions of Exercise 3.33, calculate the initial average rate of sublimation in kmol/s-m^2 for a spherical particle of 1-in. initial diameter. Compare this result to that for a bed packed with naphthalene spheres with a void fraction of 0.5.

Section 3.6

3.35 Carbon dioxide is stripped from water by air in a wetted-wall tube. At a certain location, where the pressure is 10 atm and the temperature is 25°C, the mass-transfer flux of CO_2 is 1.62 lbmol/h-ft^2. The partial pressures of CO_2 are 8.2 atm at the interface and 0.1 atm in the bulk gas. The diffusivity of CO_2 in air at these conditions is 1.6×10^{-2} cm^2/s. Assuming turbulent flow of the gas, calculate by the film theory, the mass-transfer coefficient k_c for the gas phase and the film thickness.

3.36 Water is used to remove CO_2 from air by absorption in a column packed with Pall rings. At a certain region of the column where the partial pressure of CO_2 at the interface is 150 psia and the concentration in the bulk liquid is negligible, the absorption rate is 0.017 lbmol/h-ft^2. The diffusivity of CO_2 in water is 2.0×10^{-5} cm^2/s. Henry's law for CO_2 is $p = Hx$, where $H = 9{,}000$ psia. Calculate:

(a) The liquid-phase mass-transfer coefficient and the film thickness

(b) Contact time for the penetration theory

(c) Average eddy residence time and the probability distribution for the surface-renewal theory

3.37 Determine the diffusivity of H_2S in water, using the penetration theory, from the following data for the absorption of H_2S into a laminar jet of water at 20°C.

Jet diameter = 1 cm, Jet length = 7 cm, and Solubility of H_2S in water = 100 mol/m^3

The average rate of absorption varies with the flow rate of the jet as follows:

Jet Flow Rate, cm^3/s	Rate of Absorption, mol/s × 10^6
0.143	1.5
0.568	3.0
1.278	4.25
2.372	6.15
3.571	7.20
5.142	8.75

Section 3.7

3.38 In a test on the vaporization of H_2O into air in a wetted-wall column, the following data were obtained:

Tube diameter, 1.46 cm, Wetted-tube length, 82.7 cm

Air rate to tube at 24°C and 1 atm, 720 cm^3/s

Temperature of inlet water, 25.15°C, Temperature of outlet water, 25.35°C

Partial pressure of water in inlet air, 6.27 torr, and in outlet air, 20.1 torr

The value for the diffusivity of water vapor in air is 0.22 cm^2/s at 0°C and 1 atm. The mass velocity of air is taken relative to the pipe wall. Calculate:

(a) Rate of mass transfer of water into the air

(b) K_G for the wetted-wall column

3.39 The following data were obtained by Chamber and Sherwood [*Ind. Eng. Chem.,* **29,** 1415 (1937)] on the absorption of ammonia from an ammonia-air system by a strong acid in a wetted-wall column 0.575 in. in diameter and 32.5 in. long:

Inlet acid (2-N H_2SO_4) temperature, °F	76
Outlet acid temperature, °F	81
Inlet air temperature, °F	77
Outlet air temperature, °F	84
Total pressure, atm	1.00
Partial pressure NH_3 in inlet gas, atm	0.0807
Partial pressure NH_3 in outlet gas, atm	0.0205
Air rate, lbmol/h	0.260

The operation was countercurrent, with the gas entering at the bottom of the vertical tower and the acid passing down in a thin film on the inner wall. The change in acid strength was inappreciable, and the vapor pressure of ammonia over the liquid may be assumed to have been negligible because of the use of a strong acid for absorption. Calculate the mass-transfer coefficient, k_p, from the data.

3.40 A new type of cooling-tower packing is being tested in a laboratory column. At two points in the column, 0.7 ft apart, the following data have been taken. Calculate the overall volumetric mass-transfer coefficient $K_y a$ that can be used to design a large, packed-bed cooling tower, where a is the mass-transfer area, A, per unit volume, V, of tower.

	Bottom	**Top**
Water temperature, °F	120	126
Water vapor pressure, psia	1.69	1.995
Mole fraction H_2O in air	0.001609	0.0882
Total pressure, psia	14.1	14.3
Air rate, lbmol/h	0.401	0.401
Column area, ft^2	0.5	0.5
Water rate, lbmol/h (approximate)	20	20